T.C.
İSTANBUL UNIVERSITY
INSTITUTE OF GRADUATE STUDIES IN SCIENCE AND ENGINEERING

M.Sc. THESIS

PREPARATION OF NOVEL METAL OXIDE NANOSTRUCTURES FOR ELECTRODE BASED SENSOR SYSTEMS

MAWADA MOHAMED .E TUNESI

Department of Chemistry

Chemistry Programme

SUPERVISOR
Assist. Prof. Dr. Selcan KARAKUŞ

December, 2017

İSTANBUL

This study was accepted on 22/12/2017 as a M. Sc. thesis in Department of Chemistry, Chemistry Programme by the following Committee.

Examining Committee Members

Assist. Prof. Dr. Selcan KARAKUŞ(Supervisor)
İstanbul University
Faculty

Prof. Dr. Ayben KİLİSLİOĞLU
Istanbul University
Faculty

Prof. Dr. Nilgün BAYDOĞAN
Istanbul Technical University
Faculty

Prof. Dr. Nilgün KIZILCAN
Istanbul Technical University
Faculty

Prof. Dr. Sema Demirci ÇEKİÇ
Istanbul University
Faculty

As required by the 9/2 and 22/2 articles of the Graduate Education Regulation which was published in the Official Gazette on 20.04.2016, this graduate thesis is reported as in accordance with criteria determined by the Institute of Graduate Sttudies in Science and Engineering by using the plagiarism software to which İstanbul University is a subscriber.

FOREWORD

First and foremost, I would like to thank Allah Almighty for granting me the force, ability, knowledge and opportunity to proceed this research study and complete it.

I would sincerely express my pride and appreciation to Assist. Prof.Dr. Selcan KARAKUŞ and Prof.Dr. Ayben KİLİSLİOĞLU. I thank them for the guidance, advice, patience and support during the research study and writing of my thesis.

A special thanks go to Dr. Razium Ali Soomro for his incalculable hours of contributing, reading, encouraging, motivating and most of all patience during the entire research study , this thesis would not have been possible without the priceless input.

I feel debited to my country which offered me the financial resources to pursue my study abroad.

Finally, I ought express my very deep thankfulness and gratitude to my beloved parents and to my sister, sister in law, brothers, friends for providing me with permanent support and encouragement during my years of study .This achievement would not have been possible without all of them.

December 2017   MAWADA MOHAMED .E TUNESI

TABLE OF CONTENTS

Page

LIST OF FIGURES

LIST OF TABLES

Page

LIST OF SYMBOLS AND ABBREVIATIONS

Abbreviation   **Explanation**

D   : Dimension
FTIR   : Fourier Transform Infrared Spectroscopy
XRD   : X-Ray Diffraction
SEM   : Scanning Electron Microscopy
EDX   : Energy-dispersive X-ray spectroscopy
UV/Vis   : Ultraviolet-Visible Spectrophotometry
TEM   : Transmission Electron Microscope
AFM   : Atomic Force Microscopy
NAC   : N-Acetyl-L-Cysteine
GCE   : Glassy Carbon Electrode
Nps   : Nanoparticles
NP   : Nalbuphine Hydrochloride
ASA   : Acetylsalicylic Acid
ITO   : Indium Tin Oxide
CAP   : Captopril
AD   : Adipic Acid
CA   : Citric Acid
D   : Diffusion Co-Efficient
α   : Charge Transfers Co-Efficient
DPV   : Differential Pulse Voltammetry
LOD   : Limit Of Detection
LOQ   : Limit Of   Quantification
CV   : Cyclic Voltammetry
K   : Rate Constant
MeONs   : Metal Oxide Nanostructures
Ns   : Nanostructures
DPV   : Differential Pulse Voltammetry

ÖZET

YÜKSEK LİSANS TEZİ

ELEKTROT ESASLI SENSÖR SİSTEMLERİNDE YENİ METALOKSİT NANO YAPILARININ HAZIRLANMASI

MAWADA MOHAMED .E TUNESI

İstanbul Üniversitesi

Fen Bilimleri Enstitüsü

Kimya Anabilim Dalı

Danışman : Yrd. Doç. Dr. Selcan KARAKUŞ

Son yıllarda, nanomalzemelerin ve elektrokimyanın kombinasyonu, elektro-analitik analiz için ilgi çekici hale gelmiştir. Nanoyapıların elektrot modifikasyonunda kullanımı, daha büyük aktif alanlı, verimli katalitik özellikli ve yüksek yüzey alanına sahip çeşitli önemli analitik moleküllerin hassas ve seçici olarak tespit edilmesini sağlamaktadır. Çeşitli nanoyapılar arasında, CuO, NiO ve Co_3O_4 gibi metal oksitler, daha yüksek performans kapasitesine ve sağlam yapıya sahip olduklarından, elektrot modifikasyonunda ve sensör geliştirmede tercih edilmektedirler. Bu çalışmada, nanoyapıların morfolojik büyümelerinin kontrol edilmesi ve yönetilmesi ile oldukça etkili biyo-molekül ve farmasötik ilaçlar olarak kullanılan yeni metal oksit nanoyapıların sentezi üzerinde durulmaktadır. Morfolojik açıdan ilgi çekici olan nanoyapıların sentezinde hidrotermal yöntem kullanılmış olup, SEM, FTIR, EDX ve XRD gibi gelişmiş analitik yöntemlerle karakterizasyonları gerçekleştirildi. Daha sonra sentez edilen yapılar, sensör geliştirmede kullanılan elektrotların modifikasyonunda kullanılmıştır.

Aralık 2017, 106 sayfa.

Anahtar kelimeler: Metal Oksit Nanoyapılar, Çevrimsel Voltametri, N-Asetil-L-Sistein, Nalbupin Hidroklorür, Kaptopril

SUMMARY

M.Sc. THESIS

PREPARATION OF NOVEL METAL OXIDE NANOSTRUCTURES FOR ELECTRODE BASED SENSOR SYSTEMS

MAWADA MOHAMED .E TUNESI

İstanbul University

Institute of Graduate Studies in Science and Engineering

Department of Chemistry

Supervisor : Assist. Prof. Dr. Selcan KARAKUŞ

In recent years, the combination of nanomaterials and electrochemistry has directed to the improvement of interesting platform for the electro-analytical analysis .The usage of nanomaterials for electrode modification has enabled highly sensitive and selective detection of various analytical important molecules based on high surface area, greater active sites and efficient catalytic characteristics. Among various nanomaterials, metal oxide nanostructures such as CuO, NiO and Co_3O_4 are highly considered for electrode modification and sensor development based on their greater performance capability and robust nature. The present study focuses on the synthesis of novel metal oxide nanostructures using bio-molecules and pharmaceutical drugs as highly effective templates for controlling and directing morphological growth of nanostructures. The fabrication of morphologically attractive nanostructures were achieved using hydrothermal method followed by elaborate characterization using advance analytical methods including SEM, FTIR, EDX and XRD. The fabricated materials were then utilized for electrode modification which later were considered for sensor development.

December 2017, 106 pages.

Keywords: Metal Oxide Nanostructures ,Cyclic Voltammetry,N-Acetyl-L-Cysteine, Nalbuphine Hydrochloride, Captopril.

1. INTRODUCTION

Recent progress in nanotechnology has allowed production of novel nano-materials with promising usage in almost every scientific area. The excellent characteristics of these nanomaterials are attributed to their shape and morphological features. In particular, the use of nanomaterials in electrochemical sensing has allowed effective quantification of a large number of biological important molecules. This integration of high conductive nanomaterials with electrochemistry has directed to the improvement of a novel dais for extensive electro-analysis examinations [1]. In recent, the production of electrochemical sensors using different shapes of nanomaterials and nanocomposites have attracted much interest[2][3]. In this content, due to the increasing demand of pharmaceutical drugs, the global pharmaceutical corporations, in order to cope with the growing demand worldwide, require highly sensitive protocols for the quantitative measurements related drug processing. The strict analyses ensure both the quality and stability of designed drug and also secure appropriate formulation of this drug[4]. It is therefore a high necessity to propose and produce an innovative approach for the quantification of such pharmaceuticals. So far, several conventional methods have been considereed for thier determination ranging from chromatography to turbidimetry [5] [6] [7] [8] [9] [10]. Although all mentioned methods are considered effective for quantification, they are costly, slow and complex. In contrast, the electrochemical techniques is much faster, sensitive and cost effective. This makes electro-analytical approach much suitable candidate for the fast and effective analysis pharmaceuticals[11][12][13].

1.1. THE ADVANCE NANOMATERIALS

The word nanotechnology is basically a combination of technologies where use of advance materials with design and production along with thier implementation is carried[14]. Nanotechnology is a broad field connected to multidisciplinary field with its implication in nearly every scientific area. Compared to bulk materials, nanoscale materials have superior physico-chemical characteristics which enable their usage in multiple application such as: electronics, chemical sensing, biosensing and health care. Nanomaterials are acquainted to a group of materials that have at least one dimension with approximately less than 100 nanometers in diameter (1 nm= 10^{-9} m) which is 100,000 times smaller than the diameter of a

human hair. With this extremely small size, distinctive optical, magnetic, electrical, and other physical and chemical properties appear. These superior properties have the potential for great impacts in different disciplines like chemistry, physics, biotechnology, and engineering.

1.2. THE NANO SIZE

The main obvious difference between nano and macro material is their size. Bringing down a material to a nano-size will have a pronounced effect on its properties. The most important factors contributing to this change are -: (i) quantum size effect (QSE) which means increasing Band Gap Energy (ii) increased Surface Area, therefore greater number of atoms at surface (Size =3 nm means more than 50% of its atoms at surface). Properties such as reactivity, conductivity, strength, optical and electrical features may be altered and optimized by such factors.The nanometric size of metal nanoparticles leads to its exibition of various characteristics e.g. color, reactivity and mechanical strength[15].

1.3. CLASSIFICATION OF THE NANOMATERIALS

Nanomaterial can be classified in four categories based on their macroscopic dimension, it includes: Zero (0-D), one (1-D), two (2-D) and three (3-D) dimension[16].

1.3.1. The Zero-dimension (0-D) nanomaterials

The materials that have their all dimensions (x, y, z) at nanoscale of 1 to 100 nm are called Zero dimensional (0-D) nano structures. The 0-D materials are cubes, polygonal and spherical in shape. Silver and gold nanoparticles, quantum dots with identical particle arrangements, hollow spheres and core shell quantum dots are some examples of zero dimension nanomaterials.

1.3.2. One-dimension (1-D) nanomaterials

The material that have at least their two dimensions (x, y) at the nanoscale and one dimension is greater than 100 nm out of nanoscale is called one dimensional (1-D) nano structure. Nanotubes of metal and metal oxides, nanofibers, nanowires, nanorods, spirals, columns, pillars and ropes are some examples of one dimensional nanomaterials.

1.3.3. Two-dimension (2-D) nanomaterials

The materials that have their one dimension at the nanoscale and other two dimensions are beyond the nanoscale is called two dimensional (2-D) nanomaterials. There are numerous examples of 2-D nanomaterials such as, nanolayers, fullerene powder, fullerene film, nanosheets, nanowalls, nanofilms, heteroparticles, nanostraw and nanocoatings.

1.3.4. Three-dimension (3-D) nanomaterials

The material that their all dimensions are not confined to nanoscales are called three dimensional (3-D) nanomaterials. Although, 3-D materials have some properties at the nanoscale such as they form the nanocrystalline structures with various arrangement of nanosizing crystals in different angles. In 3-D nanomaterials the different block combine together and prepared the bulk material like layer skeleton bilding, memberanes, foams, skeleton of fibers and fullerites.
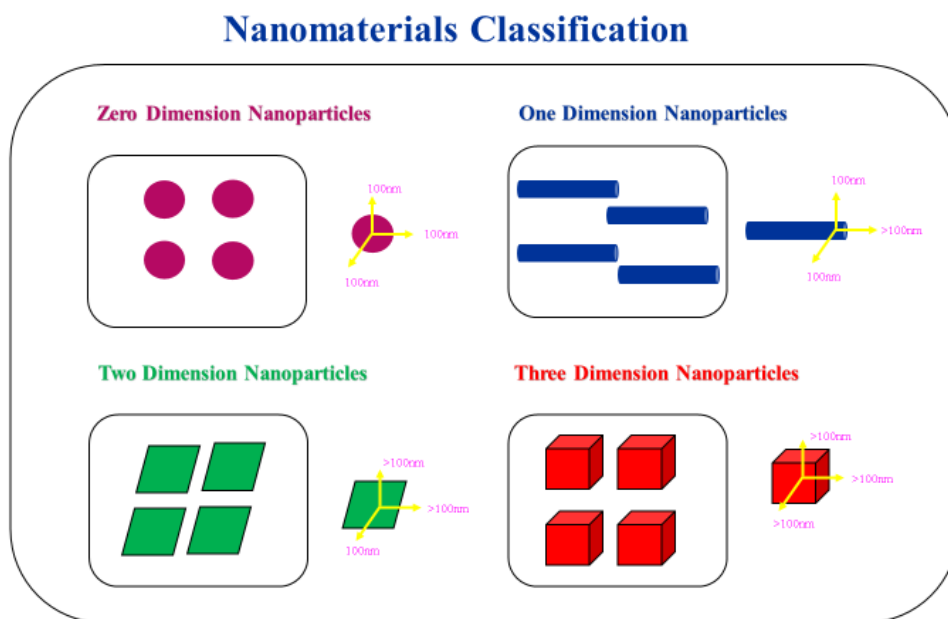
Figure 1.1: A diagram generalizing the dimensiomal classification of nanomaterials.

1.4. SYNTHESIS APPROACHES AND TECHNIQUES FOR NANOMATERALS

Generally, two methods are used for the synthesis of nanomaterials [16].

(1) The bottom-up approach and (2) the top-down approach.

1.4.1. Bottom-Up method:

Bottom up method used for the preparation of nanoparticles by the integration of atomic material. Colloidal dispersion and sol-gel method used for the formation of nanoparticles and powder respectively.

1.4.2. Top-Down method:

Top-down method used for the preparation of nanoparticles by slicing or cutting of macroscopic substance to get nano sized particles. Etching and ball milling is typical examples of top-down approach.

The above described approches are highly recommended for synthesis.
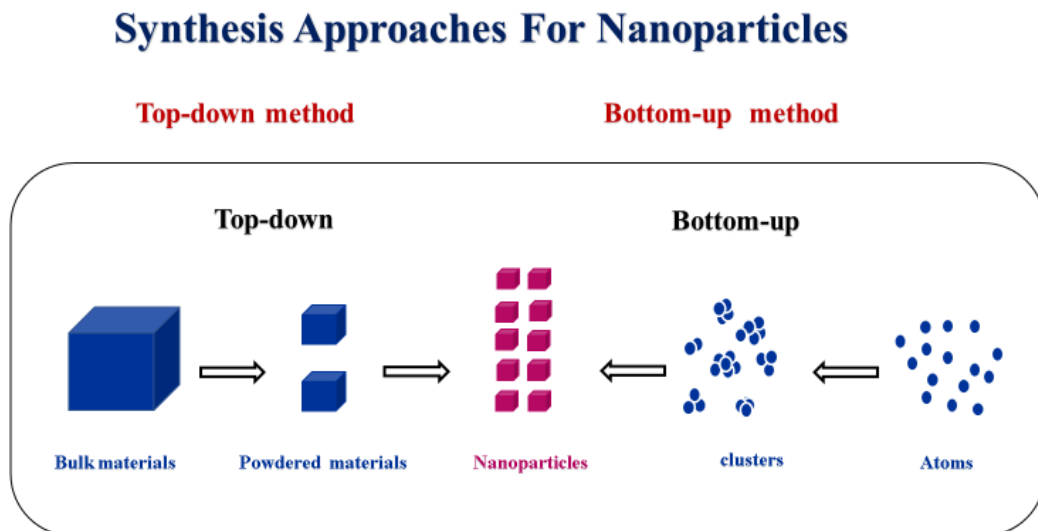
Figure 1.2: Synthesis approaches for nanoparticles.

1.5. MORPHOLOGY AND SURFACE CHARACTERIZATION OF NANOMATERIAL

Surface analysis techniques and conventional methods have been mainly used for the characterization of nanostructures and nanomaterials. FTIR can be used for the surface interactive study which can provide sufficient information of functionalization and if the surface adhered any impurity. In contrast, the XRD is an techniuqe that can easliy provide information of the cystallinity and compostion of the product under investigation.

The morphological evaluation is usaullay carried using scanning electron microscopy imaging techniques (SEM) which is the main and ideal approch to study the structral features of the nanomateiral under investigation. Similarly, the energy-dispersive x-ray spectroscopy (EDX) is used for the surface purity of the product [17].

1.6. THE METAL OXIDE NANOSTRUCTURE

The metal oxides nanostructured has recently attracted considerable attention based on their multidimensional properties and superior characteristics[18][19]. The physical and chemical features are highly contingent on the sizes, shapes, chemical composition and structures of nanocrystals. The nanostructured oxides of metal such as copper, cobalt, nickel , zinc, and iron have been found to offer interesting morphology, biocompatibility and excellent catalytic capability. They also exhibit enhanced electron-transfer kinetics, high conductivity and strong absorptivity which makes them an excellent candidate for diverse high-level applications. For example, secondary battery materials, ceramic, chemical sensors, biological sensors, solar cells and fuel cells[20].

1.6.1. Synthesis of metal oxide nanostructure

The substaintial attention towards nano-crystalline oxide materials is because of thier unique intrensic properties. The decrement in the particle size with obtaining unique morphologies resutls in the observation of remarkable characteristics. Recently, extensive efforts have been made to synthesize various metal oxide nanostructures with varying shape and size using different chemical and physical strategies including solid-state reactions, sol-gel method, coprecipitation, and hydrothermal techniques. The above mentioned method usually suffer problems such as high temperature requirments and complex protocols. In constrast, the co-precipitation approch is much prefered [21].
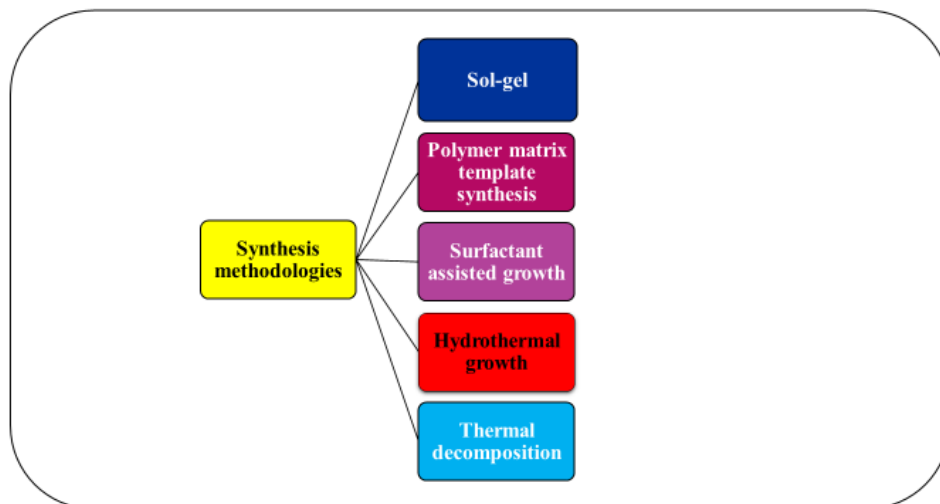
Figure 1.3: Synthesis methodologies of metal oxide nanostructures.

1.6.1.1. Hydrothermal Synthesis

The hydrothemal method is one of the most suitable methods. This method uses a sealed container with pressure buildup for synthesis. In addition, the hydrothermal method shows some advantages include simply, cost effective and ability to work with dissolved salts of many kinds. It is one of the best approach for nanocomposite preparation [22].
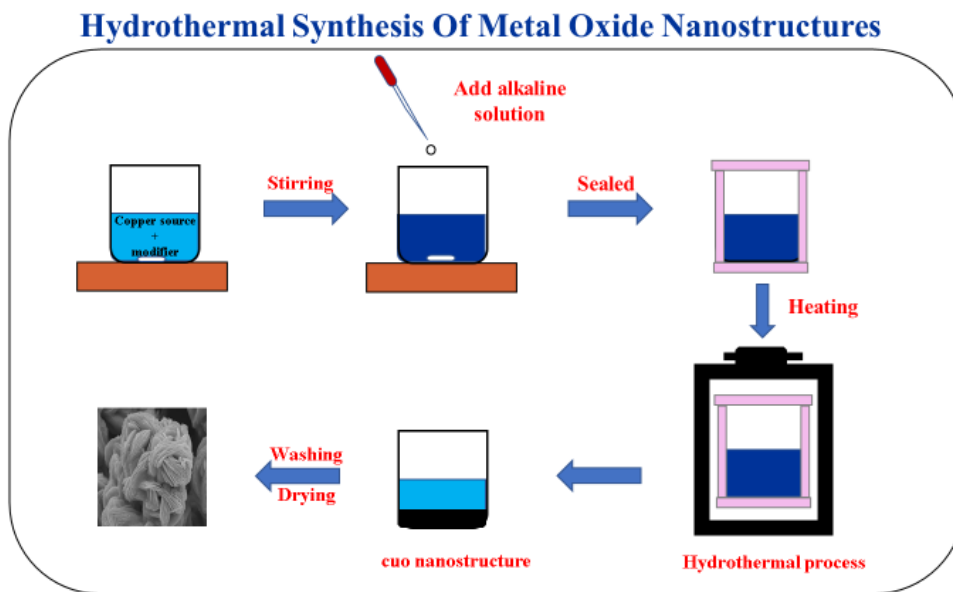
Figure 1.4: A schematic illustration of the hydrothermal synthesis of metal oxide nanostructures.

1.7. N-ACETYL-L-CYSTEINE DETECTION USING METAL OXIDE AS TRANSDUCER

The new researches of nanomaterials have contributed to the electrochemistry providing for it uneaven platform for extensive electro-analysis enquiry. The attractive nanostructures with more extensive surface area to volume ratio have provided in its turn more ability in fabricating sensitive and selective electrochemical sensor and the diversification of measuring molecules[23].Unlike the solution based homogeneous catalysis, electro-catalysis is widely affected by the morphology of the used nanomaterials. Such differences in the shape can either expedite or hinder the reaction of interest[24] .The high sensitivity and excellent conductivity of the fabricated nanosensor have provided the capability of setting high innovative standards and protocols to meet more rigorous regulations in matter of quality control of drug production. In this regard, quantitative determination of N-Acetyl-L-cysteine (NAC) is to be deemed a clinical significance due to its application, being an efficient antidote against acetaminophen poisoning ,mucolytic agent and anti-oxidant. This even though, the traditional approaches e.g. titrimetry[6], spectrophotometry[7], chemiluminescence[8],fluorimetry[9]and turbidimetry [10]are to be deemed rather sensitive techniques. Nevertheless; the complexity, timing and cost of applying such techniques make of them unsuitable ones for a rapid and effective analysis of NAC. Conversely; device miniaturization is provided with more analytical results as well as additional advantage by the electrochemical techniques of which contributes to the evolution of sensor method with both laboratory and field system.Respective to NAC analysis, several researches have showed instances of electrochemical modalities for the selective measuring. The utilization of bare glassy carbon electrode (GCE) for the purpose of direct oxidation of NAC is normaly negligible. Add to this , the utilization of noble metal electrodes, which include Au, Hg and Pt, will not be efficient in that it increases the cost of the procedure as well as its certain complexities[25]. Lately, there are evidences that the application of modified electrodes are active compared to the aforesaid constrains. The use of benzoyl ferrocene (BF) modified carbon nanotube paste electrode (BFCNPE) has already been reported [26]. Similarly, the use of iron oxide based nanocomposite has also been suggested [27].Moreover, the application of benzylferrocenyl-1H-triazole (BFT)/carbon nanotube modified glassy carbon electrode (BFT-CNT-GCE) has proven significant[28]. Moreover, the the working capacity of 1-[2-hydroxynaphthylazo]-6-nitro-2-naphthol-4-sulfonate/ CuO nanoparticles has also been achieved[29]. The use of CuO is primiarly important in this case,

as it may be easily synthesized without requiring the calcination, differently to other metal oxides (Co_3O_4, NiO and Fe_3O_4), This will permit an easier functionalization of CuO nanomaterial for any proposed functional moiety.

1.8. NIO, CUO AND CO_3O_4 NANOSTRUCTURES FOR THE DETECTION OF NALBUPHINE HYDROCHLORIDE

The Increasing use of pharmaceuticals has lead up to an increase in the aqueous environment perseverance. Although they are recognized as a class of emerging pollutants, there are no criterion regulations or limits on the maximum allocations for this new class of pollutants [30]. So, the existence of such these pollution poses considerable threat in terms of water quality especially in third world countries such as Pakistan, India and Bangladesh where hospital and industrial waste effluents are directly disposed into the river waters. The incorrect hospital effluent disposal and the lack of appropriate administration are responsible for many diseases Transmitted by water [31][32]. Thus, it is absolutely necessary to suggest and fabricate an innovative method to quantifying these pharmaceuticals. In this content, the estimation of nalboven hydrochloride NP (a phenanthrene derivative) is highly investigated due to its clinical and pharmacological significance[33]. Chromatography, spectroscopy and electrochemical methods [34] [35] [36] [37]are the most routinely approaches that have been used for the determination of these pharmaceuticals .Unlike the other techniques, the electrochemical approach is simple, fast, sensitive, and cost effective [38]. So far, sufficient progress has been observed in the application of electrochemical methods for pharmaceutical detection. One of the main factors responsible for this progress is the improved efficiency of the electrode represented by diverse new polar materials that offer much better activity than the conventional peers[39]. Right now, the nanomaterial which act as electrode modifying materials are highly considered based on their high surface area, high conductivity ,and excellent catalytic capability have proven pivotal in the amelioration of the electron-transfer kinetics permitting sensitive quantification of pharmaceuticals[40]. In this regard, The NP is much less-explored drug to its high-potential requirement sluggish/irresponsive attitude over the traditional electrodes. Recent methods which have proven efficient towards increasing the signal of NP includes modification of traditional glassy carbon electrode (GCE) with pencil graphite [41], gold nanoparticles and NiO/functional single walled carbon nanotubes [33] and nanocomposite [42]. However, signal enhancement achieved through modification of electrode with

nanostructures that having large surface area and bound charge density that faraway at the point of where structural landscapes joint with the substances of analysis[24]. It is known that, unlike the solution based catalytic reactions, the electrochemical reactions based nano catalyst such as metal oxides are hugely affected by the morphological characteristic of the synthesized nanomaterials. Although, the electro-kinetics and reduction potential value of the electrochemical reactions could be effected by different structural morphologies of produce nanomaterials that limit their success.Furthermore, the structural duplicability of nanosizing materials is additional significant case for the manufacture of electrochemical sensor method. Especially, in the example of metal oxide, the application of these small particles that can act as a model has proven to be of great importance. The use of these modifiers guarantees structural replicability for electrochemical sensors and moreover allows the producing growth of nuclei fabricating the morphology of the excellent electrochemical characteristic as associated to the larger counter parts. In this regard, diverse biological molecules like amino acids, DNA, proteins and virus [43], monosaccharide [44], polymers[45]and surfactants[46] have been reported as efficient templates. However, the extensive application of modifiers for the fabrication of nanostructures with unique structural features is still a challenging task. In context to the application of pharmaceutical drugs molecules as efficient templates is a new field of substantial research interest. The pharmaceutical drugs have proven considerable for directing the dimension of metal particles [47][48]. Newly , Soomro, R. A., et al. (2016) [49]explained the application of diclofenac sodium template to produce NiO nanostructures. In a much recent attempt Tunesi, M. M., et al. (2016) [50] demonstrated the growth controlling capability of N-acetyl-l-cysteine to fabricate CuO nanostructures.

1.9. CUO BASED ITO SUBSTRATE FOR THE SENSING OF N-ACETYL-L-CYSTEINE

The utilization of nanosizing materials in the area of electrochemical sensing has prove to be the improvement of a new platform for the extensive electrochemical examinations [23].The attractive synthesized nanostructures by higher surface area and greater charge density have presented an important improvement for the traditional electrochemical sensor system. Unlike the catalysis based on solution, the electrochemical reactions based nano catalyst like metal oxides are hugely affected via the morphological characteristic of the synthesized nanomaterials[24]. One of the most appropriate method that has been largely utilized for the

combination of nanostructure materials in the electrode system is the modification of the surface of polished electrode using drop casting approach[51]. Despite the efficiency of this methodology, it produces effective signal variation by cause of the random impeachment and organization of the nanostructure on the upper area of the electrode. In order to overcome this problem, the polymeric binders like Nafion® and chitosan are utilized to reserve the scuff of the adopted layer on the electrode to enhance the performance of the electrode system. In contrast to this, the growth of nanosizing material on the inexpensive conductive materials has confirmed the promising alternative approach for electrode modification[52].so that, the in-situ formation of nanostructures upon flexible ITO glass is an accurate, precise method with low cost process compared to the traditional approaches [53] [54]. The application of cheap ITO glass as substrate at the time of in-situ formation of nanostructure materials allows to produce precise organized nanostructure that suppressed the background current to boot the sensitivity and accuracy of the electrode system. ITO glass substrates have a low catalytic activity compared with conventional noble metal electrodes. Recently, the ability of CuO over ITO glass for the oxidation of glucose[55]. In a similar way, the direct electrochemical sensing of glucose by in-situ growth of graphene embedded Au NPs over the ITO substrate as working electrode[56]. Authors also intensified on the superior accuracy and precision of the electrode as a result of tremendous electro catalytic action of nanoparticles due to association with the conductive surface of ITO. Regardless of extravagant usage of ITO in different areas, the use of flexible electrodes as electrochemcial sensor is less explored. The controller and route of the growth procedure is a problem during the growth of nanostructures over glass substrate particularly for metal oxides, the temperature that control the synthesis of the nanostructures usually produce a bulkier nanostructures with low contact of these structure on the conductive substrate. Therefore, an effective process to design a greatly stunning nanostructures through enormous adhesion capability towards ITO substrates is needed. Alike electrode systems may be then employed in the fabrication of sensitive, selective, and effecient electrochemical sensors. In respect to the use of aforesaid materials, the robust analysis of clinically and toxicological important molecules is a growing research and one of the fastest unique research areas. In this circumstance , the adequate determination of the N-Acetyl-L-cysteine (NAC), a modified amino acid cysteine utilizes as mucolytic agent, anti-oxidant and antidote is highly investigated. Different procedures have been used for the detection of NAC include titrimetry[6], spectrophotometry[7], chemiluminescence[8], fluorimetry[9] and

turbidimetry[10] Although all these methods are highly sensitive. However, they are time taking and as well connected with numerous difficulties as result they classified them as an unsuitable candidate for the most common analytical applications.In contrast to this, the electrochemical approach is adequatly more simple, fast and cost effective .The electrochemical detection of NAC by metal electrodes such as(Au ,Pt, Ag) is a completely sluggish. Yet, the alteration of bare electrodes by appropriate mediators include:electro-active polymer, carbon nanotubes, iron oxide have established active. Currently, the use of CPE for the electrochemcial detection of NAC has been proposed using CuO with certian additives [29]. The study confirmed the conclusive role of CuO nanoparticles as an efficient charge transfer centers through the electrochemical oxidation of NAC .CuO nanostructure as a p-type semiconductor material ,with its superior physical and chemical characteristic distinctive properties and the capability to favour electron transfer kinetics. Besides this, CuO nanostucture can grow at lower temperatures without need of the calcination step offers the chance for casual functionalization of nanostructure. This functionalization can efficiently grant the effective formation of CuO nanomateiral over a flexible substrate [57].

1.10. CUO NANOSTRUCTURES BASED ITO SUBSTRATE FOR THE DETERMINATION OF CAPTOPRIL

The accurate quantification of environmental and biological serious molecules is one of the most critical challenging task for their clinical and toxicological importance[58] [59]. The numerous of traditional techniques have been utilized for the detection of such these molecules including: UV- spectrophotometry [60], HPLC [61] ,GC [62] and LC-MS [63]. Regardless of their high sensitivity and reliability, they considered them as time-consuming and complex sample preparation and analysis methods. In addition , they classified them as an unsuitable candidate for the most common analytical applications [64] .Contrary to that, the coupling of nanomaterials with electrochemical technique can guarantee a favorable pathway for the fabrication of a simple, precise, selective,and cheaper sensor system [64][63][60]. Beside that,the combination of electrochemical approach with nanosizing materials can extremely improve the distinctive properties of the classical electrodes resulting in precise and accurate determination of various clinical and toxicological substances[61][62] [65] .One of the most traditional approach that have been widely practiced for the modification of electrodes such as (gold , platin and silver) is the drop casting of the nanosizing materials above the

surface of cleaned electrode [51]. Despite the efficiency of this approach, it impedes the controllable allocation of nanostructurs throughout the surface of electrode altering the active sites as well as the electrochemical behaviour of the electrode. Moreover , the application of polymeric binders to confirm the attachment of nanomaterial on refined surface of electrode can hinder the processing of analysis specie distribution at the electrode-solution integrate [66]. Recently, the use of CuO nano based material have been tested for glucose sensing[55] . In a similar way, it is proposed that graphene-encapsulated gold nanoparticle for the non-enzymatic detection of glucose [56]. Regardless of extravagant usage of ITO in different areas, the use of the flexible material in the zone of electrode based sensors is limited investigated. Captopril (CAP), in chemical parlance, (2S)-1-[(2S)-2-methyl-3- sulfanylpropanoyl] pyrrolidine-2-carboxylic acid is a vastly drug used for the treatment need for elvated blood pressure and to monitor glucose blood level. The systems have also been utilised for kidney related issues and congestive heart failure. To date back , several electrochemical methods including the use of different mediator such as multiwall carbon nanotubes , nano-Tio2/ferrocene carboxylic acid , and chlorpromazine [67] [68] have been considered for the sensitive quantification of CAP. Recently, the direct electrochemical oxidation of CAP by CuO ions modified electrodes and CuO nanoparticles/multi-wall carbon nanotube have been defined the affinity of the electrode modified with thiol functionality connected with CAP molecules[69][70].

2. MATERIALS AND METHODS

2.1. CHEMICALS AND REAGENTS

Analytical grade Nickel based salt (Ni $(NO_3)_2.6H_2O$), Copper chloride ($CuCl_2·5H_2O$), Cobalt chloride hexahydrate ($CoCl_3.6H_2O$), Citric acid ($C_6H_8O_7$), Acetylsalicylic acid ($C_9H_8O_4$) , Adipic acid ($C_6H_{10}O_4$),Succinic acid ($C_4H_6O_4$), Malonic acid ($C_3H_4O_4$), N-Acetyl-L-cysteine ($C_5H_9NO_3S$), Ammonia solution (NH_3) 32%, Sodium hydroxide (NaOH), Britton–Robinson buffer (BRB) (0.1 M) and Phosphate buffer solution (PBS) (0.1 M) (both used as an electrolytic solution), Captopril (99.0 %), Uric acid ($C_5H_4N_4O_3$), Vitamin C ($C_6H_8O_6$), Glucose ($C_6H_{12}O_6$), Folic acid ($C_{19}H_{19}N_7O_6$), Magnesium chloride ($MgCl_2$), Aluminum chloride ($AlCl_3$), Sodium nitrate ($NaNO_3$), Potassium chloride (KCl), were procured from sigma Aldrich . ITO was purshed from TEKNOMA. Nafion$^®$ (1.5%) ($C_7HF_{13}O_5S.C_2F_4$) (Sigma) solubilized in isopropanol (C_3H_8O) (Merck) was utilized as Polymeric binder, while the remainder stock solution was prepared using deionized water.

2.2. THE SYNTHESIS OF METAL OXIDE NANOSTRUCTURES

2.2.1. The growth of CuO nanostructures functionalized utilizing N-Acetyl-L-cysteine, adipic and citric acid as controlling agents

The low-temperature hydrothermal growth method was utilized for the growth of the functionalized CuO nanostructures. In a representiative experiment, 1.68 g of $CuCl_2.5H_2O$ was allowed to vortex with 1.0 mg of NAC, AD and CA in 100 ml of deionized water. 5 ml of NH_3 (32%) was then slowly introueced to the mixture by a moderate vortex and the vessel was sealed with aluminum foil so as to prevent any chemical spillage and positioned in a pre-heated oven underneath constant temperature of 85 $^°$C for 8 hr, for the purpose of hydrothermal process. The formed CuO nanostructures were quite washed with deionized water and ethanol before subjecting to electrochemical evaluation against NAC to take out any surface associated impurities adhered to the surface.

2.2.2. The synthesis of metal oxide nanomaterials using acetylsalicylic acid as directing and controlling agent

The simple hydrothermal appproach integrated with acetylsalicylic acid (ASA) for growth stabilization is utilized for the growth of metal oxide nanostructures. In case of Nickel and

Cobalt oxide, 1.8 g of Ni $(NO_3)_2$.$6H_2O$ and 2.3 g of $CoCl_3$.$6H_2O$ were individually dissolved in total of 100 ml of de-ionized water followed by 0.1 g of ASA. To ensure entire homogenization, the solution mixtures were then stirred for 10 min. The mixtures were then introduced a fixed 6.5 mL of ammonia solution (%32) and the container was sealed with aluminum foil so as to avoid any solvent spillage and positioned in a pre-heated electrical oven underneath constant temperature of 85 °C for 6 hr, for the purpose of hydrothermal process. Then, the products were separated from the mixture solution using simple filtration and quite washed with separated water to take out any surface bound impurities followed by air-calcination at 450 ℃ for 4 h to convert the hydroxide of Nickel and Cobalt to NiO and Co_3O_4 nanostructures respectively. The Copper oxide nanostructures were grown without the calcination step. 1.68 g of $CuCl_2$·$5H_2O$ was homogenized with 0.1 g of ASA in 100 ml of deionized water. 6.5 mL of Ammonia (32%) solution was then added to the solution followed by hydrothermal treatment at 85 °C for 6 hr. The formed CuO nanostructures were thoroughly washed with deionized water and ethanol before subjecting to electrochemical evaluation against NP.

2.2.3. The fabrication of ITO based working electrode using succinic acid as directing agent

In a typical experiment, 1.68 g of $CuCl_2$.$5H_2O$ was permitted to swirl toghather with 0.5 g of succinic acid in 100 ml of deionized water. After the homogenisation is accomplished, then the pre-cleaned ITO slides (1×1 cm^2) were allocated with their conductive side directed to upside in the container. The ITO glass used as a working electrode for this purpose some part of the glass was enclosed with tape in order to prevent the nanomaterial formation on that particular portion which later was detached to allow electrical contact. 6 ml of ammonia solution (32 %) was then introduced to the mixture so as to start nucleation procedure. The mixture was hydrothermally treated for 4 h at 85℃ for completion of growth. The ITO were then taken out and washed thoroughly for removal of any impurities.

2.2.4. The fabrication of ITO based working electrode using malonic acid as directing agent

The simple hydrothermal method was utilized for the direct formaiton of CuO nanostructures with malonic acid as template. In a representative process,1.63 g of $CuCl_2$.$5H_2O$ was homogenized with 0.7 g of malonic acid in 100 ml of deionized water. After homogenisation is accomplished , the pre-cleaned ITO slides (1×1 cm^2) were allocated with their conductive

side directed to upside in the container. The ITO glass used as a working electrode for this purpose some portion of ITO was enclosed with paper tape in order to prevent the formation on that particular portion which later was detached to allow connection for working electrode. 5 ml of ammonia solution (32 %) was then introduced to the mixture so as to start nucleation procedure. The vessel was then wrapped with aluminium foil and put in a pre-heated electric oven under 80 °C for 9 h for hydrothermal process. After the finalization of reaction, the ITO coated glass slide was washed for through cleaning.

2.3. CHARACTERIZATION

2.3.1. SEM (Scanning Electron Microscopy)

The as-synthesized metal oxide nanostructures were characterized utilizing scanning electron microscopy (HR-SEM) (JEOL JSM-7001F).

2.3.2. XRD (X-ray Powder Diffractometry)

For the structural characterization of all metal oxide nanostructures, X-Ray Diffraction Measurements (XRD) was carried using (Bruker D-8).

2.3.3. EDX analysis

The compositional purity of the synthesised product were determined using Energy Dispersive Spectroscopy (EDS) (Oxford).

2.3.4. FTIR (Fourier Transform Infrared Spectroscopy)

FTIR analysis was conducted using the ALPHA-P from Bruker company within the range of $(4000–400 \text{ cm}^{-1})$.

2.3.5. Electrochemical Analysis

The electrochemical performance of the developed electrode was evaluated using bipotentiostat Gamry Instruments (Refrence 3000) (USA) with electrochemical cell, housing three electrodes. The reference electrode was a standard Ag/AgCl wire and auxiliary electrode was a platinum wire. The working electrode was a modified GCE/ITO based electrode separately linked with electrochemical cell system.

2.4. THE ELECTRODE MODIFICATION

The simple drop casting methodology was utilized for the electrode modification. Before the surface modification of (GCE)، the as-synthesized nanomaterials were primarily converted into suspension (0.1 mg into 1 mL of Methanol). After that the suspension was utilized for the alteration of pre-refined GCE with certian impeachment of volume (3 µL). The electrode was dried under gentle stream of N_2 gas and then treated with 0.8 µL of Nafion® solution (1.5 %) to make sure that nanomaterial is adhered upon polished surface of GCE. Such modified electrodes were employed as working electrode in the electrochemical system.

2.5. THE PREPARATION OF REAL SAMPLE

2.5.1. The NAC samples

A declared amount of 600 mg of NAC tablets were procured from the local pharmacy so as to estimate the viability of the established electrode. A first, the tablets were grinded and dissolved in 250 mL of water followed by ultrasonication. A particular portion of the homogenized solution was then diluted to 100 mL in 5.5 pH PBS buffer. For NAC examination 10 mL of the obtained solution was used. The standard addition strategy was also utilized to approve the assessment of NAC.

2.5.2. The CAP samples

For the quantitative analysis, also, specific amount of 25 mg of CAP tablets was procured from the local pharmacy. The tablets were crushed and diluted in BRPB buffer. A solution of 0.1 µm (CAP) was prepared before examination. To prove the quantification of CAP, the standard addition strategy was used for samples anaylsis.

3. RESULTS

Nanomaterials are reliant on various analytical and electrochemical technique in order to fame their stunning morphological building blocks and structural characteristics. Therefore, in order to visualized the aim of present research work we utilized different analytical techniques such as SEM used for the surface characterization of the synthesized nanostructures (NiO, Co_3O_4, and CuO). XRD was used for the identification of 3-dimensional arrangement of the atoms in manufactured nanomaterials and the true elemental composition of these nanomaterials was analyze by EDX. The surface functionalization of synthesized materials understood by FTIR analysis. After these characterizations the clear picture of synthesized nanomaterial has been seen that shows their ability to make a precise sensor system for the electrochemical determination of some important biological molecules such as N-acetyl cysteine, Nalbuphine hydrochloride and Captopril.

3.1. SEM ANALYSIS

SEM analysis were carried to obtain the morphological and structural characteristics of the synthesized materials .

3.1.1. SEM analysis of CuO nanostructures

The SEM analysis of CuO nanostructures obtained using N-acetyl-L-cysteine, adipic acid and citric acid as an templates are given in Figure3.1 respectively.
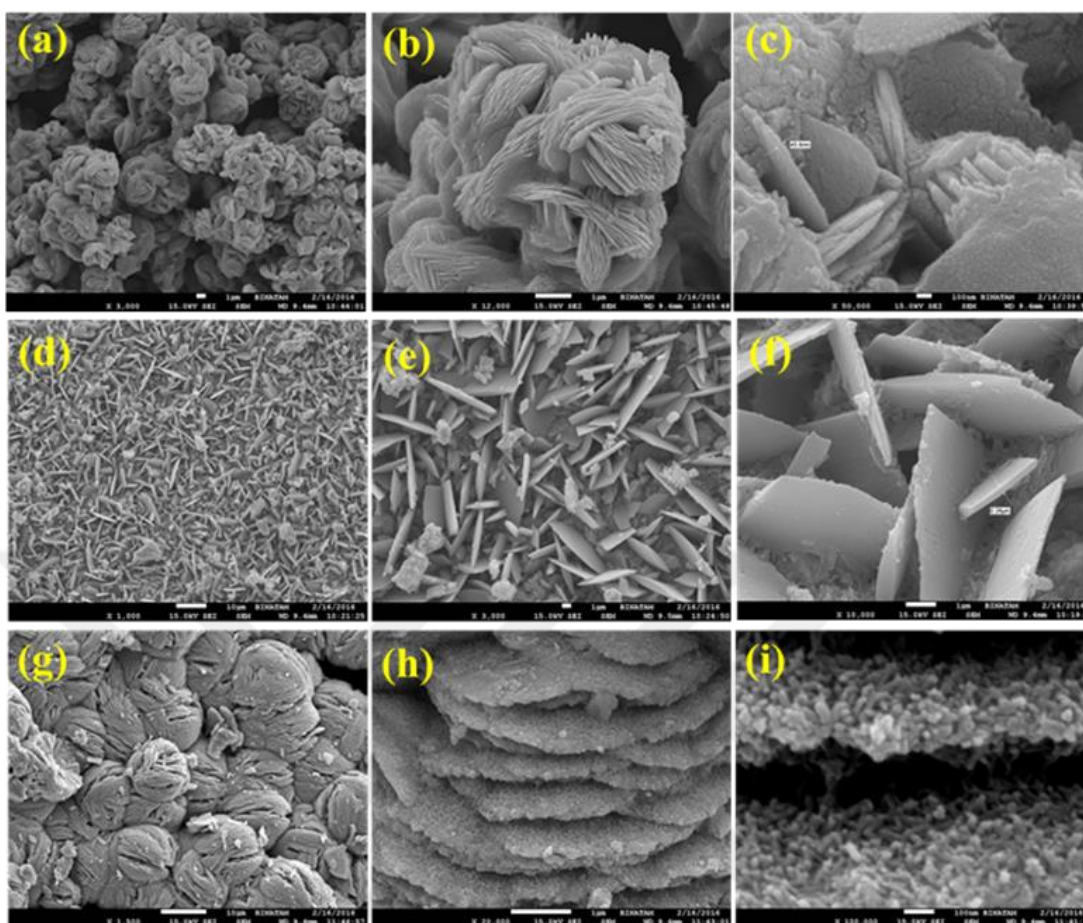
Figure 3.1: CuO nanostructures functionalized utilizing N-Acetyl-L-cysteine (a:c), adipic acid
(d:f) and citric acid (g:i) as controlling agent .

To justify the crucial role of the utilized modifiers as effective growth directing/controlling
agents the CuO material was fabricated without the application of the modifiers.
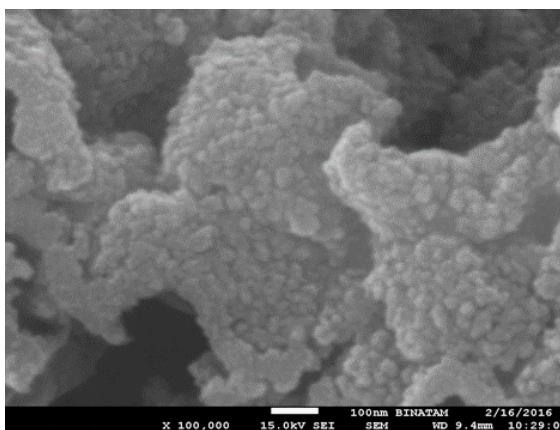
Figure 3.2: CuO material synthesized without the application of growth directing modifiers.

3.1.2. SEM images of the synthesized nanostructures (NiO, Co₃O₄, and CuO) using acetylsalicylic acid as an effective growth modifier

To evaluate the morphological characteristics of the synthesized nanostructures (NiO, Co_3O_4, and CuO) using Acetylsalicylic acid as an effective growth modifier, the FE-SEM was conducted out. The FE-SEM images for Metal oxide nanostructures is given in Figure 3.3 .
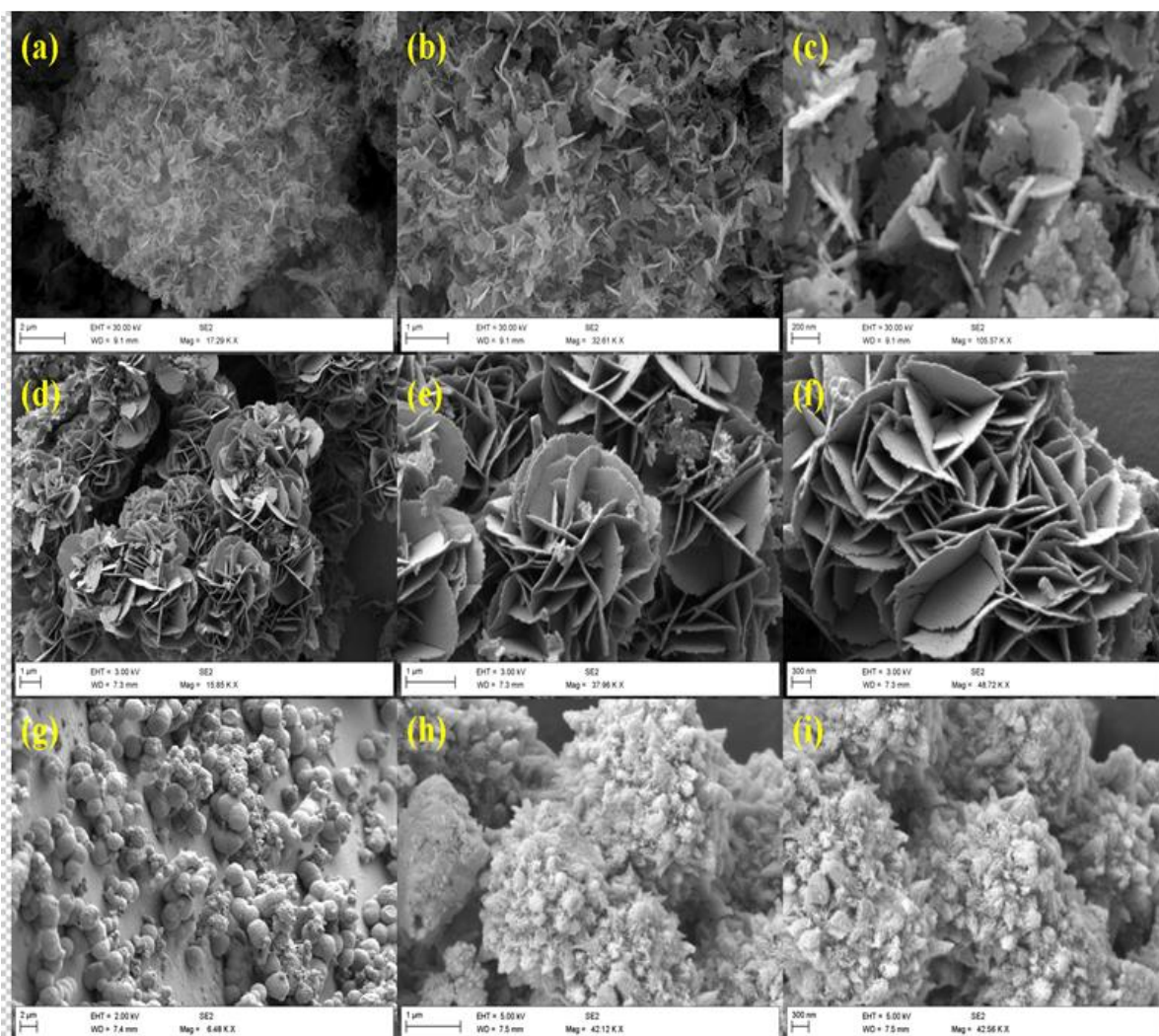
Figure 3.3: SEM images of the synthesized CuO (g:i), NiO (a:c), Co_3O_4 (d:f) nanostructures utilizing acetylsalicylic acid as directing and controlling agent.

3.1.3. SEM images of the fabricated ITO based working electrode using succinic acid as directing agent

To assess the morphological feature of the synthesized materials using succinic acid which was taken as template. The SEM images are showin in Figure 3.4.
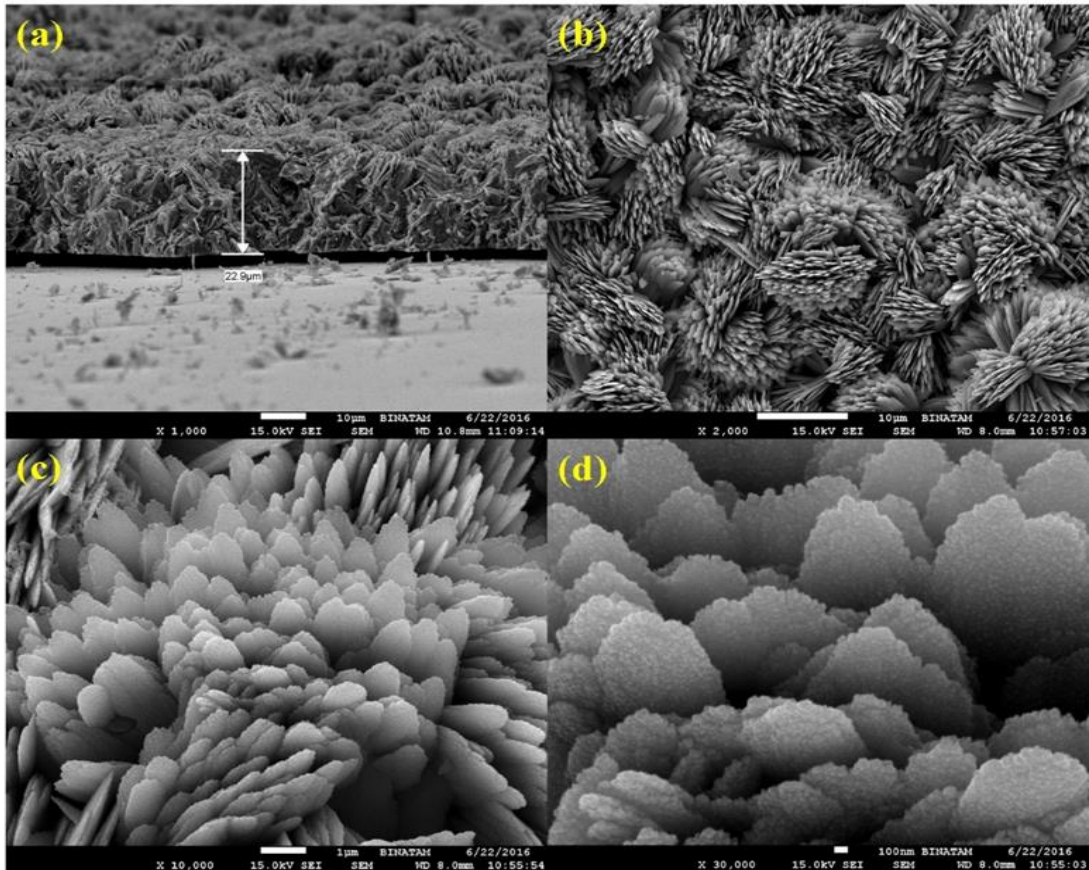
Figure 3.4: SEM patterns of the fabricated ITO based working electrode using succinic acid as directing agent.

To study the vital role of the modifier and tape paper for the grown CuO over ITO substrate, the SEM analysis was carried without the application of the modifier and tape paper.
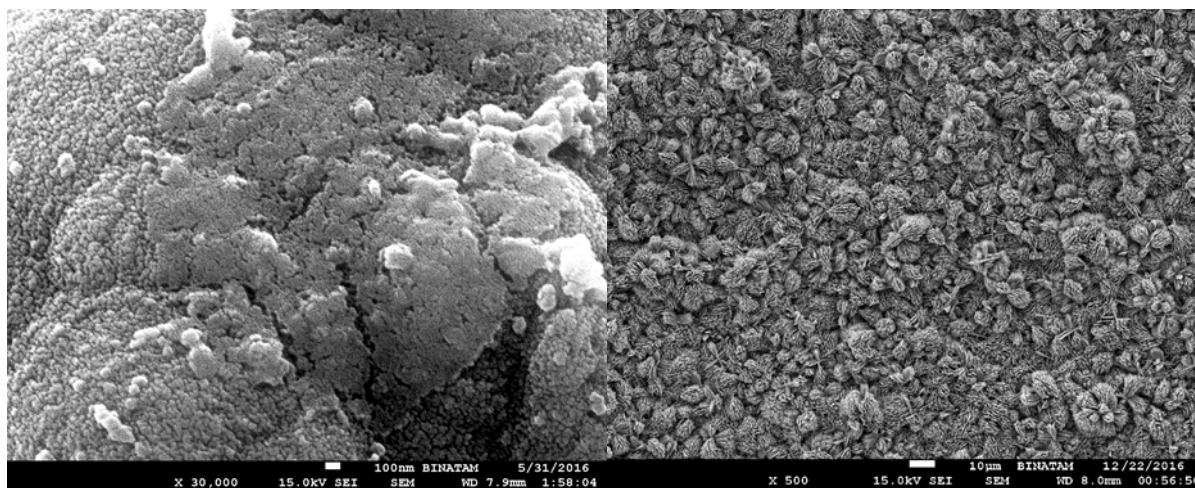
Figure 3.5: (a) HR-SEM patterns image for in-situ grown CuO without the support assistance of succinic acid as modifier and (b) CuO/ITO prepared under controlled experiment without the application of paper tape to cover the ITO electrode.

3.1.4. SEM images of the fabricated ITO based working electrode using succinic acid as directing agent

To evaluate the morphological characteristics of the synthesized material utilizing malonic acid as an efficient growth modifier, the FE-SEM was carried. The HR-SEM patterns of the fabricated ITO based working are shown in Figure 3.6.
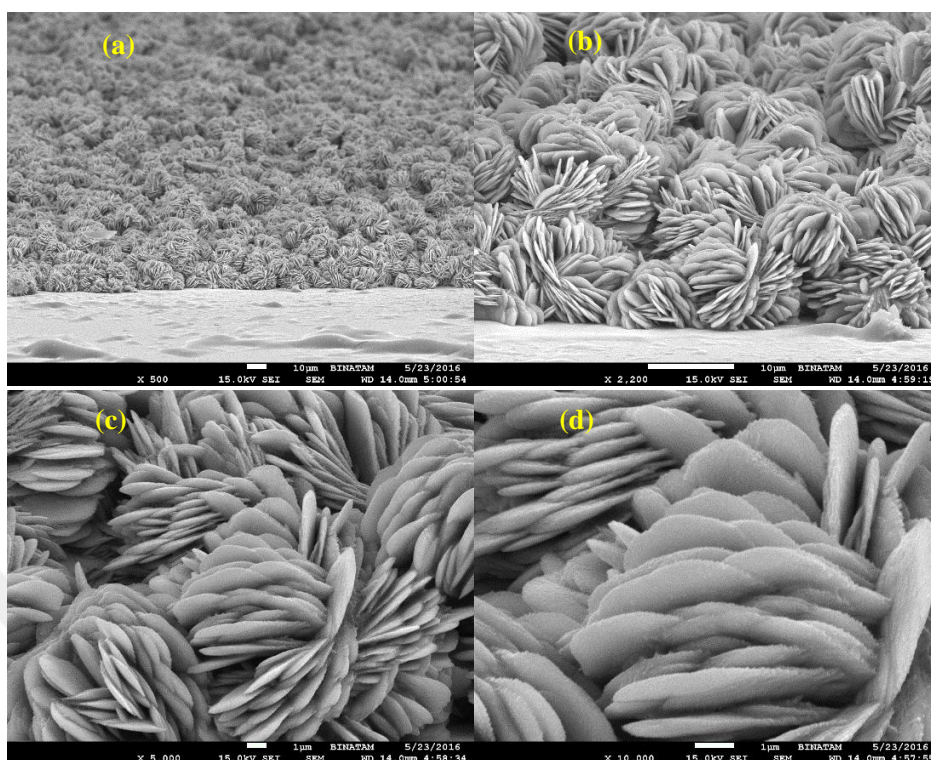
Figure 3.6: SEM patterns of the fabricated ITO based working electrode using succinic acid as directing agent.

To ensure the use of template, the material was fabricated without template where the absence of morphology is evident.
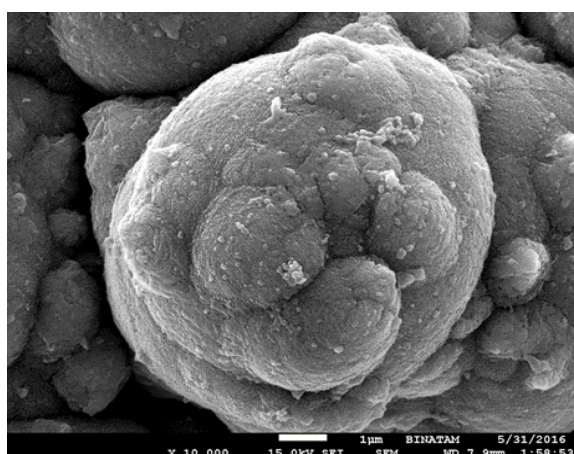
Figure 3.7: SEM patterns image of the CuO fabricated without the usage of malonic acid as directing agent.

3.2. XRD ANALYSIS

XRD measurements were carried to study the the cystallinity and compostion of the synthesized materials .

3.2.1. XRD pattern for CuO nanostructures

Figure 3.8 presents the XRD pattern for the fabricated CuO Nanostructures .
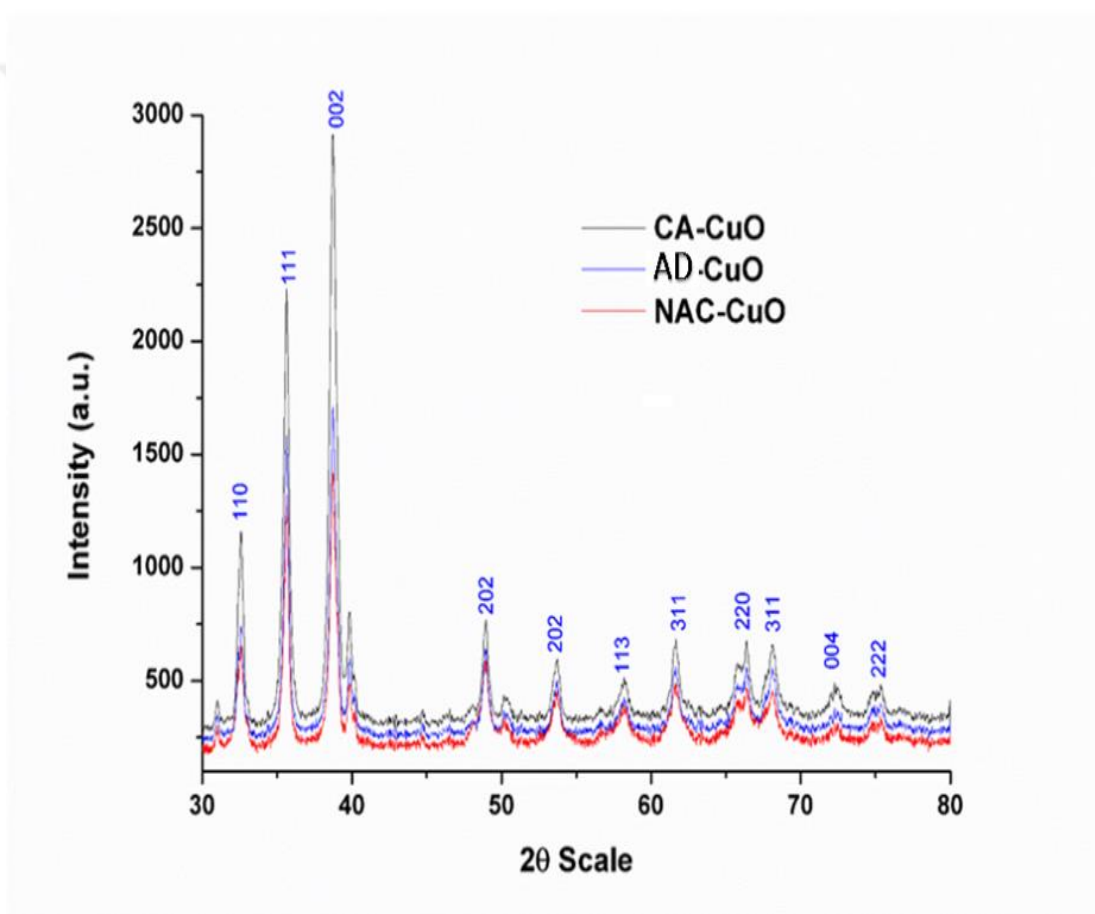
Figure 3.8: The XRD pattern for with NAC, Adipic acid, citric acid functionalized CuO nanostructures.

3.2.2. XRD patterns for the synthesized nanostructures (NiO, Co₃O₄, and CuO) using acetylsalicylic acid as an effective growth modifier

Figure 3.9 exhibits the XRD pattern for the fabricated metal oxide nanostructures .
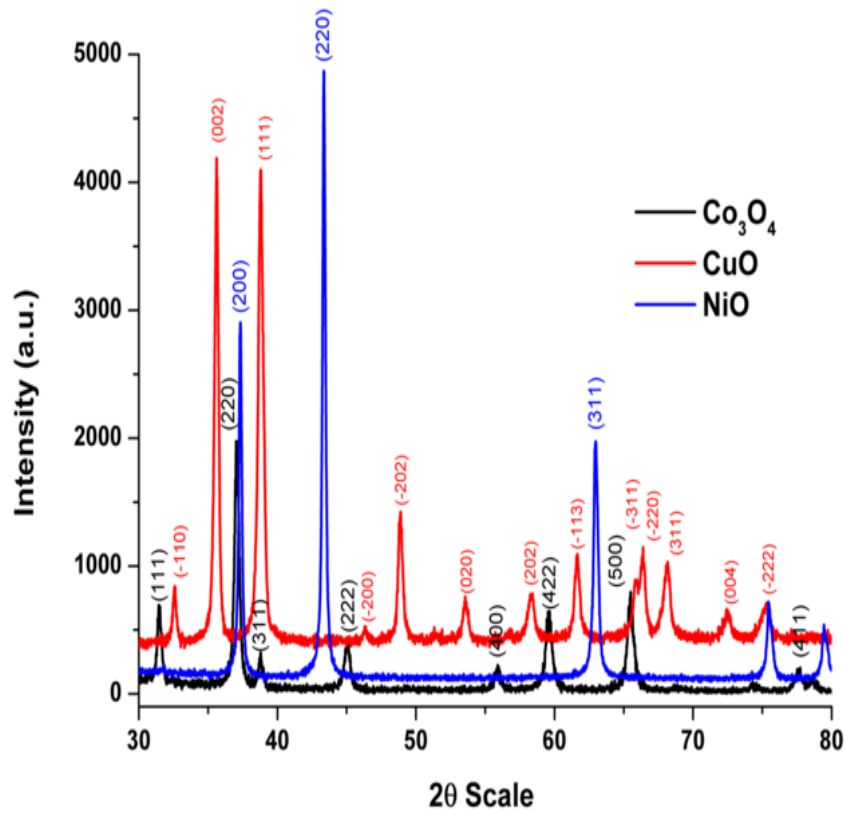
Figure 3.9: The XRD patterns measured for the fabricated   NiO, Co₃O₄ and CuO nanostructures.

3.2.3. XRD pattern for the fabricated ITO based working electrode using succinic acid as directing agent.

Figure 3.10 shows the XRD pattern for the CuO/ITO electrode.
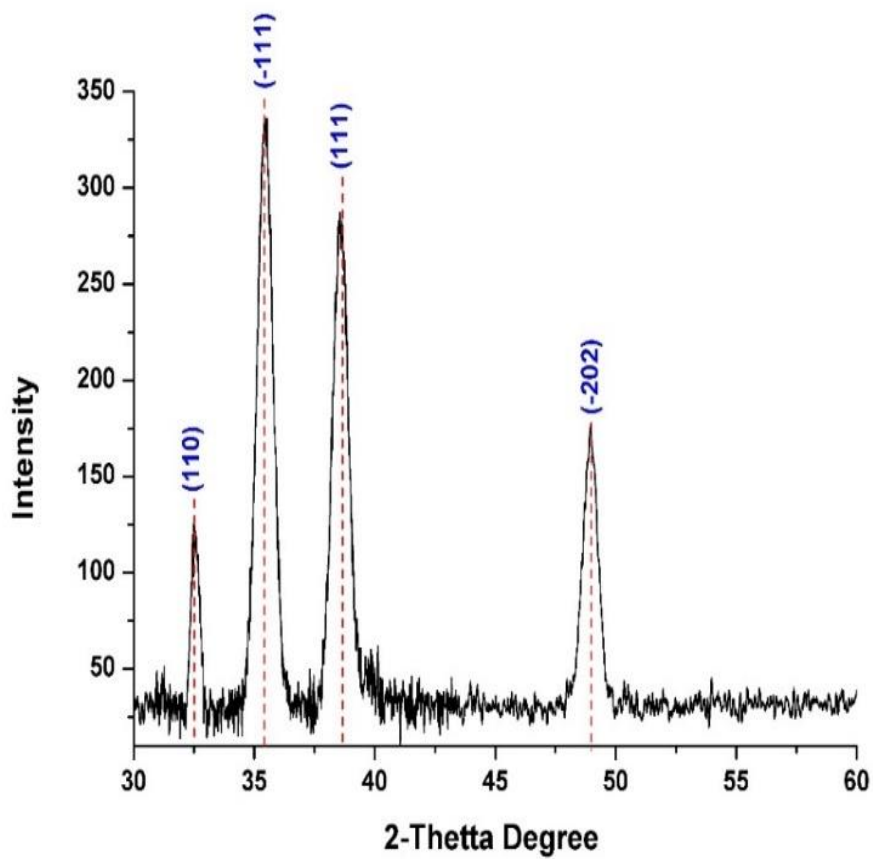
Figure 3.10: XRD pattern measured for ITO-CuO NS.

3.2.4. XRD pattern for the fabricated ITO based working electrode using malonic acid as directing agent.

Figure 3.11 depicts the XRD pattern registered for CuO/ITO.
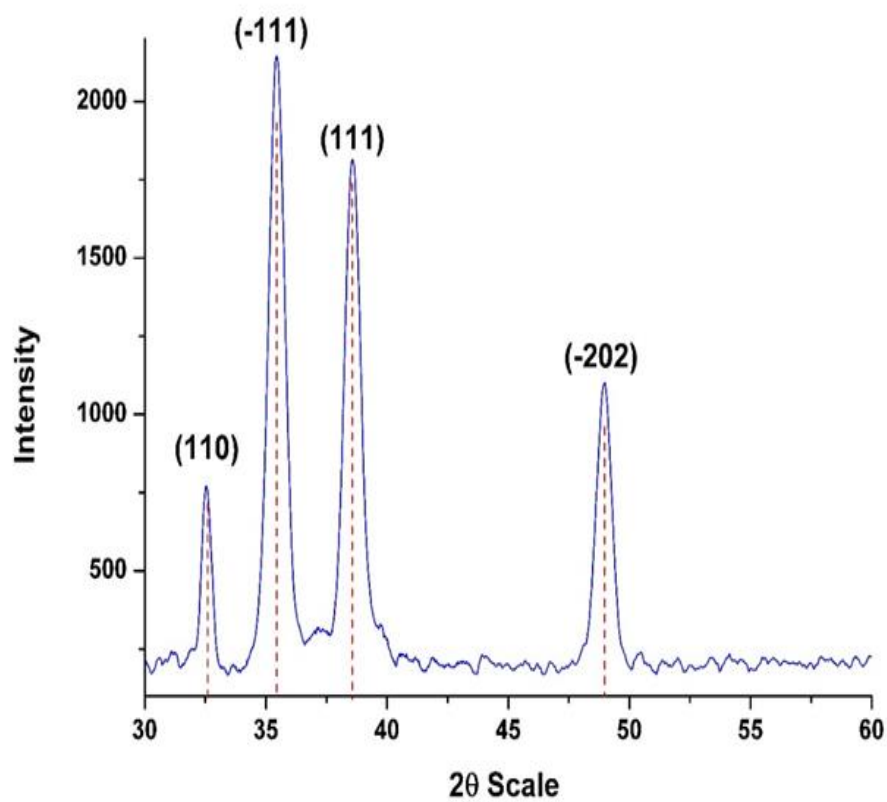
Figure 3.11: XRD pattern measured for ITO-CuO NS.

3.3. FTIR ANALYSIS

FTIR analysis was carried for all the synthesized nanostructures to understand the surface functionalization of synthesized material.

3.3.1. FTIR analysis for CuO nanostructures functionalized utilizing NAC, AD, and CA as controlling agent.

In order to check the functionality of all fabricated nanomaterial, the FTIR study was carried out. As shown in Figure 3.12, the registered FTIR spectra were assessed by way of comparison the FTIR spectrum of pure template.
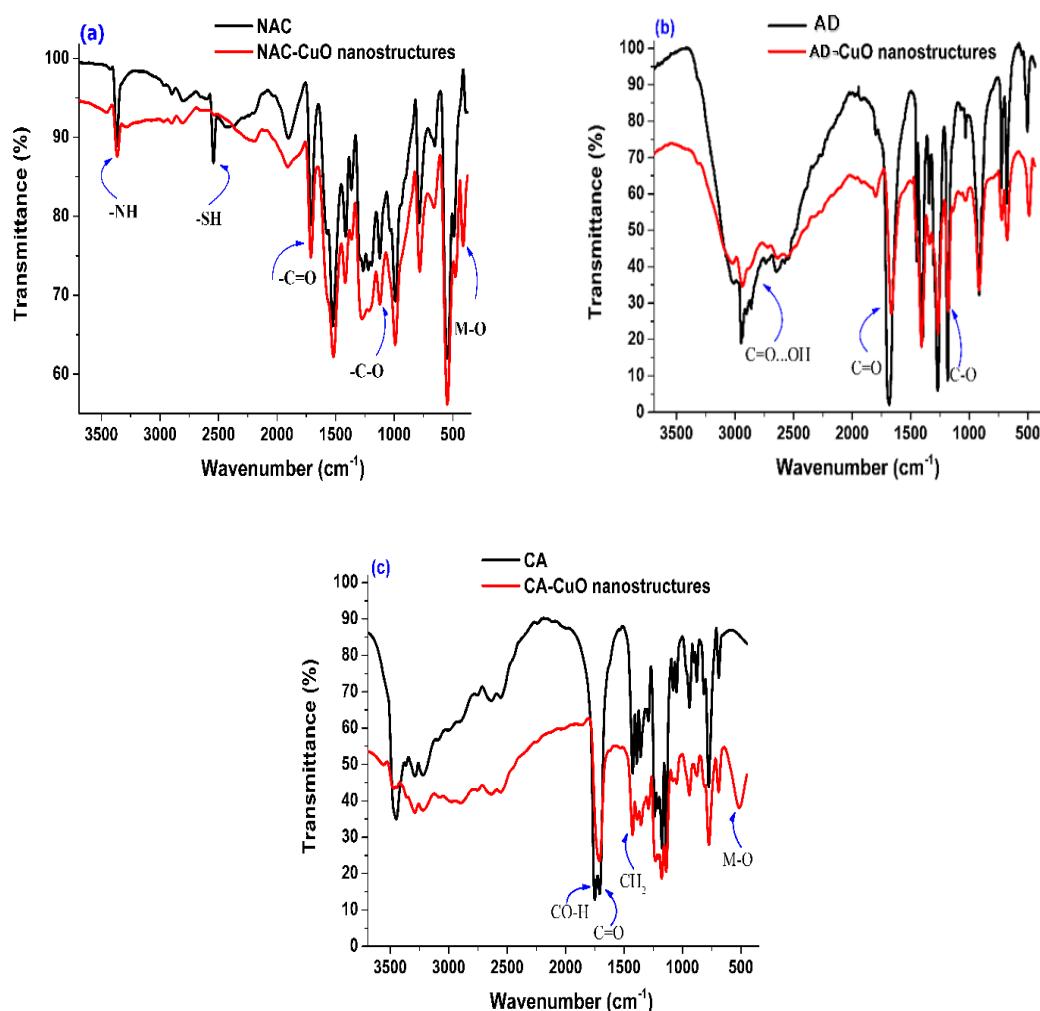
Figure 3.12: FTIR spectra of CuO nanostructures functionalized utilizing NAC, AD and CA as controlling agent .

3.3.2. FTIR analysis for the fabricated ITO based working electrode using succinic acid as directing agent

The FTIR analysis of the synthesised material was carried in accordance to pure template material. Figure 3.13 shows the overlay FTIR spectra.
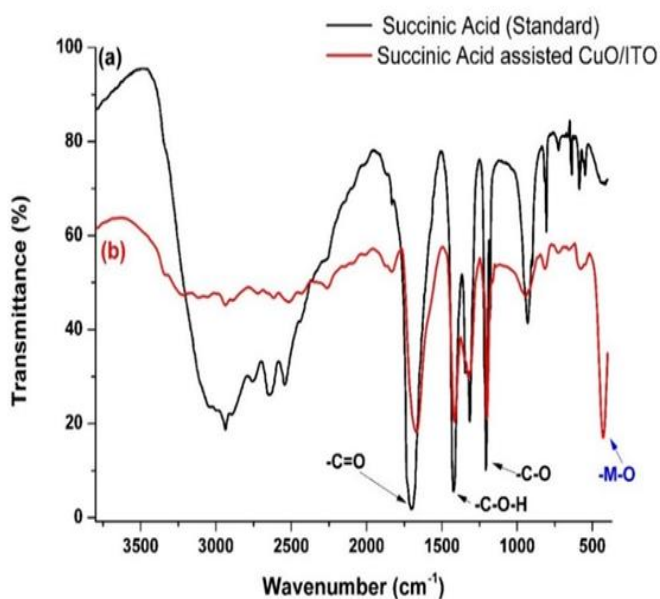
Figure 3.13: FTIR spectra of the fabricated ITO based working electrode using succinic acid as directing agent.

3.4. EDX ANALYSIS

EDX analysis was conducted so as to make sure that fabricated materials have no external impurities.

3.4.1. EDX analysis for the fabricated ITO based working electrode using succinic acid as directing agent

Figure 3.14 depicts the EDX pattern with elemental composition for further confirmation of material's purity.
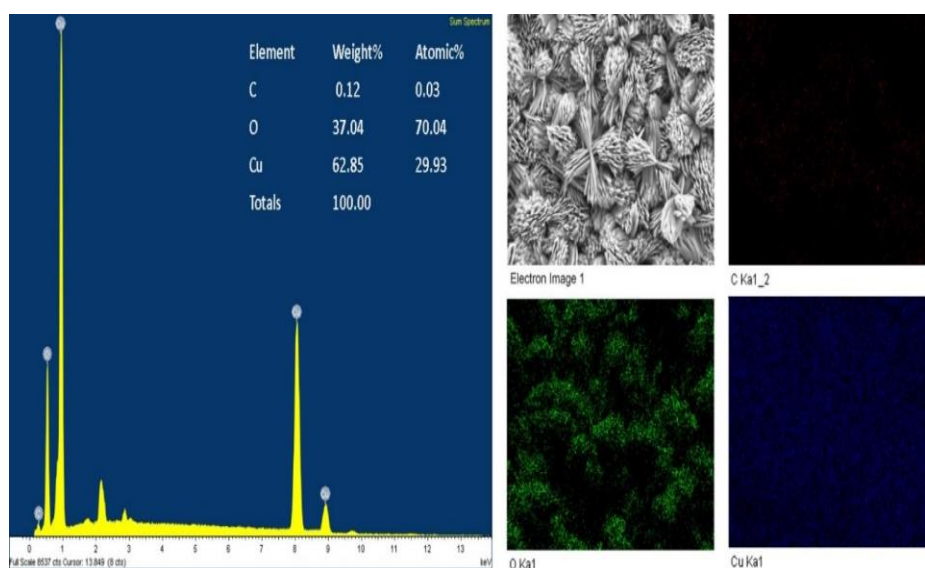
Figure 3.14: The EDX analysis with elemental mapping of in-situ grown CuO nanostructures.

3.4.2. EDX analysis for the fabricated ITO based working electrode using malonic acid as directing agent

Figure 3.15 shows the EDX pattern with elemental composition map for the as-synthesised material.
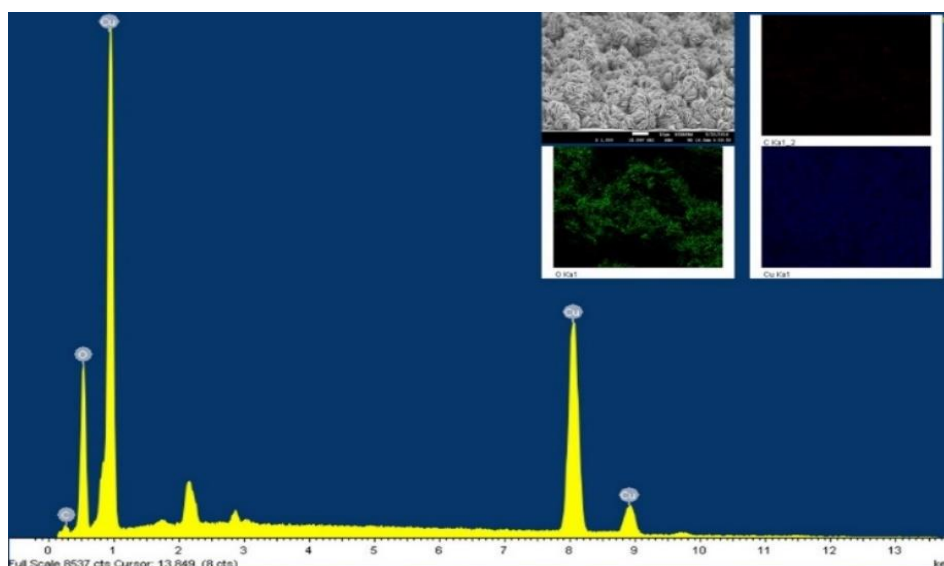
Figure 3.15: The EDX analysis with elemental mapping of in-situ grown CuO nanostructures.

3.5. THE ELECTROCHEMICAL STUDIES

The electrochemical assessment was performed using bipotentiostat Gamry Instruments (Reference 3000) (USA) housed with three electrode systems. In a typical electrochemical experiment, the Ag/AgCl was taken as reference and Pt wire as counter electrode respectively, whereas both modified GCEs and devised ITO based electrodes, separately, was recognized as efficient working electrode. The electrodes then were utilized for the electrochemical determination of some important clinical molecules such as N-acetyl cysteine, Nalbuphine hydrochloride and Captopril.

4. DISCUSSION

In this innovative research work we explore the new biosensors systems to evaluate the biological molecules. For ample of these biosensors was done through electrochemical techniques that offer the precious redox phenomena which are provide the vital evidence allied to the mechanism of reaction, concentration, kinetics and chemical status of the nanobiosensors. In order to analyze architect nanobiosensors chronoamperometry, cyclic voltammetry and differential pulse voltammetry has distinct advantages over other techniques. These electrochemical techniques are especially effective to achieve low detection limits, sensitivity, accuracy, reduce operation time, consume less amount of hazardous chemicals and they are green for environment.

4.1. HIGHLY SENSITIVE SHAPE DEPENDENT CUO NANOSTRUCTURES FOR THE DETECTION OF NAC
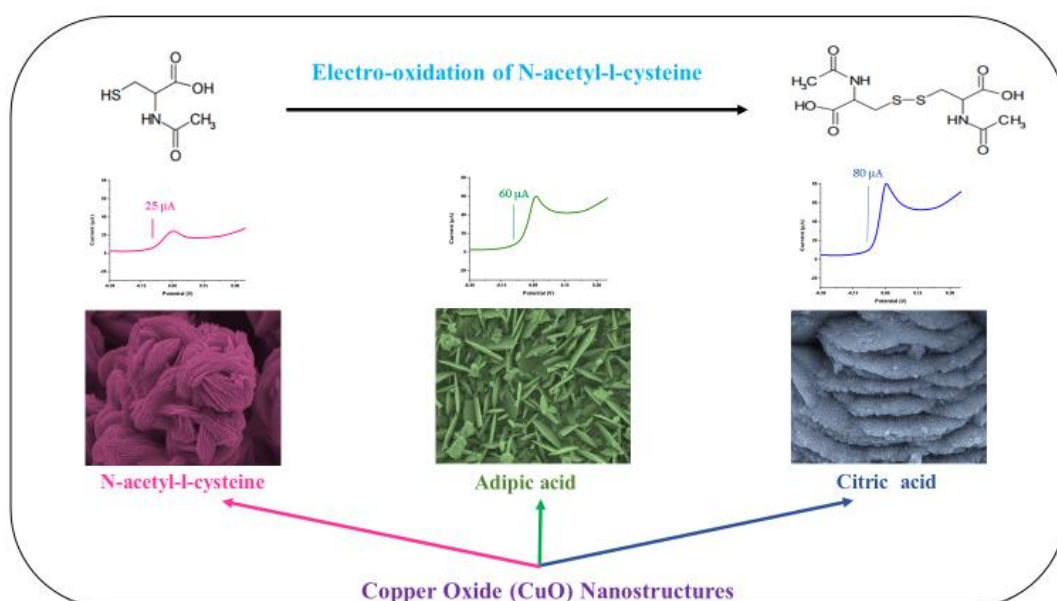
Figure 4.1: Schematic diagram representing the electro-catalytic oxidation N-acetyl-L cysteine over GCE modified with NAC, Adipic acid, citric acid functionalized CuO nanostructures.

4.1.1. The morphological and structural features of the fabricated CuO nanostructures

The analysis of HR-SEM and XRD were conducted to obtain the morphological and structural characteristics of the synthesized materials. The SEM patterns of as-synthesized material utilizing NAC, citric acid (CA) and adipic acid(AD) as an efficient template are shown in Figure3.1 respectively. As seen in Figure 3.1, the above-mentioned modifiers have been successful for directing and controlling the dimension resulting in formation of distinct morphologies. The Figure 3.1 (a-c) represents the HR-SEM patterns for CuO nanostructures utilizing NAC as modifier, the structure exhibits morphological features similar to interlaced disc like geometries with an outlook of sphere. The average thickness of each pattern was determined to be in range of 25-40 nm. The Figure 3.1(d-f) shows the nanostructures of CuO using adipic acid as modifier, the materials exhibits structural features similar to individual flakes distributed as grass with average width in range of 20-30 nm. Interestingly, the using of citric acid as modifier (Figure 3.1 (g-i)) led up to the development of bulky spheres consisting of layers made of tiny nanoparticles (10-20 nm). As seen each layer has a certain distance in-between them. Such porous material enables superior porosity for different processing e.g. catalysis and adsorption. Moreover; the CuO was grown in the absence of templates in alike experimental procedures, so as to verify the crucial role of the utilized modifiers as effective growth directing/controlling agents. As foreseen, the gained product had no a certain structure and morphological uniformity comparing to the other templates. Figure 3.2 depicts the HR-SEM images of the fabricated CuO.

Figure 3.8 presents the XRD peaks for the fabricated nanostructures. The XRD data reflects the fabrication of pure CuO nanomaterial with monoclinic phase as standarized against JCPDS Card No. 48-1548 [71]. As observed, the use of template has drastically effected the crystallinity of the product[72].

4.1.2. The Surface functionality analysis (FTIR)

The FTIR analysis carried demonstrated the surface bound functionality of all the fabricated CuO nanostructures. As shown in Figure 3.12, the registered FTIR spectra were assessed by a competative manner . Figure 3.12 (a) presents the FTIR spectra for pure NAC and NAC assisted CuO. The vanishing characteristic band near 2500 cm^{-1} indicates that the surface modification was throughout the thiol (-SH) group of NAC. Furthermore, alterating in the registred frequencies for the characteristics bands for v(N–H) and v^b(N–H) from 3370 to 3360 and 1525 to 1519 cm^{-1} respectively also propose, the participation of the -N–H group in the active interaction [73].Moreover, the –COOH functional group of NAC was observed not to contribute in the interaction as clear from unaltered frequencies nearly to 1709, 1124 attributed to C=O and C-O bands of carboxyl functionality. The existence of metal-oxygen band around 400 cm^{-1} further indicate the presence of CuO [74].Figure 3.12(b) show the FTIR spectra of pure adipic acid and adipic acid modified CuO. Considering adipic acid as di-carboxylic acid, a small alteration was anticipated in the corresponding frequencies of COOH [75].The main alteration of C = O from 1701 to 1677 cm^{-1} with decreased intensity denotes the interaction of AD with CuO via carbonyl portion. Similar alterations noted for C-O at about 1196 with decreased broad band close to 2500-3000 cm^{-1} referred to the inter-hydrogen bonds between the molecules (C-OH ... O = C). Figure 3.12(c) show the FTIR spectra of pure citric acid and citric acid modified CuO. Like adipic acid, the main shifts of C = O and C-OH were observed with a lower intensity in comparision to pure citric acid while the M-O band was noted at about 400cm^{-1} [76].

4.1.3. The sensing assessment of the developed electrode

The recorded CV profile of each of the modified GCE compared to bare GCE is depicted in Figure 4.2 (a). The responses were measured with 20 µm of NAC in existence of 0.1 M PBS (PH 6). As observed the bare electrode failed to produce any significant response were as the modified electrode proved substantially active for the elector-oxidation of NAC. In comparison, the CuO-CA/GCE produced high current intensity with less anodic potential (1.0 mV). This exquisite characteristic can be ascribed as an integrated consequence of the large surface area of the CuO nanostructure and the preferable interaction between hydroxyl portion of NAC and carbonyl group of the critic acid. This integration provides a higher signal sensitivity even at negligible quantity of the molecule of interest as Soomro et al reported in the case of

pesticides[24].Scanning rate measurements for all modified electrodes were also registered in a range of 50 to 100 mVs^{-1}.

Figure 4.3 exhibits the scan rate measurements where the maximum current intensity was plotted against the square root estimated for scan rate. The observed linear proportionality is evident of the process to be diffusion controlled. The Tafel slopes were obtained from the linear portion of CV as shown in (Figure 4.2 (b-d)). The α values were calculated as 0.61, 0.54 and 0.41 for CuO -CA/GCE, CuO-AD/GCE and CuO-NAC/GCE respectively. The greater value of charge transfer (α) with promoted current intensity noted for CA based electrode is indicative of higher kinetic favorability of the electrode[29].

The reaction of electro-oxidation can be interpreted as follows: generally, the production of Cu (II) is accompanied with the anodic current which was because of NAC empowers its oxidation to disulfide linkage in combination to the creation of Cu (I) at opposite scan as proposed by the incoming equations:

$$\textbf{Ncys} - \textbf{SH} + \textbf{2CuO} + \textbf{2e} \rightarrow \textbf{H}_2\textbf{O} + \textbf{Ncys} - \textbf{sycN} + \textbf{Cu}_2\textbf{O} \qquad\qquad (4\text{-}1)$$

$$\textbf{Cu}_2\textbf{O} + \textbf{H}_2\textbf{O} \rightarrow \textbf{2CuO} + \textbf{2e} + \textbf{2H}^+ \qquad\qquad (4\text{-}2)$$

In spite of the sensing of NAC utilizing electrodes is well-investigated nevertheless, the condition of using citric acid capped CuO empowers comparatively higher signal intensity which might be ascribed to the ideal connection between the hydroxyl portion of surface bound citric acid and – NH and - COOH group of NAC. In cases of other electrodes, the size of functionalizing agent and the morphology may be considered responsible for weaker signal.
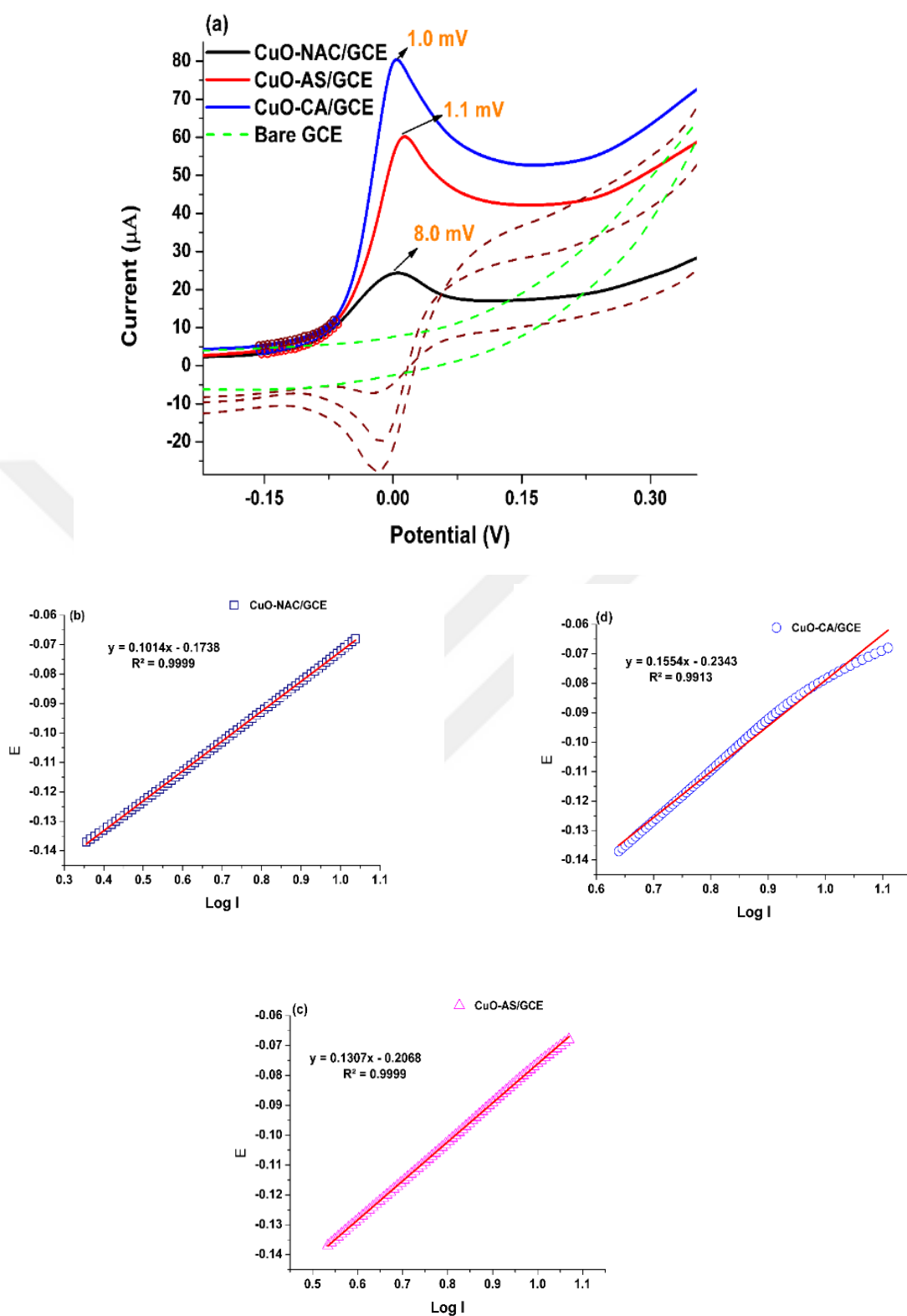
Figure 4.2: (a) CV profile of the modified electrodes GCEs along with corresponding Tafel Plots (b) CuO-NAC/GCE (c) CuO-AD/GCE and (d) CuO-CA/GCE.
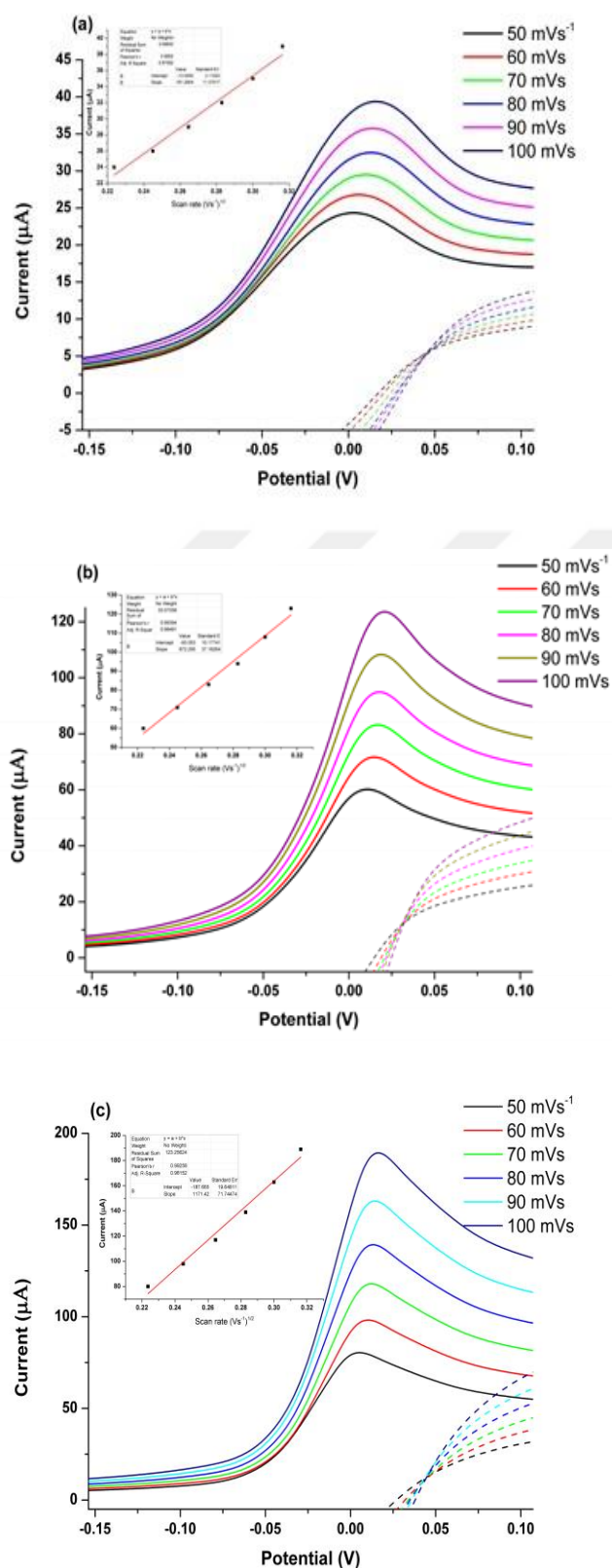
Figure 4.3: Scan rate measurement recorded for with NAC, AC, CA assisted CuO nanostructures modified GCE in range of 50 to 100 mVs^{-1}.

4.1.4. The chronoamperometric measurement

Since, the electro-oxidation of NAC over the modified electrodes is a diffusion controlled process, chronoamperometric measurements were conducted to estimate the diffusion co-efficient (D) value. Figure 4.4(a) exhibits the recorded Chronoamperometric measurements for only CuO-CA/GCE in concentratoin ranging from 0.1 to 0.9 mM. After that, the registred reading were estimation of the diffusion coefficient (D) as per the Cottrell equation [28]. The plot of current, best fitted against time ($t^{-1/2}$) is shown in Figure 4.4(b) while the slopes are plotted against concentration of NAC as depicted in Figure 4.4(c)., whereby the final slope value is utilized to estimated D using the incoming modified formula of Cottrell equation:

$$I = nFAD^{1/2} \, C_b \, \pi^{-1/2} \, t^{-1/2} \qquad (4\text{-}3)$$

$$D = \left[\frac{m}{nFA \, C_b \, \pi^{-1/2}} \right] \qquad (4\text{-}4)$$

Where m is the slope from Figure 4.4 (c), C_b is the NAC concentration , A is the active area of electrode (0.07 cm^2), n, F and π possess their regular meanings. The value of D for CuO-CA/GCE was 6.059 $\times 10^{-4}$ cm^2/s. The acquired D measurement for CuO-CA/GCE are considerably larger than showin in (Table 4.1).
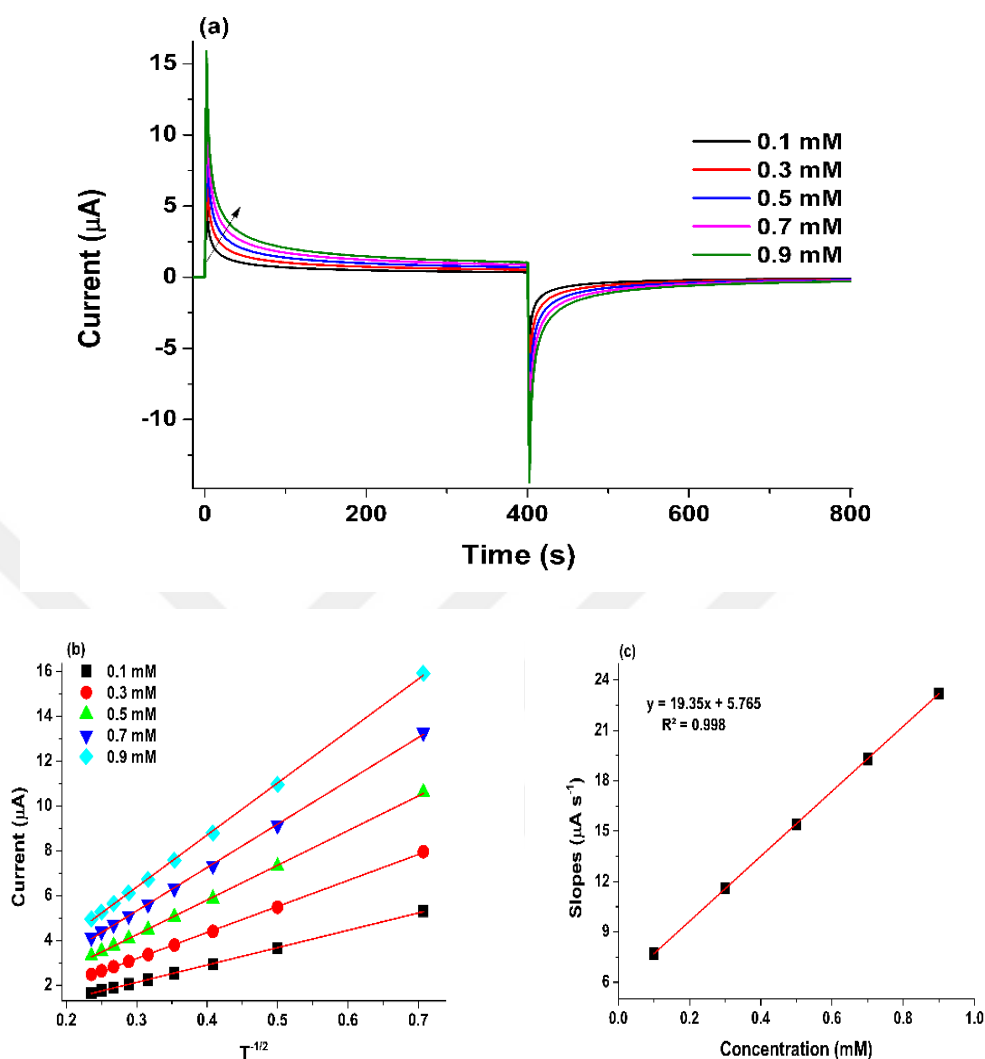
Figure 4.4: Chronoamperometric characteristics of CuO-CA/GCE against NAC in concentration range of 0.1 to 0.9 mM with inset graphs reflecting linear fit analysis for current v/s $t^{-1/2}$ and their corresponding slopes against the utilised concentration of NAC respectively.

4.1.5. The optimization of the modified electrode

Critical metrics were optimized to guarantee the maximum current for the sensor. These include: catalyst deposition volume, pH and accumulation time for measurement. The impact of pH over electrochemical oxidation of NAC was taken from 2 to 10. Figure 4.5 (a) the most current intensity value was registered at pH value of 6. The decrease in the current at higher pH values can be attributed to the production of Cu(II) hydroxide upon the surface of CuO [77]. The difference in the current against deposition volume of catalyst was also examined in

concentration ranging from of 2 to 5 µL. The Figure 4.5 (b) shows a decrease in current was registered at higher volumes that might be the outcome of catalyst disrobing from the surface of GCE owing to its discrepancy with used volume of Nafion®. The accumulation time was examined within a range of 0-360 seconds under constant conditions. Figure 4.5 (c) shows an increase in the density of current up to 240 s of accumulation time. After that, the current intensity was observed to be stable indicating the attainment of the saturation point.
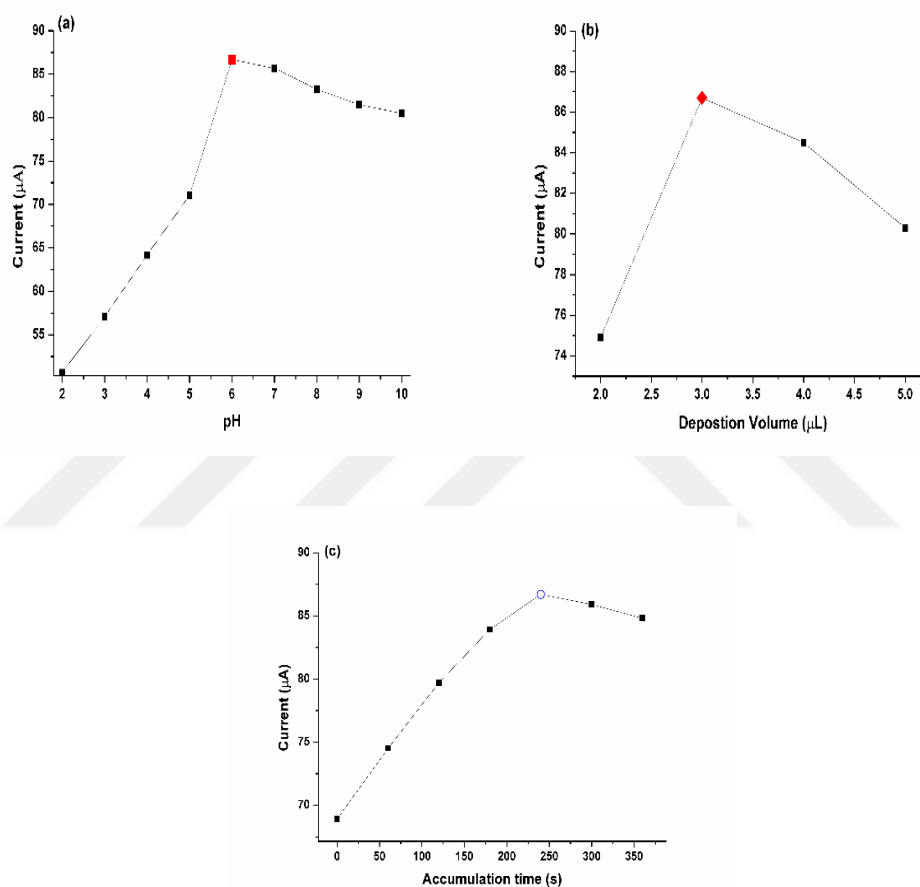
Figure 4.5: Variation in current response for CuO-CA/GCE under different experimental condition (a) PBS buffer system pH   (b) deposition volume of CA assisted CuO nanostructures on the GCE and (c) accumulation time.

4.1.6. Sensing of NAC using DPV

The DPV for NAC was recorded in range of 0.1 to 5.5 µm. Figure 4.6(a) shows the registered DPV waves for the aforesaid concentration range whereas Figure 4.6(b) shows the calibration with linear fit analysis. The LOD and LOQ were calculated to be 0.01 and 0.15 µM (S/N=3) respectively. The acquired analytical features were contrasted with different electrode-based system that was used before to determine NAC. Table 4.1 presents the collected data. As clear, the modified electrode owns better analytical features in terms of electro-oxidation potential and limit of detection value.
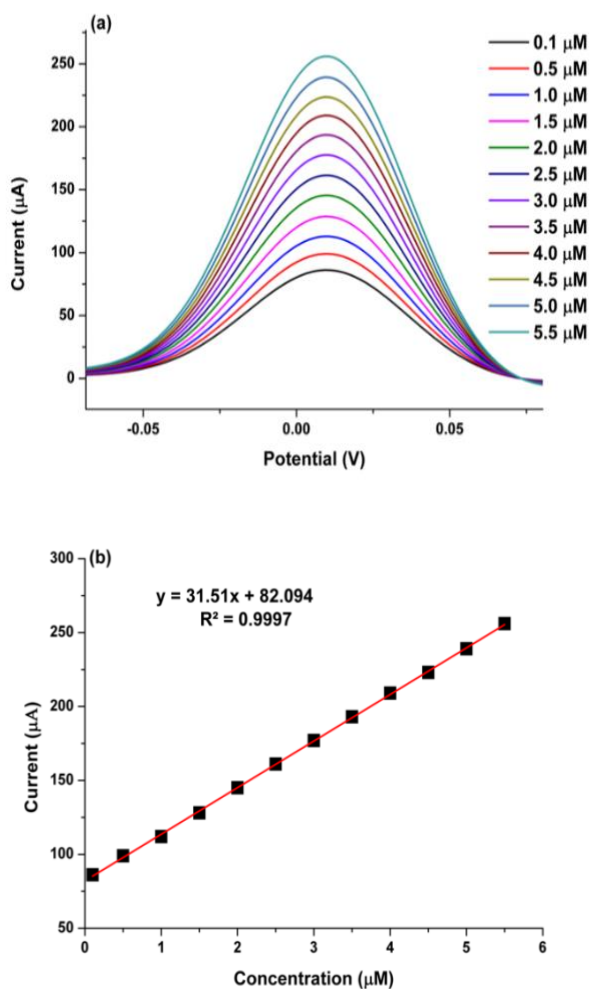
Figure 4.6: The DPV response recorded for the modified electrode against NAC and (b) the corresponding calibration plot.

Table 4.1: Comparison of CuO-CA/GCE based electrochemical sensor with other sensor system utilising for quantification of NAC.

Electrode	Modifier	pH	Oxidation Potential (mV)	LOD (M)	LDR (M)	Electron transfer Coefficient (D)	Diffusion Coefficient cm^2.s^{-1}	Reference
Graphite Paste Electrode	Si Cu NP	7	760	4.18×10^{-5}	9.9×10^{-5}-8.4×10^{-4}	-	-	[78]
Glassy Carbon Electrode	BFT-CNTs	8	330	6.2×10^{-8}	1.0×10^{-7} - 6.0×10^{-4}	0.6	3.5×10^{-5}	[28]
Carbon Paste Electrode	DMBQ-Pt-CNTS	7	250	7.0×10^{-8}	1.0×10^{-7}-6.0×10^{-4}	0.4	7.88×10^{-5}	[79]
Carbon Paste Electrode	2CBF	7	665	2.6×10^{-8}	5.0×10^{-8} - 4.0×10^{-4}	0.47	6.8×10^{-5}	[64]
Glassy Carbon Electrode	**CuO-CA**	**6**	**1.0**	$\mathbf{1 \times 10^{-8}}$	$\mathbf{1.0 \times 10^{-7}}$ - $\mathbf{5.5 \times 10^{-6}}$	**0.61**	$\mathbf{6.059 \times 10^{-4}}$	**This Work**

4.1.7. The selectivity and stability of the developed electrode

The selectivity of the developed electrode was measured for interfering species which are usually exist with NAC within biological fluids. The measurment was performed to determine NAC (0.1 μM) in the existance of interfering species like fructose, glucose, cysteine, glutathione, Ca^{2+}, Al^{3+}, Mg^{2+},Cl^-,F^- and CO_3^{-2} with a concentration ten folds larger than NAC. Figure 4.7 (a) clealry reflects trivial variation in the recorded current. The stability of the modified electrode was ascertained by measuring 100 cycles of CuO-CA/GCE in 0.1 μM of NAC within 0.1 M PBS (pH 6.0) as seen in Figure 4.7 (b). The small change is indicative of the electrode stability and reproducibility.
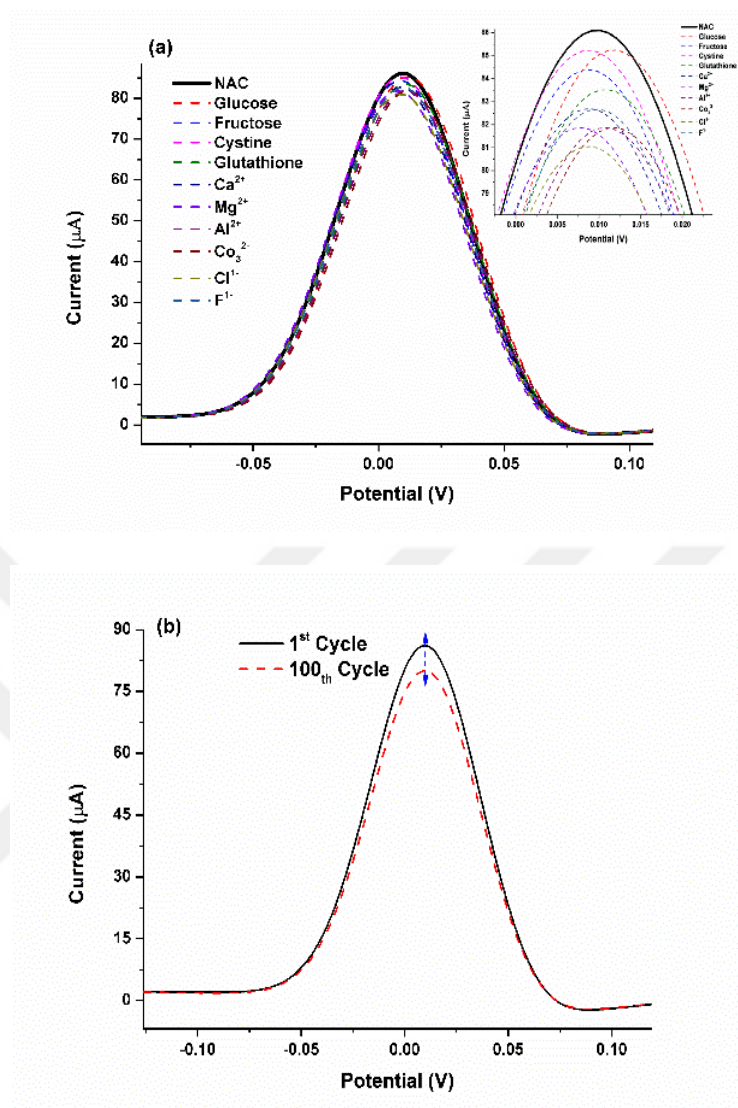
Figure 4.7: The selectivity of CA-CuO/GCE towards NAC in the presence of common interferents with 10 folds higher concentration and (b) the stability of the electrode response after 100 cycles recorded in 0.1 μM NAC with 0.1 M PBS (pH 6).

4.2. THE GROWTH OF NIO, CUO, CO3O4 NANOSTRUCTURES WITH THE ASISTANCE OF ACETYLSALICYLIC ACID AND THEIR UTILIZATION AS EFFICIENT ELECTRODE MATERIAL FOR THE EVALUTATION OF NALBUPHINE HYDROCHLORIDE
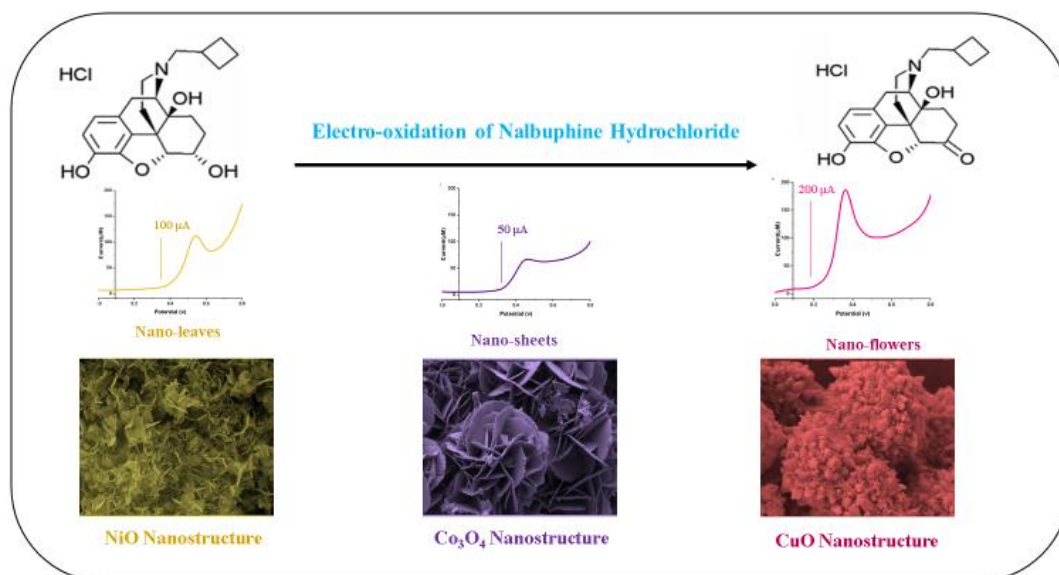
Figure 4.8: Schematic diagram representing the electro-catalytic oxidation of NP over GCE modified with ASA assisted metal oxide nanostructures.

4.2.1. The characterization of acetylsalicylic acid assisted metal oxide nanostructures

To evaluate the morphological characteristics of the synthesized nanostructures (NiO, Co_3O_4, and CuO) using acetylsalicylic acid as an effective growth modifier, the FE-SEM was conducted out. The FE-SEM images for NiO nanostructures is shown in Figure 3.3 (a-c). The material exhibits morphological features comparable to thin sheets resembling scattered leaves. The size of these sheets were estimated to be 2-10 nm $\pm$ 1.2 nm. This is proof that the as-synthesized nanosheets are nicely distributed and exempt from growth aggregation. The Figure 3.3 (d-f) shows the FE-SEM images of Co_3O_4 nanostructures which exhibit morphological features comparable to flowers with wide petals and helical pattern. It is interesting that, the ASA have facilitated quite different growth path for Co_3O_4 compared to NiO nanostructures. Such variation in the morphological structure can be attribute to the difference between the non-covalent interaction between the metal (Ni, Co and Cu) and the modifier. These interaction permit nuclei crystallization along the modifier molecule

encouraging distinct clustering and re-arrangements patterns to achieve prominent morphologies. The helicity in case of nanoflowers might be associated with the chirality of the modifier in the system. The average thickness of the petal was estimated in the range of 10-15 nm ±1.4 nm. The FE-SEM images for CuO nanostructures is shown in Figure 3.3 (g-i). the material exhibits completely different morphology. Despite that the synthesized nanostructures possess spherical shape nevertheless; each sphere consists of tiny spines which are hollow in nature and composed of thin wire-like structural features. The average size of each spine was estimated in the range of 10-25 nm ±1.1nm while, each wire-like feature had an average width of 5 nm.

Figure 3.9 shows the XRD data for the as-synthesized metal oxide nanostructures. The XRD pattern for NiO consists of major peaks indexed to (200), (220), (311) while for Co3O4 for (111), (220), (311) (222), (400), (422), (511) and (400) crystal planes were noted. The observed peaks are consistent with pure face-centered cubic (FCC) as referenced against ICDD card 71-1179 and 42-1467 respectively [80][81] [44]. The XRD pattern for CuO involve major peaks indexed to (-110) (002) (111) (-200), (-202), (020), (202), (-113), (311), (-220), (311), (004) and (-222) planes of pure monoclinic phase as standardized against ICDD No: 45-0937[45]. As is clear from the XRD patterns, that the as-synthesized nanostructures own distinguished crystallinity. This difference in structural crystallinity can be attribute to the deviation in the texture/morphology of the as-synthesized nanostructure [45].

4.2.2. Electrochemical oxidation of NP at metal oxide nanostructures modified GCEs

The electrochemical behavior of modified electrodes against NP ($0.001\mu M$) was studied using cyclic voltammetry as the basic investigation mode. The CV for NiO/GCE, Co_3O_4/GCE and CuO/GCE in GCEs in comparison to bare and GCE modified with Nafion is shown in Figure 4.9. As noted, the modified electrodes demonstrate diverse electrochemical features towards NP and also in each case the shape of CV peak is distinct. The lower-peak potential with maximum current intensity observed for CuO/GCE in comparsion to its other counterparts. This noted electro-catalytic features may be ascribed to the distinctive morphological characteristics of CuO nanostructures. these materials with their higher active surface area and largely exposed structural features (spikes) might have simplified the electron transfer kinetics and electrochemical reactivity during electro-catalytic oxidation of NP. Tafel plots were obtained from the rising portion of the CV profiles to estimate the electron transfer

co-efficient for all the modified electrodes (Figure 4.10). The α values were calculated to be 0.69, 0.63 and 0.73 for NiO/GCE, Co_3O_4/GCE and CuO/GCE respectively. The active surface area for the modified electrodes was calculated from the CV profiles of each modified electrode measured in $K_3[Fe(CN)_6]$ (1.0 mM) against scan rate in range of 50-120 $mV.s^{-1}$ (Figure 4.11). The slopes obtained from the graphs plotted between anodic peak current verses the square root of scan rate was considered for active area using the following Randles-Sevcik equation:

$$I_p = 0.4463 n^{3/2} F^{3/2} AC (v D/RT)^{1/2} \tag{4-5}$$

where I is the current, A is the active area of modified electrode, C is the concentration of $K_3[Fe(CN)_6]$, D is the diffusion co-efficient (0.76×10^{-5} $cm^2.s^{-1}$) and the symbol F, R, v,n, T possess their regular meanings. The active areas values were calculated as 0.044, 0.101 and 0.232 cm^2 for the NiO/GCE, Co_3O_4/GCE and CuO/GCE respectively . Interestingly, CuO nanostructures was observed to possess higher greater surface area (0.232 cm^2) although their large size of (10-20 nm), this can be ascribed to the hollow/cavity based structural features which allows greater electrochemical responses based on higher surface area provided by the internal hollow structural features of the CuO nanostructures. Furthermore, these nanostructures give preferable analyte diffusion which can positively affect the electron-transfer kinetics of the reaction under investigation.
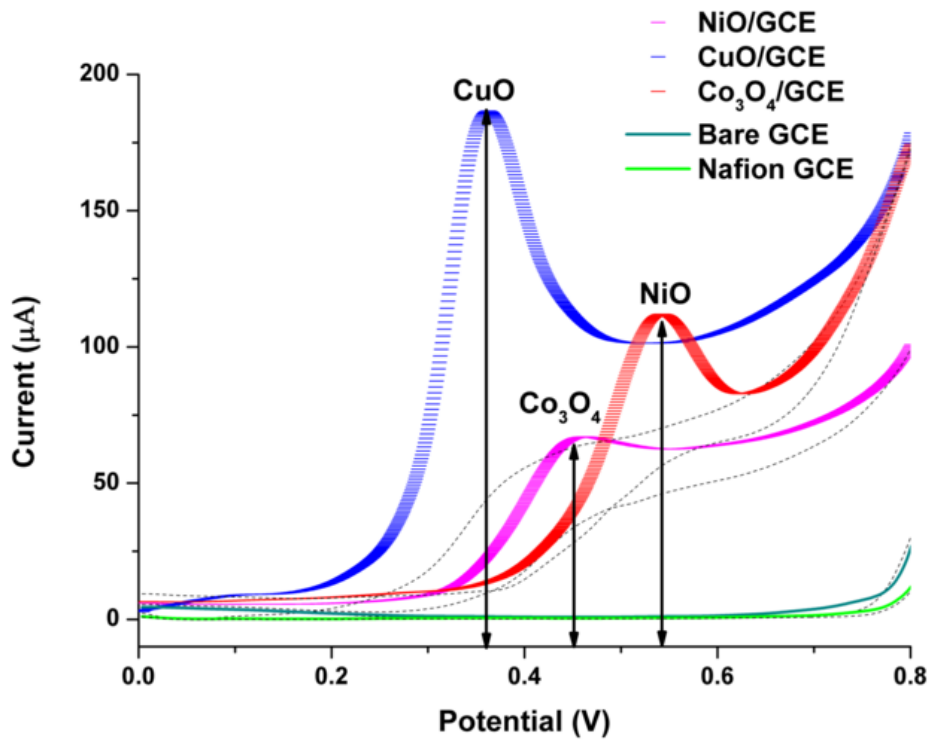
Figure 4.9: CV characteristics of electrodes modified with ASA assisted metal oxide nanostructures measured against 0.001 μM NP in BRB (0.1 M pH 7.0) in reference to bare and Nafion modified GCEs.
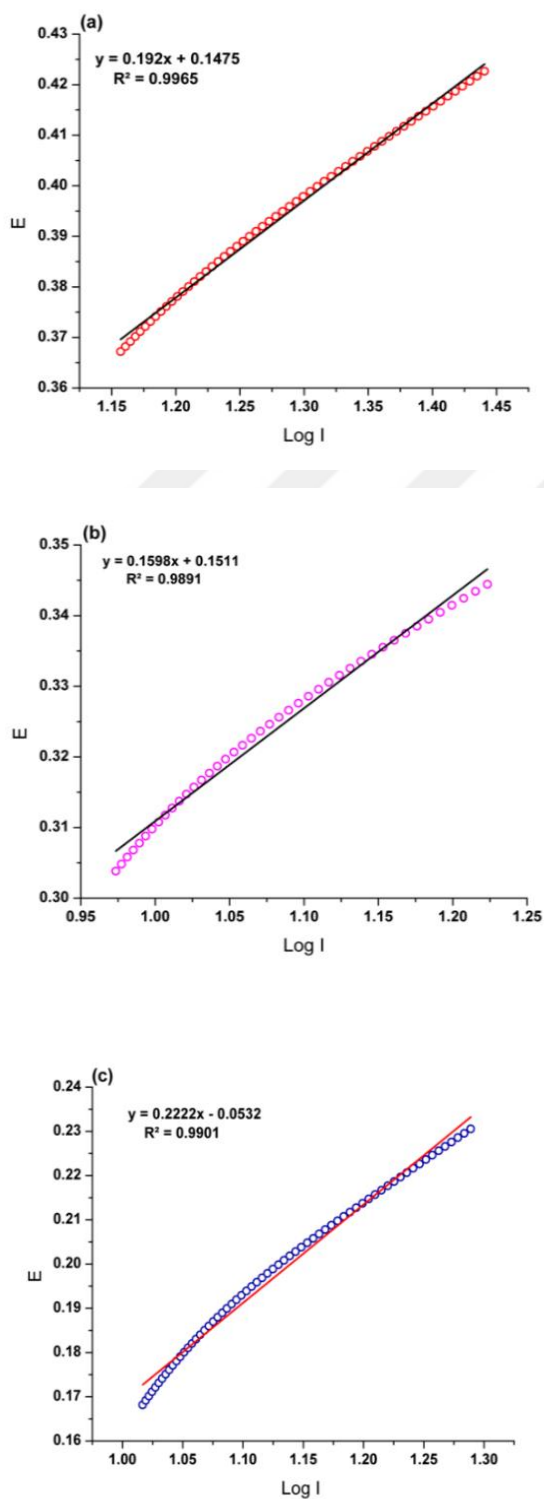
Figure 4.10: Tafel slopes plotted for (a) NiO/GCE, (b) Co_3O_4/GCE and (c) CuO/GCE against 0.001µM of NP with 0.1 M BRB (pH 7.0).
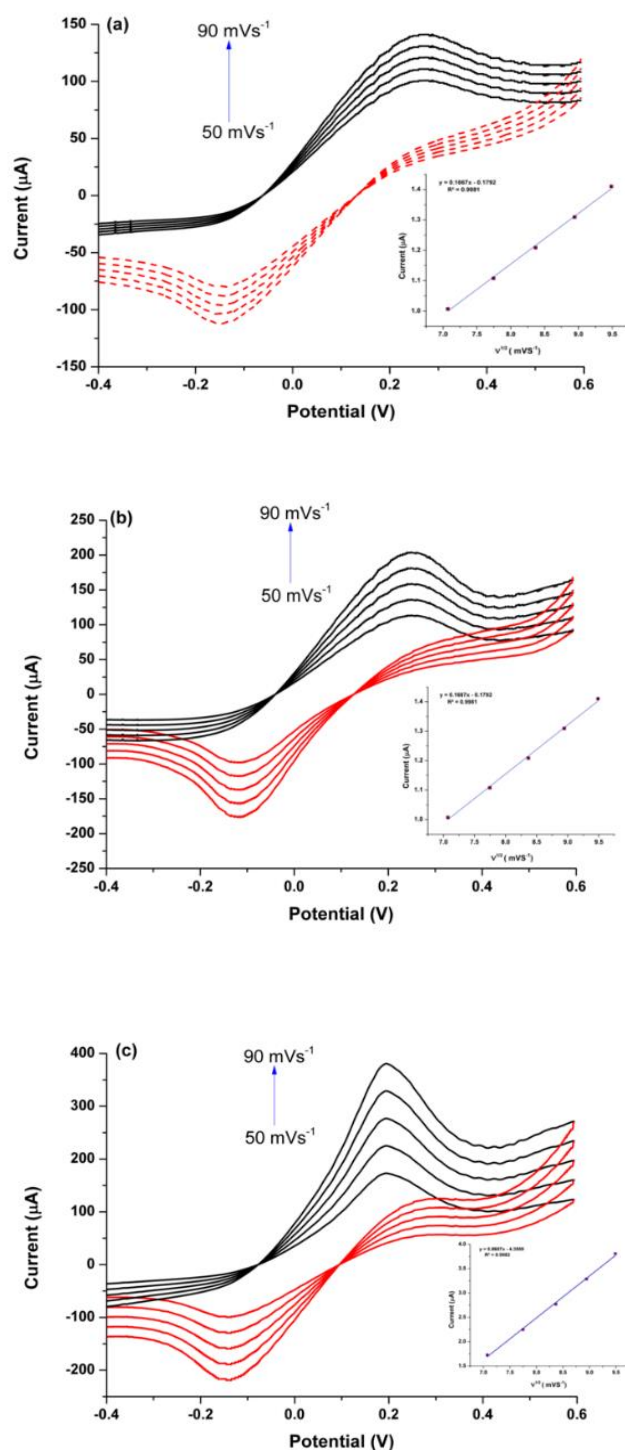
Figure 4.11: CV profiles measured in $K_3[Fe(CN)_6]$ (1.0 mM) against scan rate ranging from 50-120 mV.s^{-1} for (a) NiO/GCE, (b) Co_3O_4/GCE and (c) CuO/GCE with inset figure reflecting the corresponding plots of square root of scan rate v/s current density.

Figure 4.12 exhibits a general schematic representation of NP oxidation over CuO/GCE. The electrochemical oxidation begins through Cu (II)/(I) redox couple. The Cu (II) ions are generated during the anodic sweep which led to the electro-oxidation of NP molecules at the surface of CuO/GCE. After that, the transferred electrons generate a large anodic peak current and in the meantime reducing the Cu (II) to Cu (I) which can again oxidize under the anodic sweep. In this way, the redox cycle of Cu (II)/ (I) continues to electrochemical oxidize NP molecules which its concentration is proportional to the generated current density.
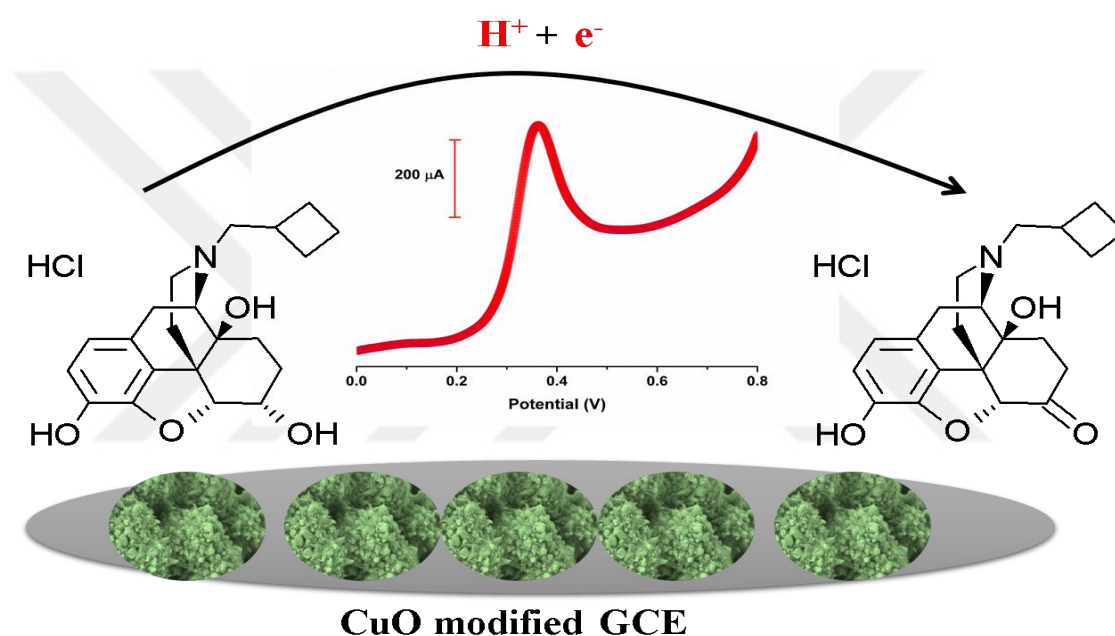
Figure 4.12: Schematic diagram representing the electro-catalytic oxidation of NP over GCE modified with ASA assisted CuO nanostructures.

4.2.3. Optimization of CuO/GCE for electrochemical assessment of Nalbuphine (NP)

Since the CuO/GCE exhibited the best electrochemical features compared to its competitors, the electrochemical performance of CuO/GCE was further processed by optimizing crucial experimental parameters such as scan rate and pH. The impact of scan rate on electrochemical oxidation of NP was studied by recording the CV responses of CuO/GCE against 0.001 µM NP solubilized in 0.1 M BRB (pH 7) solution in the scan range of 50 to 90 mV.s^{-1}. Figure 4.13 (a) exhibits the linear relationship between the square root of scan rate and current density

suggesting the noted catalytic electrochemical reaction to be diffusion controlled. For more details, the response of CuO/GCE was estimated in NP containing solution under open circuit potential condition (OPC) (figure 4.13 (b)). The CV measurements were conducted on after duration time of 100 s up to 600 s. The maximum increase in current density was attained after 500 s of free standing time, which allowed maximum accumulation of NP molecules on the electrode surface. Figure 4.13 (c) shows the impact of pH on the oxidation of NP in the range of 3 to 10. The maximum current density was recorded when the pH value was near 7. The change in the peak potential and shape with the variation of pH is evident of the variance in the reaction rate as the pH of the system is changed.
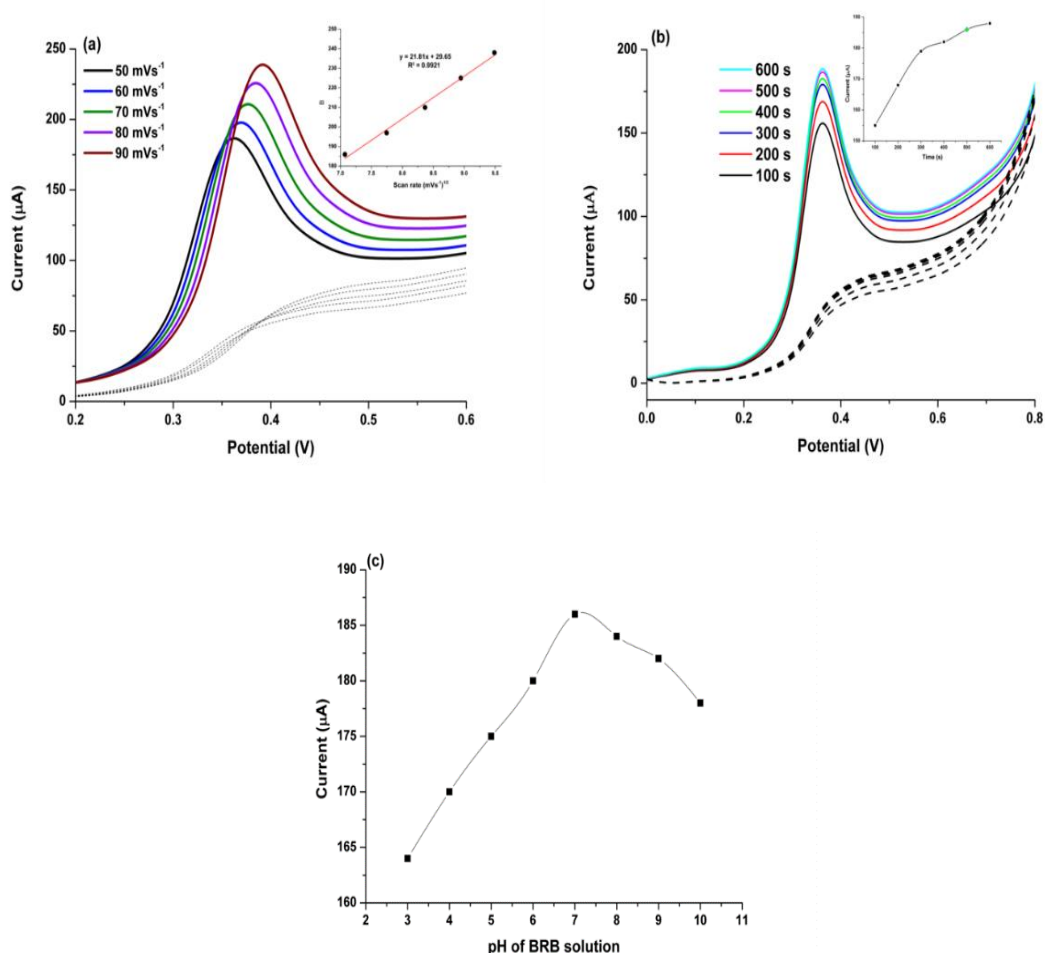
Figure 4.13: CV measurements carried for CuO/GCE for (a) variation of scan rate in concentration ranging from 50 to 90 mVs^{-1} with inset figure depicting graph of $\upsilon^{1/2}$ v/s current density, (b) increase in current density measured against accumulation time at open circuit potential in range of 100 to 600 s and (c) variation in measured current density against the pH of the NP containing solution.

4.2.4. The chronoamperometric measurements

The diffusion co-efficient (D) for the electro-catalytic oxidation of NP were estimated using chronoamperometric measurements. The measurements were obtained for NP in concentration ranging from 0.1 to 0.6 mM. The recorded chronoamperometric graph is shown in Figure 4.14. To obtain D value, the plot of current I, best fitted against time ($t^{-1/2}$) (Figure 4.14 (b)) while the obtained slopes are then plotted against the chosen concentration of NP (Figure 4.14 (c)). whereby the final slop values is utilized to estimated D utilizing the incoming modified formula of Cottrell equation [26]:

$$I = nFAD^{1/2} C_b \pi^{-1/2} t^{-1/2} \qquad (4\text{-}6)$$

$$D = \left[\frac{m}{nFA\, C_b\, \pi^{-1/2}}\right] \qquad (4\text{-}7)$$

Where m is the slope from Figure 4.14 (c), A is the area of electrode ($0.07\ cm^2$), Cb is the NP concentration of and F, π, n possess their regular meanings. The value of D was estimated to be $3.99 \times 10^{-3}\ cm^2/s$ which is much higher than lately reported for CuO based electrode [42].

The catalytic rate constant (k) for the electro-oxidation of NP at CuO/GCE was also derived from the chronoamperometry data using the modified form of Galus equation:

$$\frac{IC}{IL} = \gamma^{\frac{1}{2}} \pi^{\frac{1}{2}} ((k_h C_b t))^{1/2} \qquad (4\text{-}8)$$

Where I_c is the catalytic current at CuO/GCE in the presence of NP and I_L is the limiting current measured in the absence of NP (blank). while k_h, C_b and t denote the rate constant, concentration of NP and elapsed time respectively. The plot of Ic/I_L v/s $t^{1/2}$ against the used concentration of NP provides K_h value of $9.44 \times 10^3\ mol^{-1}Ls^{-1}$ (Figure 4.14 (d))
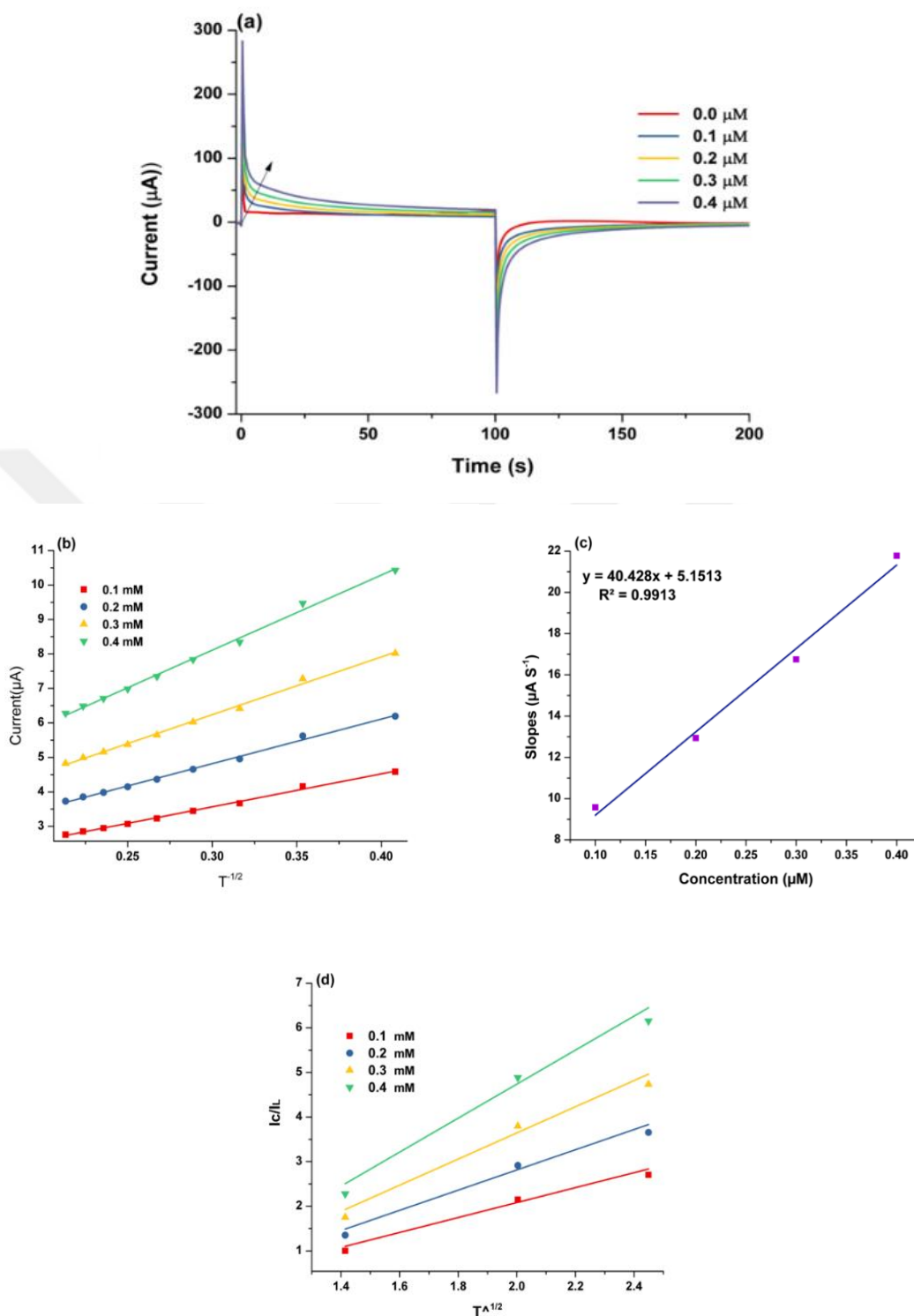
Figure 4.14: (a) Chronoamperometric characteristics of CuO/GCE against NP in concentration ranging from 0.1 to 0.4 mM (b) graph of current v/s $t^{-1/2}$, (c) plot of the corresponding slopes against the standard concentration of NP and (d) Linear fit analysis for the graphs plotted between I_c/I_L and $t^{-1/2}$ against NP.

4.2.5. Analytical quantification of NP

The sensing of NP ranging from 0.001 to 2.25 µM within 0.1M BRB (pH 7.0) utilizing DPV as a fundamental mode of measurement. Figure 4.15 (a) shows the registered DPV waves for the chosen concentration range. Figure 4.15 (b) shows the linear fit analysis of the corresponding calibration plot. The LOD and LOQ were calculated to be 1×10^{-4} and 0.06 µM respectively. The estimated characteristics are clearly reflecting the greater analytical ability of the developed sensor compared to the recent reported system proposed for quantification of NP (Table 4.2).
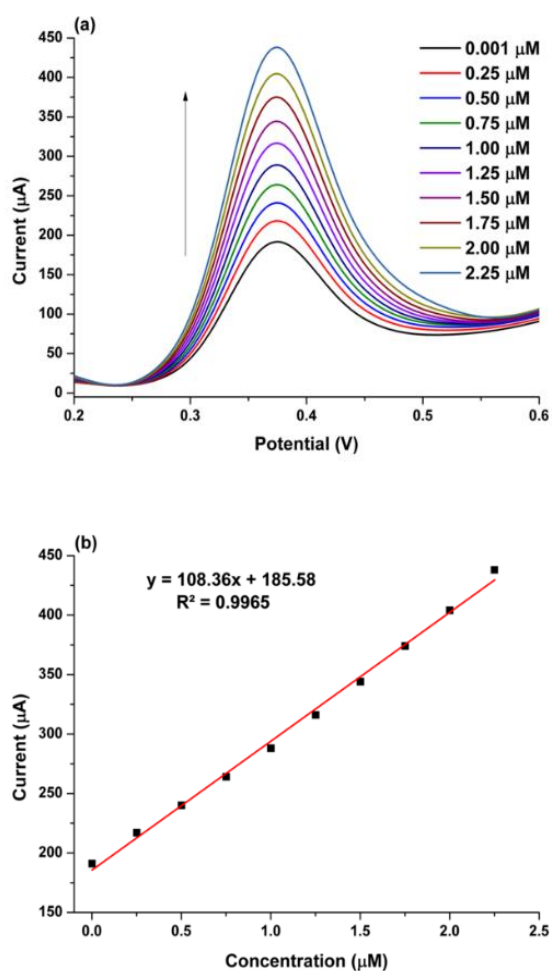
Figure 4.15: (a) The DPV waves measured for NP in the concentration range of 0.001 to 2.25 µM with 0.1 M BRB (pH 7.0) and (b) the corresponding calibration plot with linear fit analysis depicting the proposed sensor's linear working range.

Table 4.2: Comparison of proposed sensor system with other electrochemical methods for the quantification of NP.

Method	Electrodes	Sensing range (μmol L^{-1})	sensing limit (μmol L^{-1})	Reference
Voltammetry	Au NPs modified GCE	0.14 to 3.5	0.037	[41]
Voltammetry	IL/NiO/CNT/CPE	0.2 to 500.0	0.07	[42]
Voltammetry	Pencil Graphite electrodes	0.015 to 0.16	12.5	[33]
Voltammetry	**ASA-assisted CuO modified GCE**	**0.001 to 2.25**	**1×10^{-4}**	**This work**

NiO/functional single walled carbon nanotubes nanocomposite incorporated with ionic liquid (IL/NiO/CNT/CPE), gold nanoparticles (Au NPs).

4.2.6. Selectivity of CuO/GCE against interferents

To check the analytical feasibility of the proposed electrode, the selectivity of CuO/GCE towards NP was assessed in the presence of common co-existing pharmaceutical drugs and some chemical species such as: diclofenac sodium, N-acetyl cysteine, and captopril,glycine, glucose, l-cysteine, uric acid and folic acid. The neasurment was conducted for evaluation of NP (0.01 µM) in the existence of the mentioned interfering species with concentration 100 folds higher than NP. Figure 4.16 depicts the corresponding DPV responses. As noted, the response of CuO/GCE insignificantly has changed in the presence of interferents. Therefore, it is evident that the NP can be selectively oxidized at potential of 0.37 V using the proposed sensor system.
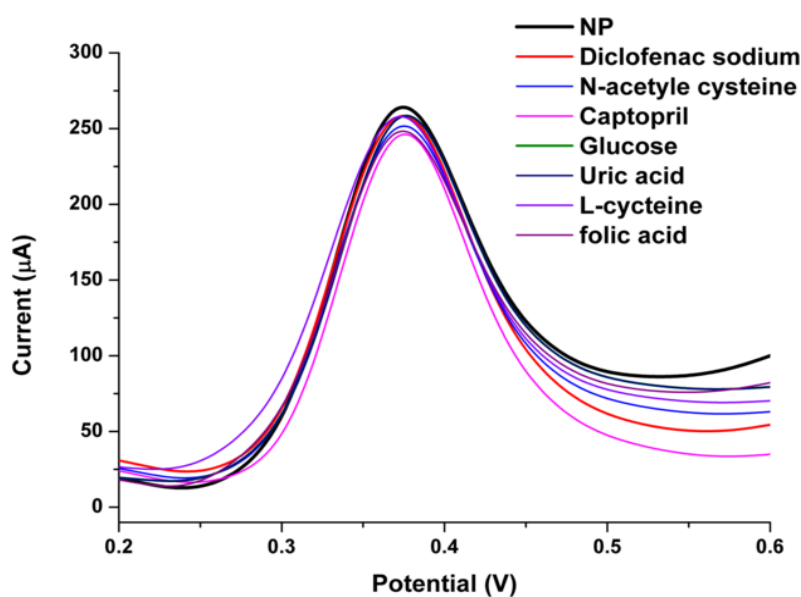
Figure 4.16: DPV curves measured for NP (alone) and in presence of common co-existing chemical species.

4.2.7. Quantification of NP from spike human urine samples and clinical waste water

The CuO/GCE was examined in complex matrices like human urine and clinical waste water to guarantee the validity of the proposed sensors. The recovery data gained after quantification of NP from pre-spiked samples is shown in Table 4.3. The superior recovery of NP from such complex matrices is clearly reflect the practical workability of the proposed sensor system.

Table 4.3: Recovery of NP from urine and waste water samples using CuO/GCE.

S. No	Sample	Spiked (µM)	Detected (µM) *	Recovery (%)	RSD (%)
1	Urine	0.15	0.14	93.3	1.7
2	Urine	0.21	0.19	90.0	1.1
3	Urine	0.019	0.018	94.7	2.2
4	Waste Water	0.22	0.20	90.9	1.4
5	Waste Water	2.25	2.24	99.5	1.3
6	Waste Water	1.25	1.24	99.2	2.6

* Mean value for three measurements

4.3. SENSING OF N-ACETYL-L-CYSTEINE USING FLEXIBLE ELECTRODE
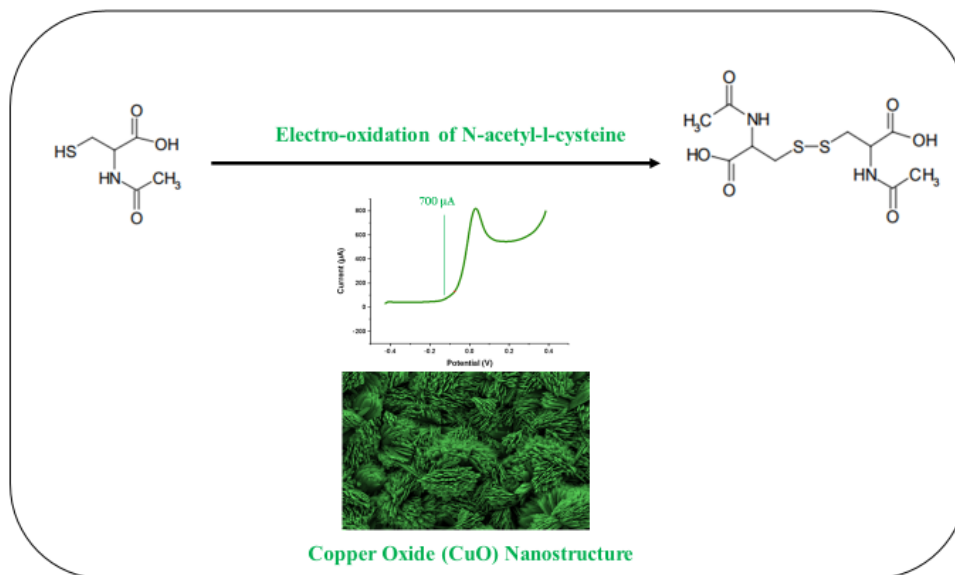
Figure 4.17: Schematic diagram representing the electro-catalytic oxidation of NAC over the in-situ growth of succinic acid assisted CuO nanostructures on ITO substrate.

4.3.1. The SEM analysis of CuO over ITO electrode

Figure 3.4 displays the SEM images for the as-synthesised product. The representative images clarified that the nanostructures possess structural characteristic features similar to large flowers composed of thin sharp flakes. Figure 3.4 (d) exhibits the high magnification image which further demonstrates the fabrication of flakes from nanoparticles [23] .This variation is because of the growth pattern over ITO glass [82]. Figure 3.5 (a) shows the CuO formed without any template. The absence of any structural features is a clear evidence of template importance. The pattern of the CuO clearly signify the importance of Succinic acid in controlling the morphology and as an adhesive material for adhesion of nanomaterial over ITO glass. The average thickness was estimated in rang of 20-50 nm. The Figure 3.5 (b) depicts the corresponding SEM image. The image shows no morphological variation in formed nanostructures. This is the evidence that the used tape does not affect the growth of material over conductive substrate.

Figure 3.14 depicts the EDX spectrum and the elemental mapping which emphasize the compositional of the material. Figure 3.10 shows the XRD pattern for the CuO/ITO substrate.

The noted patterns consist of peaks consists of (110), (111), (–111), (–202) indexes which are because of the pure CuO nanomateiral as compared to ICCD Card No. 80-0076[83]. The proposed method provides high crystallinity compared to other reported method such as chemical deposition and electro-deposition method [83][84].

The FTIR analysis was carried for both the pure template and nanostrucutre. The comparative evaluation has been shown in Figure 3.13. Succinic acid shows major characteristic bands at 1700 cm^{-1}, 1420 cm^{-1} and at 1208 cm^{-1} for C-O-H bending vibration and C-O stretching vibration [85]. The frequency shift from 1700 to 1660 cm^{-1} is evidence of the successive interaction. The smaller shifts in the measured frequencies were noted for C-O-H bending vibration (1420 to 1407 cm^{-1}) and C-O stretching vibration (1208to 1201cm^{-1}). The band at 400 cm^{-1} is evidence of M-O bond [74].

Although the formation pattern of copper oxide over substrates is still not completely clear. Nevertheless, it is known that the growth begins by the formation of copper hydroxide nuclei which results from the dissociation of [Cu(NH3)4]$^{2+}$ complex as described in below:

$$\mathbf{Cu^{+2} + 4NH_3 \rightarrow [Cu(NH_3)_4]^{+2}} \tag{4-9}$$

$$\mathbf{[Cu(NH_3)_4]^{+2} + 2OH^- \rightarrow Cu(OH)_2 + \ NH_4\ OH} \tag{4-10}$$

$$\mathbf{Cu(OH)_2 \rightarrow CuO + H_2O} \tag{4-11}$$
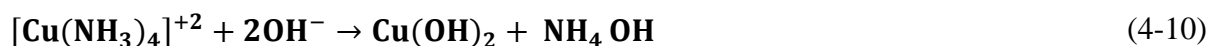
The growth of nuclei controlled by the Succinic acid and propped by ITO substrate allowed formation of aggregates. These aggregates with time convert from orthorhombic phase to monoclinic phase of CuO with the resultant morphology of flowers. The provision of support such as ITO would minimize the surface effects allowing good adhesion of nanomaterial to the substrate [82]. A pictorial view of the slides is shown in Figure 4.18. As noted ‹the complete coverage of electrode with negligible pin holes have been obtained which inverts the Validity of the proposed method.
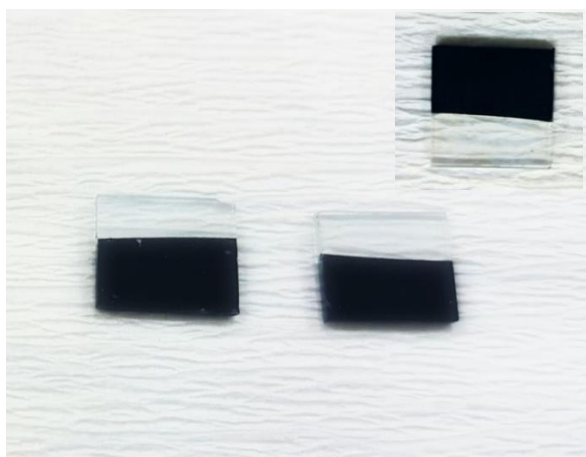
Figure 4.18: The microscopic view of the developed CuO/ITO substrates.

4.3.2. The electrodes electrochemical characteristics

The electrochemical behaviour of the developed electrode was tested in 0.01 μM solution of NAC against bare electrode and electrode modified with CuO prepared with the template. Figure 4.19 shows the CV curves for the electrodes. As seen, the developed electrode has a higher current and low-over potential value compared to the bare and modified electrode.

As the utilised material is copper oxide in both cases. The variability in the signal measurement is because of the morphological features. The use of flexible substrate provides more uniform nanostructure formation with greater contact with the conducting substrate. The charge transfer co-efficient (α) was determined to be 0.653, 0.564 for CuO/ITO and CuO/GCE respectively (Figure 4.19(b, c)). The larger value in case of CuO over conductive substrate is evident of greater electron transfer kinetics associated with such electrodes.

The oxidation of NAC using the described electrode can be illustrated in the given equations:

$$\text{Ncys} - \text{SH} + 2\text{CuO} + 2\text{e} \rightarrow \text{H}_2\text{O} + \text{Ncys} - \text{sycN} + \text{Cu}_2\text{O} \tag{4-12}$$

$$\text{Cu}_2\text{O} + \text{H}_2\text{O} \rightarrow 2\text{CuO} + 2\text{e} + 2\text{H}^+ \tag{4-13}$$
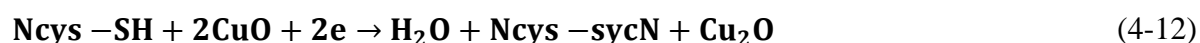
Generally, Cu(II)/(I) redox couple allow the NAC oxidation. The Cu(II) formed via anodic sweep led to the oxidation of NAC as shown in equation (4-12). The cathodic sweep again

generates the Cu(II) as suggested by equation (4-13). The EIS measurement for CuO/ITO conducted out in 0.01 µM NAC with 0.1 M PBS (pH 5.5) is shown in Figure 4.20. The Nyquist diagram shows a smaller semi-circle for modified electrode which is indicative of low-resistance achieved at the electrode. The scan rate of the modified electrode was measured from 50 to 100 mVs^{-1}. Figure 4.21 shows the variation of current density and square of scan rate. The rise in current with scan rate shows the process to be diffusion controlled.
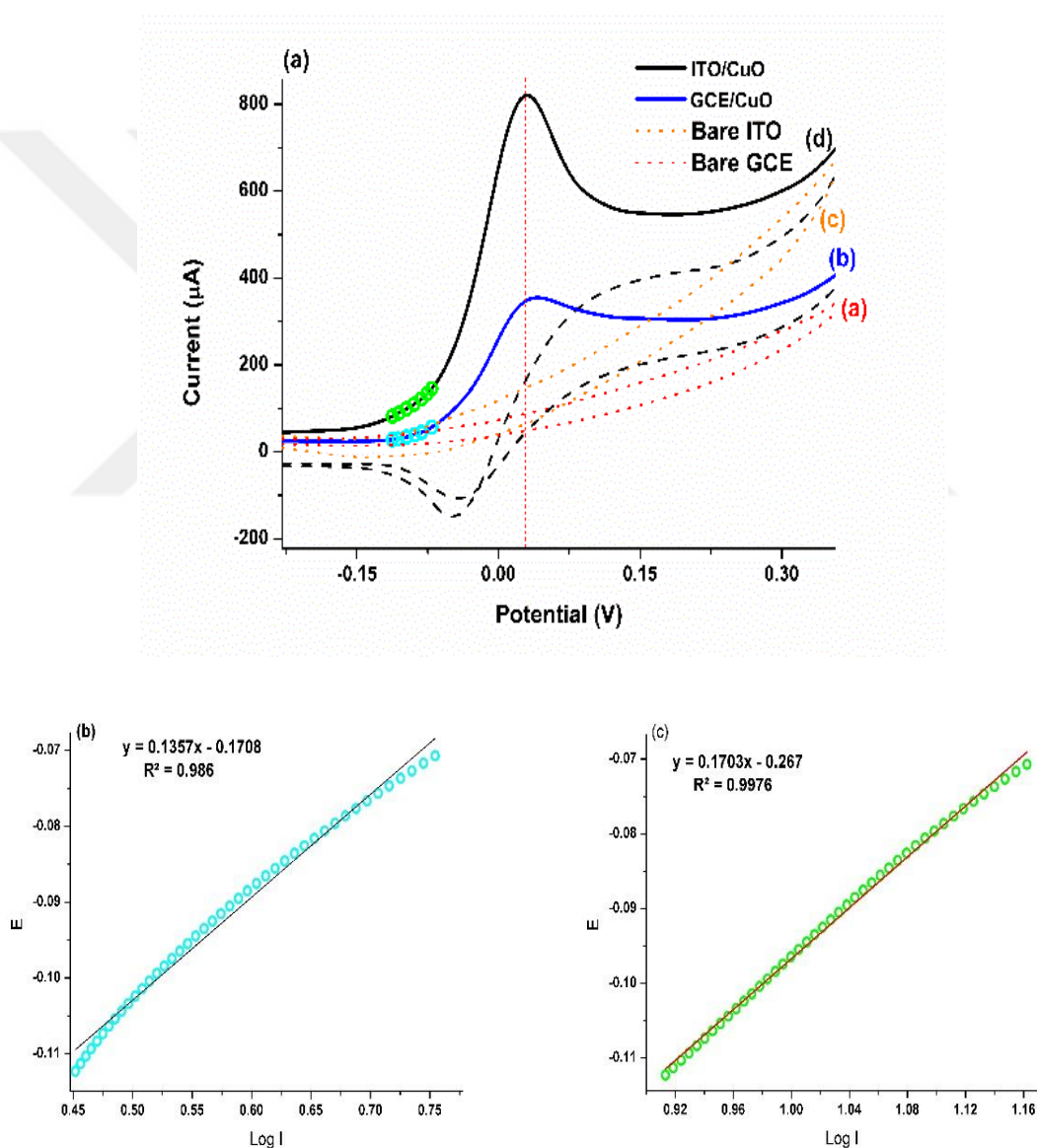
Figure 4.19: (a) CV characteristics recorded for CuO/ITO and CuO/GCE for NAC (b) and (c) Tafel slope of the corresponding plots.
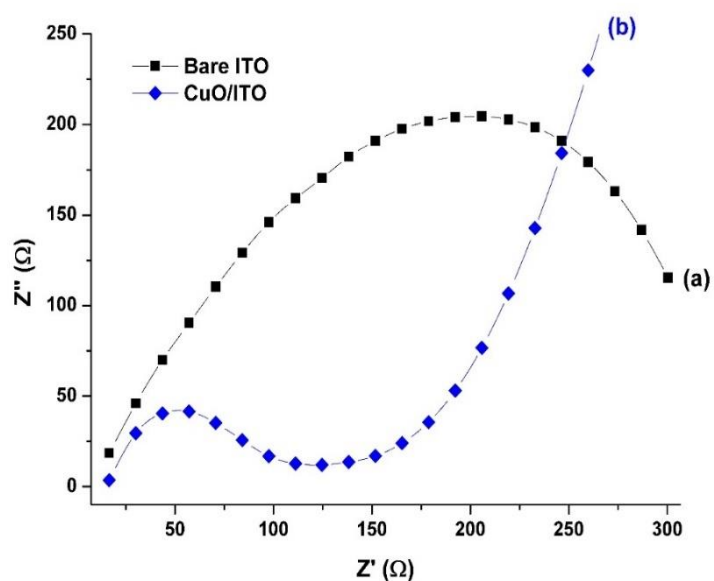
Figure 4.20: Electrochemical impedance spectra in 0.01µM NAC with 0.1 M PBS (pH 5.5) at (a) bare ITO and (b) CuO/ITO.
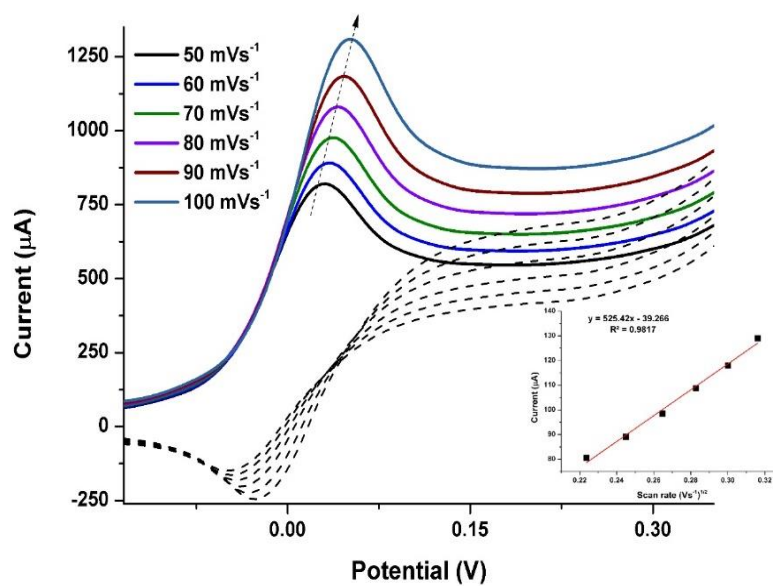
Figure 4.21: The scan rate measurement for CuO/ITO electrode in range of 50 to 100 mVs^{-1}.

4.3.3. The chronoamperometric measurement for CuO/ITO electrode

The chronoamperometric measurements was carried for diffusion constant [26]. The recording was obtained for current versus different concentration of NAC ranging from 0.1-0.5 mM. Figure 4.22 shows the obtained chronoamperometric graph. Figure 4.22 (a) shows the plot of I vs $t^{-1/2}$ while the final obtained slopes were then plotted for NAC concentration as shown in Figure 4.22 (b). After that the slope of the figure 4.22 (b) was utilized to calculate the D value utilizing the incoming modified formula of Cottrell equation:

$$I = nFAD^{1/2} C_b \, \pi^{-1/2} \, t^{-1/2} \tag{4-14}$$

$$D = \left[\frac{m}{nFA \, C_b \, \pi^{-1/2}}\right] \tag{4-15}$$

Where m is the slope from figure 4.22 (b), C_b represents the strength of NAC, A is the active area of electrode (0.031 cm^2), n, F and π possess their regular meanings. 1.62×10^{-2} cm^2/s was obtained as the D value of the discussed electrode. Table 4.4 represents the noticed analytical features of the newly advanced electrode. The obtained data is evident that the proposed electrode system exhibits sufficient analytical features compared to its other counterparts.
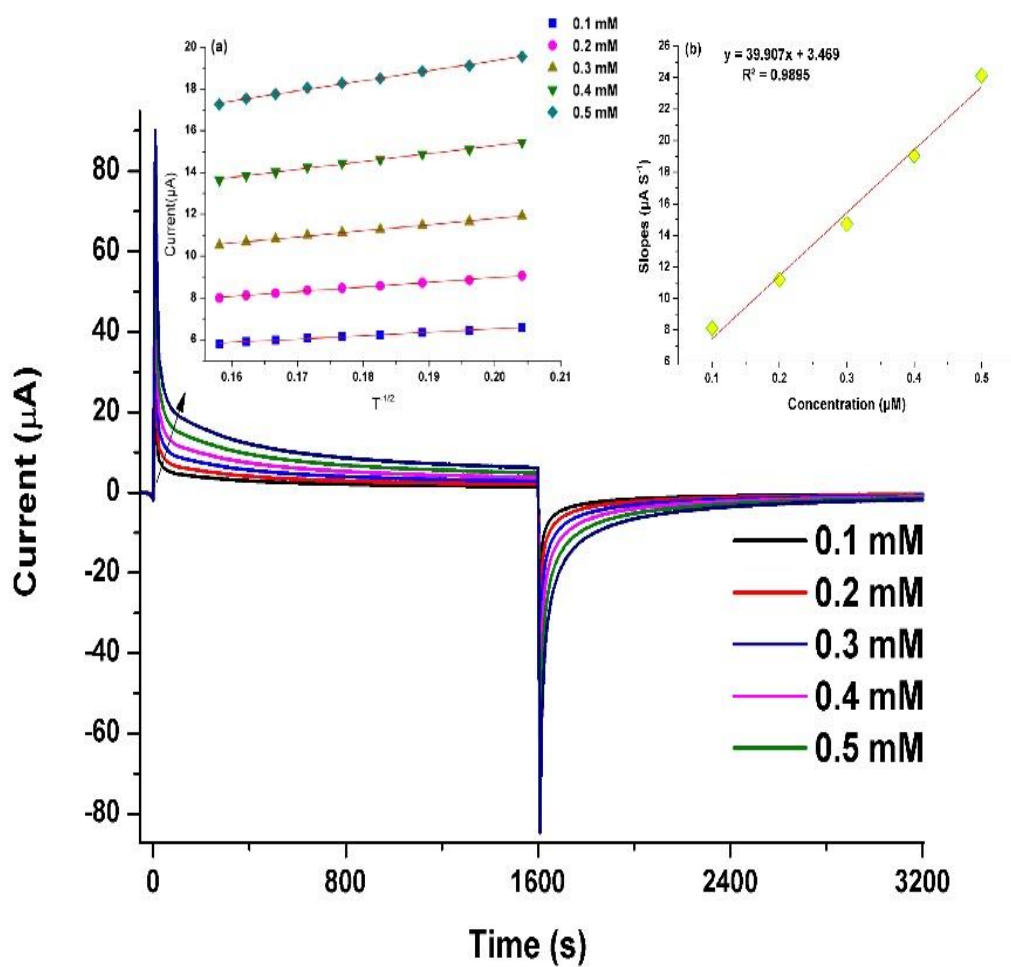
Figure 4.22: Chronoamperometric characteristics of ITO/CuO against NAC in concentration ranging from 0.1 to 0.5 mM (a) graph of current v/s $t^{-1/2}$,(c) plot of the corresponding slopes against the standard concentration of NAC.

Table 4.4 : Comparision of the devised electrode with conventiaonal methods.

Electrode	Transducer	Sensing limit (M)	Electron transfer Coefficient	Diffusion Coefficient (cm^2.s^{-1})	Reference
CPE	DMBQ-Pt-CNTS	7.0×10^{-8}	0.4	7.88×10^{-5}	[79]
CPE	2,7-BFCNPE	5.2×10^{-8}	0.43	2.87×10^{-5}	[26]
CPE	Q–MWCNT	4.4×10^{-7}	0.30	1.22×10^{-6}	[86]
GCE	CuO-CA	1.0×10^{-8}	0.61	6.05×10^{-4}	[50]
CPE	2CBF	2.6×10^{-8}	0.47	6.80×10^{-5}	[64]
CPE	Cobalt salophen complexes	5.0×10^{-8}	--	--	[87]
CPE	Catechol	1.0×10^{-5}	--	3.49×10^{-5}	[88]
Palladized aluminum	Prussian blue film	5.4×10^{-7}	0.5	3.20×10^{-2}	[89]
ITO Electrode	**CuO**	**1.2×10^{-9}**	**0.65**	**1.62×10^{-2}**	**This work**

4.3.4. The optimization of devised electrode

The impact of of pH on the electro-oxidation of NAC was measured from 2.5 to 7.5 with concentration (0.01µM). Figure 4.23 (a) shows the current variation against pH. The best signal was achieved to pH 5.5 [90] [77]. Figure 4.23 (b) shows the optimization of accumulation time. The measurement was studied in range of 0-120 s under continuous stirring.
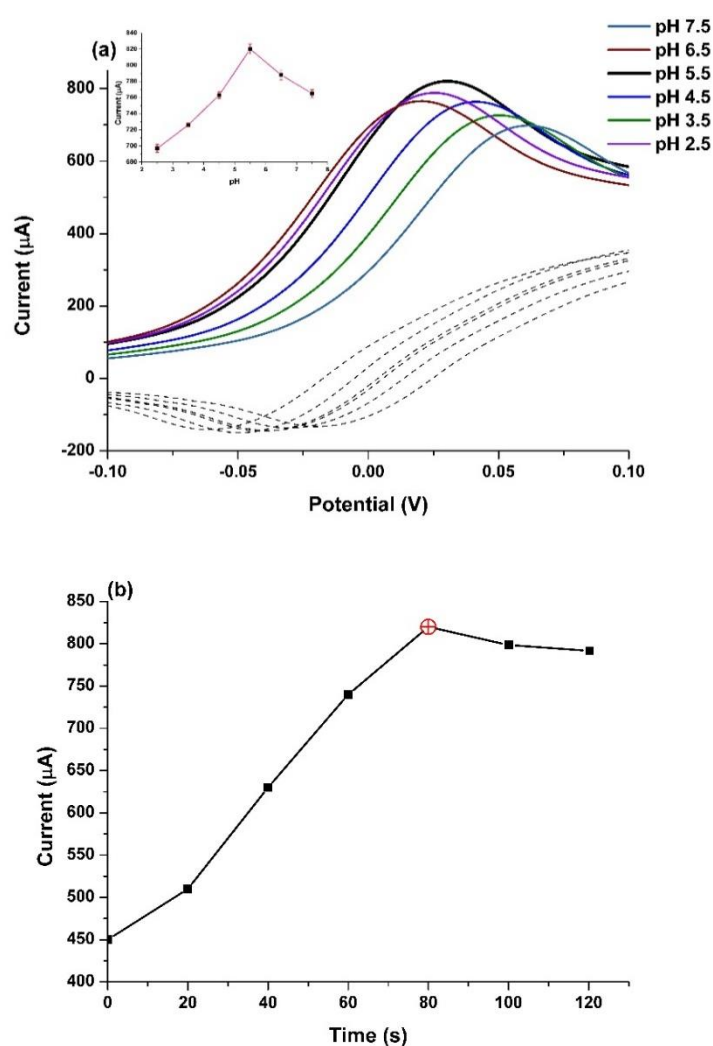
Figure 4.23: (a) The pH variation for the observed current and (b) Current against different accumulation time.

4.3.5. The quantification of NAC using DPV

The sensing of NAC was conducted in concentration ranging from 0.01 to 0.28 µM. The concentration was measured with differential pulse voltammetry. Figure 4.24 (a) depicts the DPV profile where Figure 4.24 (b) shows the calibration with linear fit analysis. The LOD and LOQ were estimated to be 1.2×10^{-3} (S/N=3) and 1.7×10^{-2} µM (S/N=10) respectively.
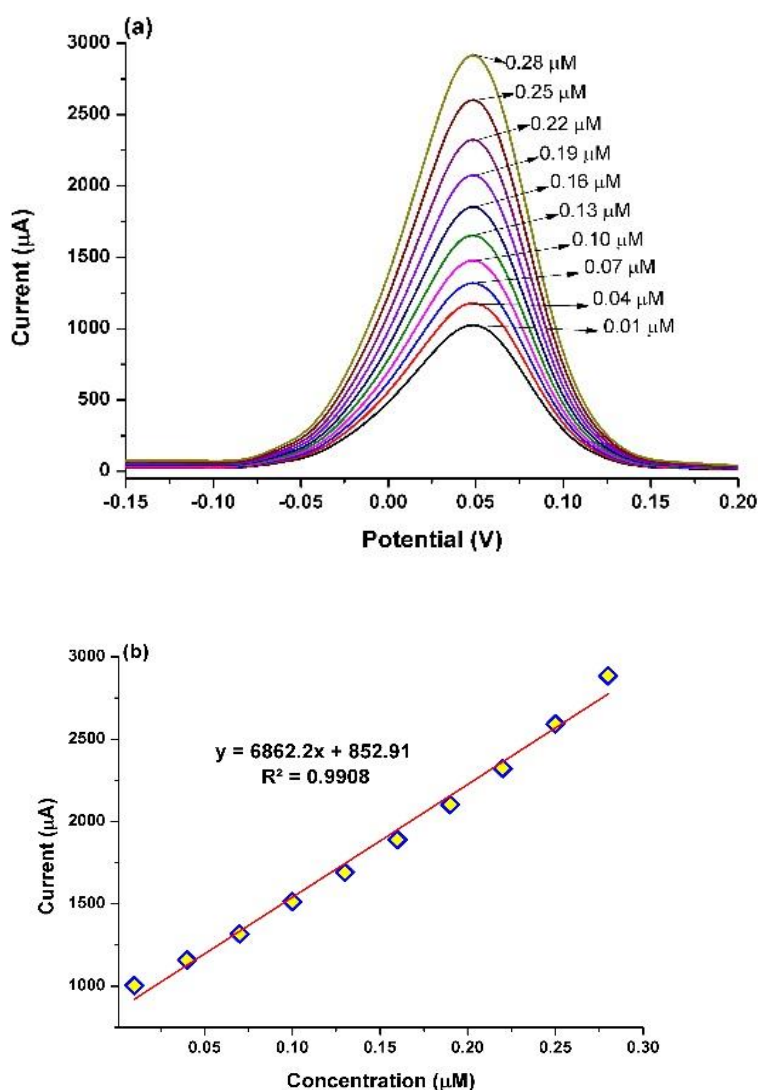
Figure 4.24: (a) Calibration registered for ITO/CuO electrode for NAC concentration and (b) corresponding analysis.

4.3.6. The characteristics of the devised electrode

The interference measurements were carried for various species including biomolecules. Figure 4.25(a) shows the corresponding DPV waves in the presence of NAC. The trial variation in the observed current response indicates the selectivity of electrode. The repeatability of the electrode was assessed by measuring the 100 cycles of the electrode in the same solution. The inconsiderable drop in the observed current density shows the high reproducibility of the electrode.
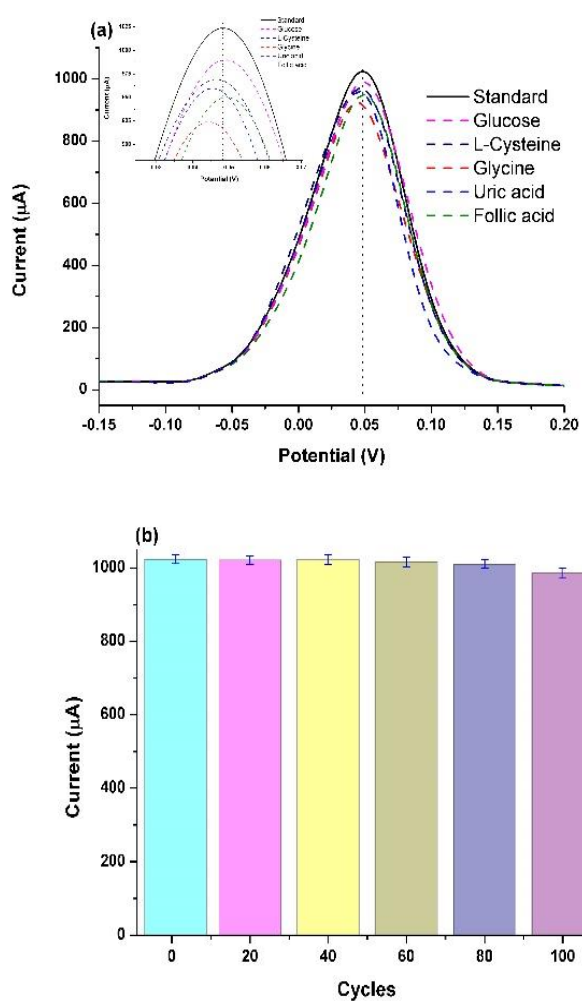
Figure 4.25: (a) The DPV waves recorded for ITO/CuO in presence interference species with 10 folds higher concentration then NAC (0.1 µM) and (b) Variation in current density recorded for 100 cycles of ITO/CuO electrode in 0.1 µM NAC.

4.3.7. The validation of method

The electrode capability was validated using pre-spiked samples. Table 4.5 shows the good recoveries of the samples which is suggestive of the greater analytical performance of electrode.

Table 4.5: The employment of CuO/ITO for the determination of NAC.

Original concentration (μM)*	Added (μM)	Determined Content (μM)	Recovery (%)
1.0	0	0.98	98
1.0	0.1	1.98	99
1.0	0.4	1.39	99.3
1.0	0.8	1.77	98.3

*600 mg of NAC crushed to make diulted samples.

4.4. SENSING OF CAPTOPRIL USING ELECTRODE BASED SENSING SYSTEM
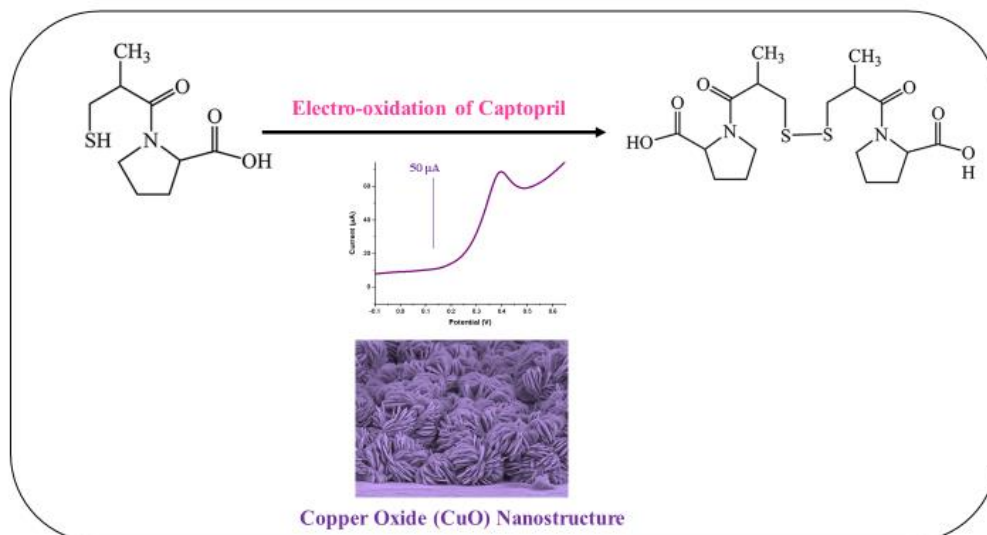
Figure 4.26: Schematic diagram representing the electrochemical oxidation of Captopril over CuO/ITO electrode synthesized using malonic acid as modifier.

4.4.1. The characterization of ITO based electrode

Figure 3.6 shows the synthesized nanostructures are heavily populated with flower-like morphological characteristic which are consisted of interconnected thin flakes. To ensure the vital role of template, a similar experiment was conducted without the template. Figure 3.7 is evident that the material lacks the the appropriate morphological features . In addition, the material has zero adhesion to electrode. The width was noted in range of 10-20 nm where EDX analysis comfirmed the purity of the product.

Figure 3.11 depicts the XRD pattern with (110), (111), (–111), (–202) indexed to monoclinic phase of CuO ICCD Card No:80-0076[83]. Figure 4.27 shows the pictures of the developed electrode. The use of malonic acid as modifier enables the direct formation fo nanostrctures over conductive platform. The growth method can be illustrated as per given equations:

$$Cu^{+2} + 4NH_3 \rightarrow [Cu(NH_3)_4]^{+2} \tag{4-16}$$

$$[Cu(NH_3)_4]^{+2} + 2OH^- \rightarrow Cu(OH)_2 + NH_4OH \qquad (4\text{-}16)$$

$$Cu(OH)_2 \rightarrow CuO + H_2O \qquad (4\text{-}17)$$
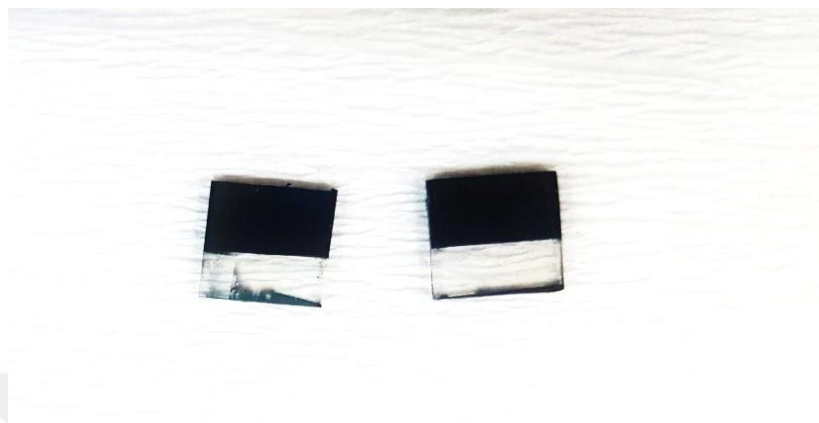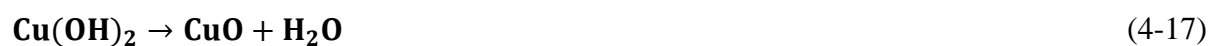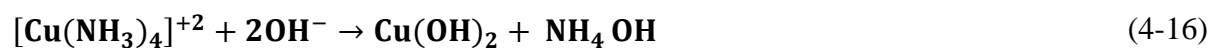
Figure 4.27: Microscopic view of the modified ITO electrodes.

4.4.2. The sensing of CAP with devised electrode

The measurement was conducted out in comparison to bare ITO, GCE and CGE modified with nanomaterials fabricated without template. Figure 4.28 (a), shows that the electrode demonstrated greater current intensity compared to other electrodes. The CuO /ITO shows entire coverage of surface area of the electrode with negligible pin-hole formation as seen from SEM images[56]. The electron transfers co-efficient (α) were evaluated using Tafel slopes (Figure 4.28 (b), (c)). The α value were0.83,0.73 for both electrode respectively.
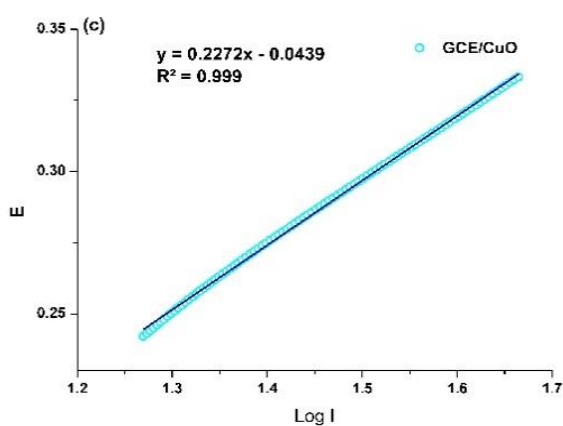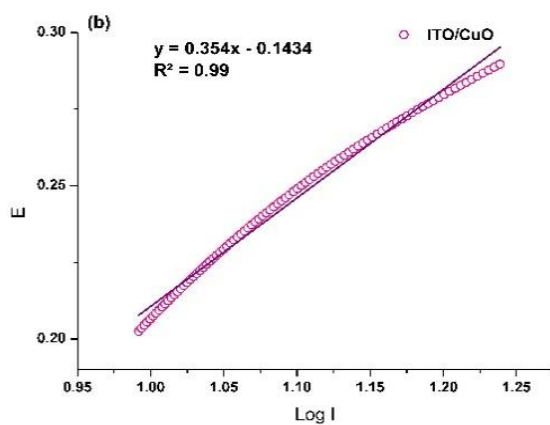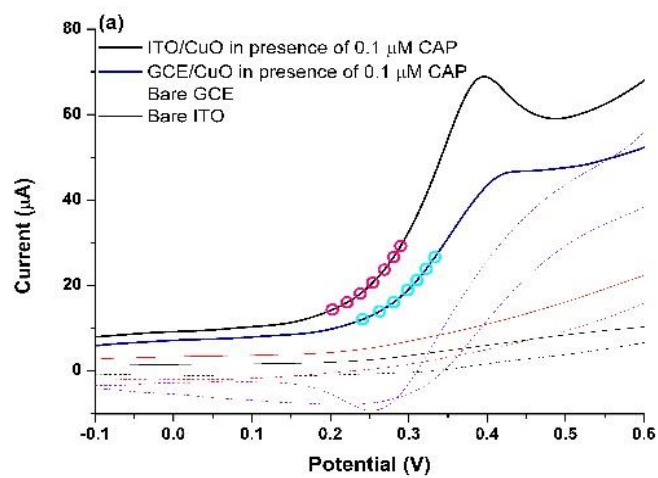
Figure 4.28: (a)CV characteristics of electrodes against 0.1 μM CAP while (b),(c) exhibits the Tafel slopes.

Table 4.6: Comparison of CuO /ITO based electrochemical sensor with other sensor system utilising for quantification of CAP.

Electrode	Modifier	LOD (M)	LDR (M)	Coefficient of electron transfer (D)	Coefficient of diffusion ($cm^2.s^{-1}$)	Rate constant ($mol^{-1}Ls^{-1}$)	Reference
Carbon paste Electrodes	CuO NPs /MWCNTs -CPE	2.9×10^{-7}	4.6×10^{-7} - 1.0×10^{-5}	0.43	2.1×10^{-7}	1.449×10^5	[70]
Carbon Paste Electrode	NiO/NPs /DED/CPE	7.0×10^{-9}	3.5×10^{-8}– 5.5×10^{-4}	0.72	2.9×10^{-5}	1.49×10^3	[91]
Carbon Paste Electrode	Si/Al-APTMS-BPK-Mn	9.0×10^{-8}	3.0×10^{-7} – 300×10^{-4}	0.69	1.55×10^{-4}	6.21×10^2	[92]
Carbon paste Electrodes	2CBFZC CPE	9×10^{-8}	5.0×10^{-7}- 9.0×10^{-4}	0.64	1.2×10^{-6}	8.9×10^3	[93]
ITO Electrode	**CuO**	2.0×10^{-9}	1.0×10^{-8}- 4.3×10^{-7}	*0.83*	9.28×10^{-5}	3.5×10^3	**This Work**

4.4.3. The chronoamperometric measurement

The chronoamperometric measurements were carried for CuO/ITO for 0.1 to 0.5 mM of CAP under constant potential of 0.39 V. Cottrell equation was used for the estimation of D value [26]:

$$I = nFAD^{1/2} C_b \pi^{-1/2} t^{-1/2} \tag{4-19}$$

$$D = [\frac{m}{nFA C_b \pi^{-1/2}}] \tag{4-20}$$

The plot of current (I) versus ($t^{-1/2}$) is given in (Figure 4.29 (b)) .Thereafter the obtained slopes are plotted against the chosen concentration of CAP as shown in Figure 4.29 (c). The D value for CuO/ ITO was calculated to be 9.28×10^{-5} cm^2/s which is relatively higher in comparison to the conventional electrodes modified utilizing the drop casting process (Table 4.6). The rate

constant (k) was derived from the chronoamperometry graph using the modified form of Galus equation:

$$\frac{IC}{IL} = \left[\gamma^{1/2}\left[\pi^{\frac{1}{2}}erf\left(\gamma^{\frac{1}{2}}\right) + \frac{exp(-\gamma)}{\gamma^{1/2}}\right]\right] \tag{4-21}$$

Where Ic is observed current and I_L is blank current. Since the γ value exceeds two, the error function can be considered unity and thus equation cna be simplified to equation (4-22).

$$\frac{IC}{IL} = \gamma^{\frac{1}{2}}\pi^{\frac{1}{2}}(k_hC_bt)^{1/2} \tag{4-22}$$

The symbols k_h, C_b and t denote the rate constant, CAP concentration and elapsed time respectively. The plot of I_c/I_L v/s $t^{1/2}$ against the used concentration of CAP provides K_h value of 3.5×10^3 mol^{-1}Ls^{-1}as shown in Figure 3.30.
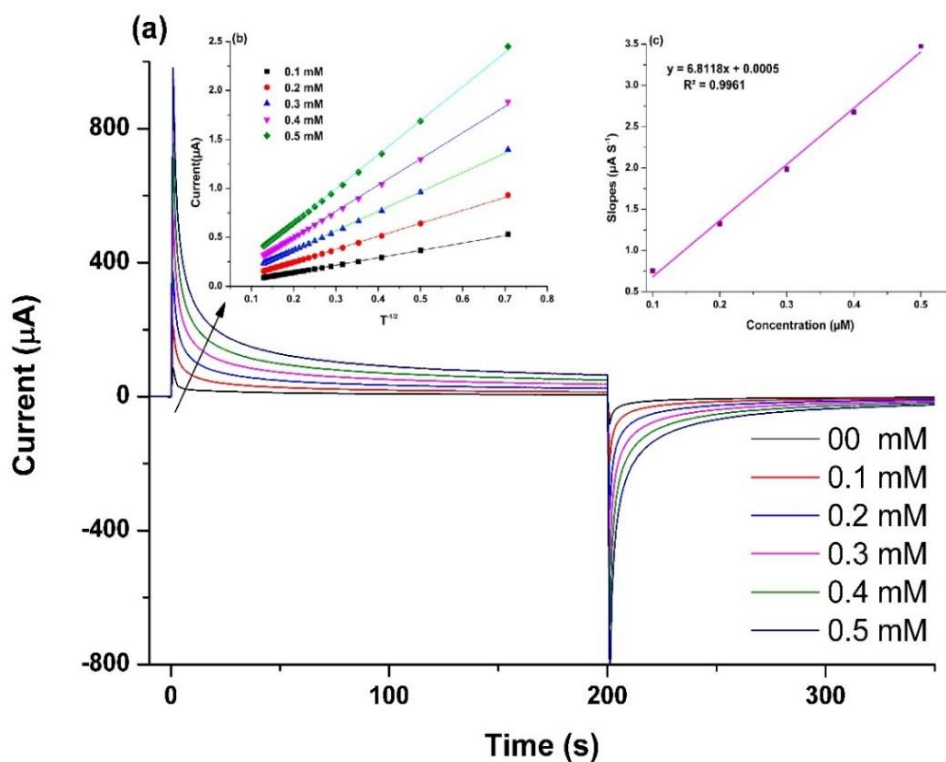
Figure 4.29: (a) Chronoamperometric characteristics (b) graph of current v/s $t^{-1/2}$, (c) graph of slopes plotted against concentration of CAP.
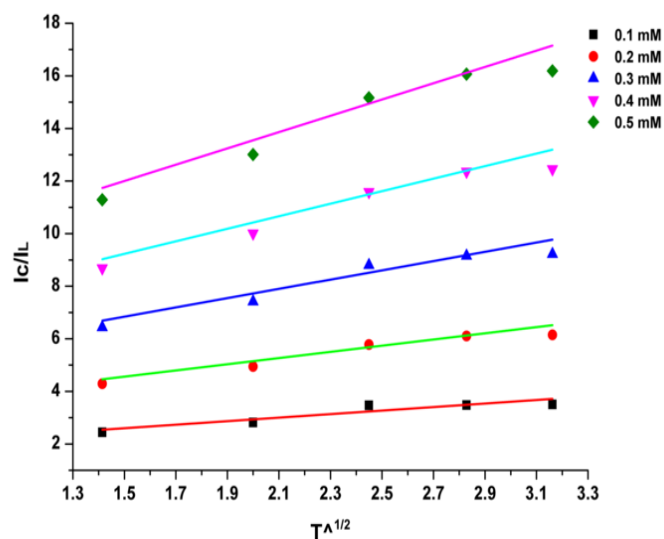
Figure 4.30: Linear fit analysis for the graphs plotted between I_c/I_L and $t^{-1/2}$.

4.4.4. The optimization

The pH of the system was studied in range of 2.5 to 8.5 (Figure 4.31(a)). The best signal response was noted for pH value of 4.5. The scan rate of the developed electrode was also studied (Figure 4.32) which shows increase in current with respect to rate of scan. The accumulation time was also studied (Figure 4.31(b)) in range of 50 to 90 mVs^{-1}.
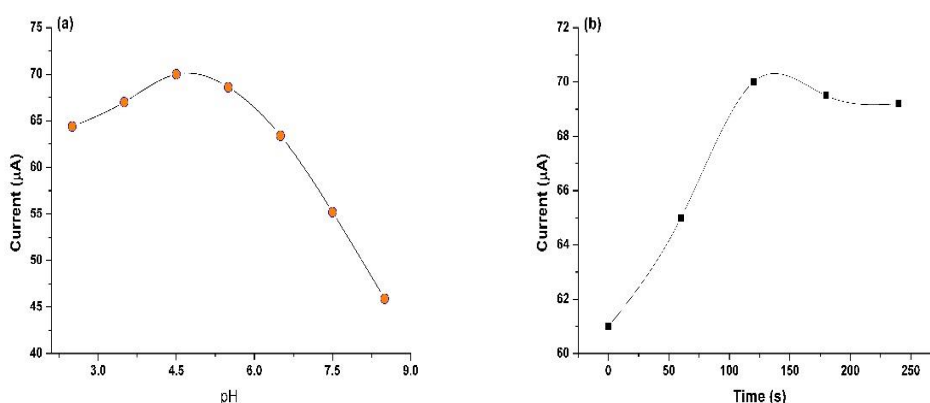
Figure 4.31: Current response of CuO/ ITO against (a) variation in the pH of BRB buffer and (b) variation in accumulation time ranging from 0 to 250 s.
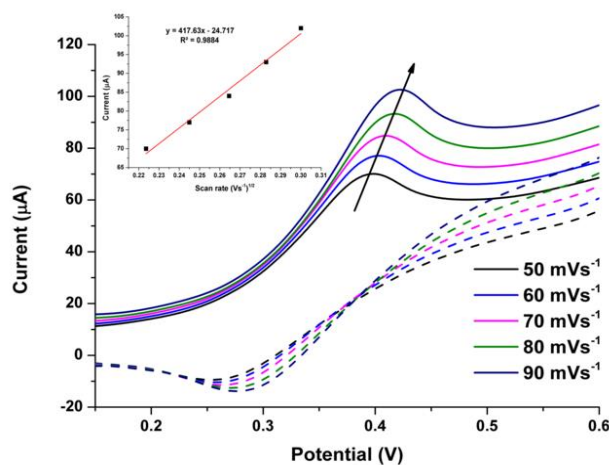
Figure 4.32: Scan rate measurement for CuO/ITO ranging from 50 to 90 mVs^{-1} .

4.4.5. The quantification of drug using developed electrode

The quantification was carried in concentrations range of 0.01 to 3.43 µM. The Figure 4.33 displays the plotted calibration and linear fit analysis. The LOD was estimated to be 0.002(S/N=3) while the LOQ was estimated to be 0.08 µM. The table 4.7 shows the comparison of the electrode with the conventional one.
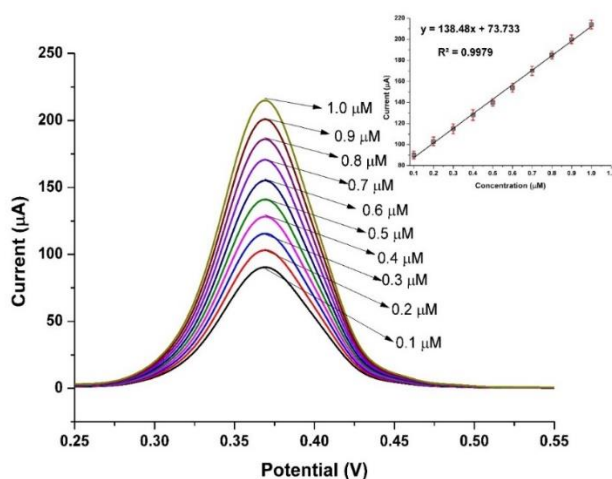
Figure 4.33: The DPV waves for different concentration of CAP and the inset shows the linear fit analysis.

4.4.6. Selectivity of CuO/ITO against interferents

The experiment was recorded for foreign substances including Mg^{2+}, K^+, Al^{3+}, Fe^{3+}, Ca^{2+}, NO_3^- , SO_4^{2-} , CO_3^{2-}, and various biological important molecules with concentration greater than CAP analyte. The small current variation is indicative of the selectivity of the electrode. The electrode stability was evaluated from the ten sequential runs of ITO/CuO where the reproducibility of devised electrode was also evaluated by testing the response of five ITO/CuO electrodes were individually synthesized utilizing the same procedure mentioned in part 2.2.4 as shown in Figure 4.34 (b), (c).
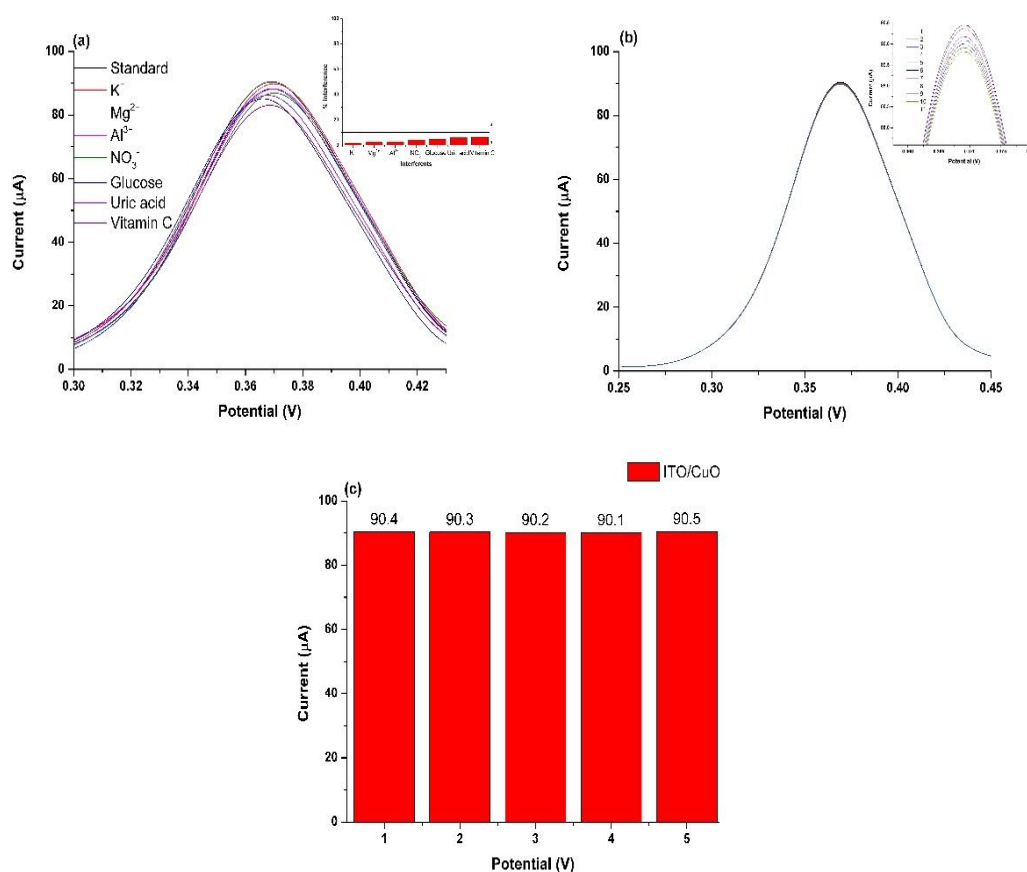
Figure 4.34: The DPV waves recorded for ITO/CuO in presence interference species and(b) repeatability of the developed electrode for 0.1 µM of CAP(c) difference in current intensity registered for five similar electrodes.

4.4.7. The sensing of CAP from urine samples

These collected urine samples were added fixed amount of CAP and tested utilizing method aforesaid in part 2.5.2. The perfect recoveries with lower RSD values proves the working feasibility of the devised electrode (Table 4.7).

Table 4.7: The employment of CuO/ITO for the determination of CAP.

Sample	spiked (μM)	Determined (μM)	RSD (%)	Recovery (%)
Tablet*	0	0.098 ±0.002	2.0	98
Urine	0.25	0.24 ±0.005	2.1	96
Urine	0.15	0.14 ±0.001	0.7	93

*25 mg of CAP crushed to make diulted samples.

5. CONCLUSION AND RECOMMENDATIONS

To better understand and easier for readers, the summary of the full thesis has been divided into a number of paragraphs according to the study parts.

Part 1

This study depicts electro-oxidation of NAC in aquatic environment utilizing electrode based sensor. The low-temperature hydrothermal growth method was utilized for the growth of the functionalized CuO nanostructures utilizing diverse growth controlling agents e.g. Citric acid, N-acetyl-L-cysteine, and Adipic acid. The unique growth controlling abilities of these modifier allowed the development of highly attractive morphological CuO nanostructure sensitive for the direct oxidation of NAC. The modified electrode utilizing citric acid demonstrated excellent electro-oxidation capability for NAC, compared to to its other peers with charge transfer coeffecient value of 0.61 and diffusion coefficient value of 6.059×10^{-4} cm^2/s . The sensor worked linearly in range from 0.1 to 5.5 μM with LOD value of 0.001 μM .

Part 2

This study represents the successful electro-catalytic oxidation of nalbuphine hydrochloride (NP) in aqueous medium. The low-temperature hydrothermal growth route was utilized for the growth of unique nanostructures of NiO, CuO, and Co$_3$O$_4$. The study examines the potential of pharmaceutical drug, in particular acetyl salicylic acid (ASA) as controlling and directing agent. The utilized drug owns unique ability for different metal oxides which enabled formation of nanostructures with diverse morphologies and structural features. It is interesting that the as-synthesized nanostructures showed evident electro-catalytic behavior against NP with CuO nanostructures encouraging higher current density and low-over potential value. This competitive electrochemical exploration of metal oxide nanostructures enabled fabrication of highly effective NP electrochemical sensor system which relied both on the active structural morphology and enhanced electron-transfer kinetics. The sensor system was also tested in human urine samples and clinical waste water where excellent recoveries of the spiked NP reflected its analytical workability.

Part 3

The study reports the use of flexible electrode for the sensing of NAC using CuO nanostructures unqiue morphology. The electrode was developed using hydrothermal approch with the assistance of a template known as succinic acid. The sensor system was sensing linearly in range of 0.01 to 0.28 µM with sensitivity up to be 1.2×10^{-3} µM. Furthermore, the developed electrode was applicapble to real samples.

Part4

The study deals with another approch of obtaining CuO nanostrctures over conductive substrate with malonic acid as template during hydrothermal method. The developed electroe was tested for sensing of CAP molecule using electrochemical technique. The sensor performed well in linear range of 0.1 to 1.0 µM. The deveised electrode was also suitable for practical application such as clinical and enviromental samples.

REFERENCES

[1] A. Afkhami, H. Khoshsafar, H. Bagheri, and T. Madrakian, "Preparation of NiFe2O4/graphene nanocomposite and its application as a modifier for the fabrication of an electrochemical sensor for the simultaneous determination of tramadol and acetaminophen," *Anal. Chim. Acta*, vol. 831, pp. 50–59, 2014.

[2] A. Afkhami, H. Khoshsafar, H. Bagheri, and T. Madrakian, "Facile simultaneous electrochemical determination of codeine and acetaminophen in pharmaceutical samples and biological fluids by graphene-CoFe2O4 nancomposite modified carbon paste electrode," *Sensors Actuators, B Chem.*, vol. 203, no. November, pp. 909–918, 2014.

[3] H. Bagheri, A. Afkhami, P. Hashemi, and M. Ghanei, "Simultaneous and sensitive determination of melatonin and dopamine with Fe3O4 nanoparticle-decorated reduced graphene oxide modified electrode," *RSC Adv.*, vol. 5, no. 28, pp. 21659–21669, 2015.

[4] B. J. Sanghavi, O. S. Wolfbeis, T. Hirsch, and N. S. Swami, "Nanomaterial-based electrochemical sensing of neurological drugs and neurotransmitters," *Microchim. Acta*, vol. 182, no. 1–2, pp. 1–41, 2015.

[5] V. Concha-Herrera, J. R. Torres-Lapasió, and M. C. García-Alvarez-Coque, "Chromatographic Determination of Thiols After Pre-column Derivatization with *o* - Phthalaldehyde and Isoleucine," *J. Liq. Chromatogr. Relat. Technol.*, vol. 27, no. 10, pp. 1593–1609, 2004.

[6] S. M. Al-Ghannam, A. M. El-Brashy, and B. S. Al-Farhan, "Fluorimetric determination of some thiol compounds in their dosage forms," *Farmaco*, vol. 57, no. 8, pp. 625–629, 2002.

[7] W. T. Suarez, H. J. Vieira, and O. Fatibello-Filho, "Generation and destruction of unstable reagent in flow injection system: Determination of acetylcysteine in pharmaceutical formulations using bromine as reagent," *J. Pharm. Biomed. Anal.*, vol. 37, no. 4, pp. 771–775, 2005.

[8] J. Du, Y. Li, and J. Lu, "Investigation on the chemiluminescence reaction of the phenylhydrazine- luminol-peroxide system," *Anal. Chim. Acta*, vol. 448, pp. 79–83, 2001.

[9] W. T. Suarez, A. A. Madi, F. C. Vicentini, and O. Fatibello-Filho, "Flow-injection spectrophotometric determination of N-acetylcysteine in pharmaceutical formulations with on-line solid-phase reactor containing Zn(II) phosphate immobilized in a polyester resin," *Anal. Lett.*, vol. 40, no. 16–18, pp. 3417–3429, 2007.

[10] W. T. Suarez, H. J. Vieira, and O. Fatibello-Filho, "Flow injection turbidimetric determination of acetylcysteine in pharmaceutical formulations using silver nitrate as precipitant reagent," *J. Braz. Chem. Soc.*, vol. 18, no. 5, pp. 1028–1033, 2007.

[11] J. Gong, X. Miao, T. Zhou, and L. Zhang, "An enzymeless organophosphate pesticide sensor using Au nanoparticle-decorated graphene hybrid nanosheet as solid-phase

extraction," *Talanta*, vol. 85, no. 3, pp. 1344–1349, 2011.

[12] C. W. Liao, Y. R. Chen, J. L. Chang, and J. M. Zen, "A Sensitive Electrochemical Approach for Melamine Detection Using a Disposable Screen Printed Carbon Electrode," *Electroanalysis*, vol. 23, no. 3, pp. 573–576, 2011.

[13] H. Bagheri, A. Afkhami, Y. Panahi, H. Khoshsafar, and A. Shirzadmehr, "Facile stripping voltammetric determination of haloperidol using a high performance magnetite/carbon nanotube paste electrode in pharmaceutical and biological samples," *Mater. Sci. Eng. C*, vol. 37, no. 1, pp. 264–270, 2014.

[14] A. K. C. C. N. R. Rao, A. Muller, *The Chemistry of Nanomaterials_ Synthesis, Properties and Applications*. 2004.

[15] G. C. Bond and D. T. Thompson, "Catalysis by Gold Downloaded by [University of Tokyo] at 01 : 24 24 December 2011," *Catal. Rev. - Sci. Eng.*, vol. 41, no. December, p. 319, 2011.

[16] V. K. Gupta, Tawfik Abdo Saleh, *Synthesis , Classification , and Properties of Nanomaterials*, vol. 101. 2016.

[17] T. A. S. and V. K. Gupta, "Morphology and Surface Characterization of Nanomaterial and Polymer Membranes," 2016.

[18] G. Tontini, A. Koch, V. A. V Schmachtenberg, C. Binder, A. N. Klein, and V. Drago, "Synthesis and magnetic properties of nickel micro urchins," *Mater. Res. Bull.*, vol. 61, no. January, pp. 177–182, 2015.

[19] S. De and S. Mandal, "Surfactant-assisted shape control of copper nanostructures," *Colloids Surfaces A Physicochem. Eng. Asp.*, vol. 421, pp. 72–83, 2013.

[20] Q. Zhang *et al.*, "CuO nanostructures: Synthesis, characterization, growth mechanisms, fundamental properties, and applications," *Prog. Mater. Sci.*, vol. 60, no. 1, pp. 208–237, 2014.

[21] M. Outokesh, M. Hosseinpour, S. J. Ahmadi, T. Mousavand, S. Sadjadi, and W. Soltanian, "Hydrothermal synthesis of CuO nanoparticles: Study on effects of operational conditions on yield, purity, and size of the nanoparticles," *Ind. Eng. Chem. Res.*, vol. 50, no. 6, pp. 3540–3554, 2011.

[22] Z. Zhuang, Q. Peng, and Y. Li, "Controlled synthesis of semiconductor nanostructures in the liquid phase," *Chem. Soc. Rev.*, vol. 40, no. 11, p. 5492, 2011.

[23] R. A. Soomro *et al.*, "A highly selective and sensitive electrochemical determination of melamine based on succinic acid functionalized copper oxide nanostructures †," *RSC Adv.*, vol. 5, no. December, pp. 105090–105097, 2015.

[24] R. A. Soomro *et al.*, "Amino acid assisted growth of CuO nanostructures and their potential application in electrochemical sensing of organophosphate pesticide," *Electrochim. Acta*, vol. 190, pp. 972–979, 2016.

[25] Z. N. Gao, J. Zhang, and W. Y. Liu, "Electrocatalytic oxidation of N-acetyl-l-cysteine by acetylferrocene at glassy carbon electrode," *J. Electroanal. Chem.*, vol. 580, no. 1, pp. 9–16, 2005.

[26] H. Beitollahi, M. A. Taher, F. Mirrahimi, and R. Hosseinzadeh, "Electrochemical sensor for selective determination of N-acetylcysteine in the presence of folic acid using a modified carbon nanotube paste electrode," *Mater. Sci. Eng. C*, vol. 33, no. 3, pp. 1078–1084, 2013.

[27] H. Heli, S. Majdi, and N. Sattarahmady, "Ultrasensitive sensing of N-acetyl-l-cysteine using an electrocatalytic transducer of nanoparticles of iron(III) oxide core-cobalt hexacyanoferrate shell," *Sensors Actuators, B Chem.*, vol. 145, no. 1, pp. 185–193, 2010.

[28] A. Salmanipour, M. A. Taher, H. Beitollahi, and R. Hosseinzadeh, "New voltammetric strategy for simultaneous determination of N-acetylcysteine and folic acid using a carbon nanotube modified glassy carbon electrode," *Colloids Surfaces B Biointerfaces*, vol. 102, pp. 385–390, 2013.

[29] H. Beitollahi and S. Nekooei, "Application of a Modified CuO Nanoparticles Carbon Paste Electrode for Simultaneous Determination of Isoperenaline, Acetaminophen and N-acetyl-L-cysteine," *Electroanalysis*, vol. 28, no. 3, pp. 645–653, 2016.

[30] V. H. R. Souza *et al.*, "Flexible, Transparent and Thin Films of Carbon Nanomaterials as Electrodes for Electrochemical Applications," *Electrochim. Acta*, vol. 197, pp. 200–209, 2016.

[31] R. J. Bull, J. Crook, M. Whittaker, and J. A. Cotruvo, "Therapeutic dose as the point of departure in assessing potential health hazards from drugs in drinking water and recycled municipal wastewater," *Regul. Toxicol. Pharmacol.*, vol. 60, no. 1, pp. 1–19, 2011.

[32] C. Adams, Y. Wang, K. Loftin, and M. Meyer, "Removal of Antibiotics from Surface and Distilled Water in Conventional Water Treatment Processes," *J. Environ. Eng.*, vol. 128, no. 3, pp. 253–260, 2002.

[33] H. M. Elqudaby, H. A. M. Hendawy, E. R. Souaya, G. G. Mohamed, and G. M. G. Eldin, "Utility of Activated Glassy Carbon and Pencil Graphite Electrodes for Voltammetric Determination of Nalbuphine Hydrochloride in Pharmaceutical and Biological Fluids," *Int. J. Electrochem.*, vol. 2016, pp. 1–10, 2016.

[34] et al. Dube, L.M., "Determination of nalbuphine by high-performance liquid chromatography with electrochemical detection," *J Chromatogr*, vol. 427, pp. 113–120, 1988.

[35] F. Bressolle, S. Khier, A. Rochette, J. M. Kinowski, C. Dadure, and X. Capdevila, "Population pharmacokinetics of nalbuphine after surgery in children," *Br. J. Anaesth.*, vol. 106, no. 4, pp. 558–565, 2011.

[36] L. J. Cai *et al.*, "Validated LC-MS/MS assay for the quantitative determination of nalbuphine in human plasma and its application to a pharmacokinetic study," *Biomed. Chromatogr.*, vol. 25, no. 12, pp. 1308–1314, 2011.

[37] C. Spectrometry, J. Y. Kim, and M. K. In, "Simultaneous Determination of Nalbuphine and Opiates in Human Hair by Gas," no. 3, pp. 219–226, 2004.

[38] R. A. Soomro, Z. H. Ibupoto, Sirajuddin, M. I. Abro, and M. Willander, "Electrochemical sensing of glucose based on novel hedgehog-like NiO nanostructures," *Sensors Actuators, B Chem.*, vol. 209, pp. 966–974, 2015.

[39] S. Kempahanumakkagari, A. Deep, K. H. Kim, S. Kumar Kailasa, and H. O. Yoon, "Nanomaterial-based electrochemical sensors for arsenic - A review," *Biosens. Bioelectron.*, vol. 95, no. April, pp. 106–116, 2017.

[40] L. Lan, Y. Yao, J. Ping, and Y. Ying, "Recent advances in nanomaterial-based biosensors for antibiotics detection," *Biosens. Bioelectron.*, vol. 91, pp. 504–514, 2017.

[41] T. Shaikh *et al.*, "Tranexamic acid derived gold nanoparticles modified glassy carbon electrode as sensitive sensor for determination of nalbuphine," *Sensors Actuators, B Chem.*, vol. 211, no. September, pp. 359–369, 2015.

[42] M. Fouladgar, "A new sensor for determination of nalbuphine using NiO/functional single walled carbon nanotubes nanocomposite and ionic liquid," *Sensors Actuators, B Chem.*, vol. 230, pp. 456–462, 2016.

[43] A. R. Voet and J. R. Tame, "Protein-templated synthesis of metal-based nanomaterials," *Curr. Opin. Biotechnol.*, vol. 46, no. Figure 1, pp. 14–19, 2017.

[44] X. Wang *et al.*, "Synthesis and lithium storage properties of Co3O4 nanosheet-assembled multishelled hollow spheres," *Adv. Funct. Mater.*, vol. 20, no. 10, pp. 1680–1686, 2010.

[45] Y. Duan *et al.*, "Optically active chiral CuO 'nanoflowers,'" *J. Am. Chem. Soc.*, vol. 136, no. 20, pp. 7193–7196, 2014.

[46] K. Khojier, H. Savaloni, and Z. Sadeghi, "A comparative investigation on growth, nanostructure and electrical properties of copper oxide thin films as a function of annealing conditions," *J. Theor. Appl. Phys.*, vol. 8, no. 1, p. 116, 2014.

[47] M. Safdar, Y. Junejo, and A. Balouch, "Efficient degradation of organic dyes by heterogeneous cefdinir derived silver nanocatalyst," *J. Ind. Eng. Chem.*, vol. 31, pp. 216–222, 2015.

[48] Y. Junejo, A. Baykal, and Sirajuddin, "Cefditorene-Mediated Synthesis of Silver Nanoparticles and Its Catalytic Activity," *J. Inorg. Organomet. Polym. Mater.*, vol. 24, no. 2, pp. 401–406, 2013.

[49] R. A. Soomro, Z. H. Ibupoto, Sirajuddin, S. T. H. Sherazi, M. I. Abro, and M. Willander, "Practice of diclofenac sodium for the hydrothermal growth of NiO nanostructures and their application for enzyme free glucose biosensor," *Microsyst. Technol.*, vol. 22, no. 10, pp. 2549–2557, 2016.

[50] M. M. Tunesi, R. A. Soomro, and R. Ozturk, "CuO nanostructures for highly sensitive

shape dependent electrocatalytic oxidation of N-acetyl-L-cysteine," *J. Electroanal. Chem.*, vol. 777, pp. 40–47, 2016.

[51]   R. A. Soomro, O. P. Akyuz, R. Ozturk, and Z. H. Ibupoto, "Highly sensitive non-enzymatic glucose sensing using gold nanocages as efficient electrode material," *Sensors Actuators, B Chem.*, vol. 233, no. April, pp. 230–236, 2016.

[52]   P. J. Lamas-Ardisana, P. Fanjul-Bolado, and A. Costa-Garc??a, "Manufacture and evaluation of cup-stacked carbon nanofiber-modified screen printed electrodes as electrochemical tools," *J. Electroanal. Chem.*, vol. 775, pp. 129–134, 2016.

[53]   A. Von Weber, E. T. Baxter, H. S. White, and S. L. Anderson, "Cluster Size Controls Branching between Water and Hydrogen Peroxide Production in Electrochemical Oxygen Reduction at Pt n /ITO," *J. Phys. Chem. C*, vol. 119, no. 20, pp. 11160–11170, 2015.

[54]   N. Q. Dung, D. Patil, H. Jung, J. Kim, and D. Kim, "NiO-decorated single-walled carbon nanotubes for high-performance nonenzymatic glucose sensing," *Sensors Actuators, B Chem.*, vol. 183, pp. 381–387, 2013.

[55]   T. Wang, W. Su, Y. Fu, and J. Hu, "Controllably annealed CuO-nanoparticle modified ITO electrodes: Characterisation and electrochemical studies," *Appl. Surf. Sci.*, vol. 390, pp. 795–803, 2016.

[56]   T. D. Thanh, J. Balamurugan, J. Y. Hwang, N. H. Kim, and J. H. Lee, "In situ synthesis of graphene-encapsulated gold nanoparticle hybrid electrodes for non-enzymatic glucose sensing," *Carbon N. Y.*, vol. 98, pp. 90–98, 2016.

[57]   X. Ji, A. Wang, and Q. Zhao, "Direct growth of copper oxide films on Ti substrate for nonenzymatic glucose sensors," *J. Nanomater.*, vol. 2014, 2014.

[58]   M. Mazloum-Ardakani, M. A. Sheikh-Mohseni, H. Beitollahi, A. Benvidi, and H. Naeimi, "Electrochemical determination of vitamin C in the presence of uric acid by a novel TiO2 nanoparticles modified carbon paste electrode," *Chinese Chem. Lett.*, vol. 21, no. 12, pp. 1471–1474, 2010.

[59]   Z. Taleat, M. M. Ardakani, H. Naeimi, H. Beitollahi, M. Nejati, and H. R. Zare, "Electrochemical Behavior of Ascorbic Acid at a 2,2′-[3,6-Dioxa-1,8-octanediylbis(nitriloethylidyne)]-bis-hydroquinone Carbon Paste Electrode," *Anal. Sci.*, vol. 24, no. 8, pp. 1039–1044, 2008.

[60]   H. Karimi-Maleh, A. A. Ensafi, H. Beitollahi, V. Nasiri, M. A. Khalilzadeh, and P. Biparva, "Electrocatalytic determination of sulfite using a modified carbon nanotubes paste electrode: Application for determination of sulfite in real samples," *Ionics (Kiel).*, vol. 18, no. 7, pp. 687–694, 2012.

[61]   R. A. Soomro *et al.*, "Highly sensitive determination of atropine using cobalt oxide nanostructures: Influence of functional groups on the signal sensitivity," *Anal. Chim. Acta*, vol. 948, no. November, pp. 30–39, 2016.

[62] M. M. Foroughi, H. Beitollahi, S. Tajik, M. Hamzavi, and H. Parvan, "Hydroxylamine electrochemical sensor based on a modified carbon nanotube paste electrode: Application to determination of hydroxylamine in water samples," *Int. J. Electrochem. Sci.*, vol. 9, no. 6, pp. 2955–2965, 2014.

[63] L. Tian and B. Liu, "Fabrication of CuO nanosheets modified Cu electrode and its excellent electrocatalytic performance towards glucose," *Appl. Surf. Sci.*, vol. 283, pp. 947–953, 2013.

[64] H. Beitollahi, M. A. Taher, M. Ahmadipour, and R. Hosseinzadeh, "Electrocatalytic determination of captopril using a modified carbon nanotube paste electrode: Application to determination of captopril in pharmaceutical and biological samples," *Measurement*, vol. 47, pp. 770–776, 2014.

[65] M. Mazloum-Ardakani *et al.*, "Simultaneous determination of levodopa, carbidopa and tryptophan using nanostructured electrochemical sensor based on novel hydroquinone and carbon nanotubes: Application to the analysis of some real samples," *Electrochim. Acta*, vol. 56, no. 25, pp. 9113–9120, 2011.

[66] Y. Jing *et al.*, "Determination of nicotine in tobacco products based on mussel-inspired reduced graphene oxide-supported gold nanoparticles," *Sci. Rep.*, vol. 6, no. July, p. 29230, 2016.

[67] A. B. Ferreira Vitoreti, O. Abrahão, R. A. da Silva Gomes, G. R. Salazar-Banda, and R. T. S. Oliveira, "Electroanalytical determination of captopril in pharmaceutical formulations using boron-doped diamond electrodes," *Int. J. Electrochem. Sci.*, vol. 9, no. 3, pp. 1044–1054, 2014.

[68] S. A. Chermini, H. Krimi, M. Keyvanfard, and K. Alizad, "Voltammmetric determination of captopril using multiwall carbon nanotubes paste electrode in the presence of isoproterenol as a mediator," *Iran. J. Pharm. Res.*, vol. 15, no. 1, pp. 107–117, 2016.

[69] M. C. C. Areias, K. Shimizu, and R. G. Compton, "Voltammetric Detection of Captopril Using Copper(II) and an Unmodified Glassy Carbon Electrode," *Electroanalysis*, vol. 28, no. 7, pp. 1524–1529, 2016.

[70] B. Zargar, H. Parham, and A. Hatamie, "Electrochemical investigation and stripping voltammetric determination of captopril at CuO nanoparticles/multi-wall carbon nanotube nanocomposite electrode in tablet and urine samples," *Anal. Methods*, vol. 7, no. 3, pp. 1–10, 2015.

[71] D. Huo, Q. Li, Y. Zhang, C. Hou, and Y. Lei, "A highly efficient organophosphorus pesticides sensor based on CuO nanowires-SWCNTs hybrid nanocomposite," *Sensors Actuators, B Chem.*, vol. 199, pp. 410–417, 2014.

[72] D. P. Singh, A. K. Ojha, and O. N. Srivastava, "Synthesis of different Cu(OH)2 and CuO (nanowires, rectangles, seed-, belt-, and sheetlike) nanostructures by simple wet chemical route," *J. Phys. Chem. C*, vol. 113, no. 9, pp. 3409–3418, 2009.

[73] M. Picquart, Z. Abedinzadeh, L. Grajcar, and M. H. Baron, "Spectroscopic study of N-acetylcysteine and N-acetylcystine/hydrogen peroxide complexation," *Chem. Phys.*, vol. 228, no. 1–3, pp. 279–291, 1998.

[74] S. Mandal, G. Das, and H. Askari, "Interactions of N-acetyl-l-cysteine with metals (Ni2+, Cu 2+ and Zn2+): An experimental and theoretical study," *Struct. Chem.*, vol. 25, no. 1, pp. 43–51, 2014.

[75] K. D. Dobson and A. J. McQuillan, "In situ infrared spectroscopic analysis of the adsorption of aliphatic carboxylic acids to TiO2, ZrO2, Al2O3, and Ta2O5 from aqueous solutions," *Spectrochim. Acta Part A Mol. Biomol. Spectrosc.*, vol. 55, no. 7–8, pp. 1395–1405, 1999.

[76] I. W. Siriwardane, "Adsorption of citric acid on cerium oxide nanoparticles (nanoceria) : effects of pH , surface charge and aggregation," 2012.

[77] W. Toito Suarez, L. H. Marcolino, and O. Fatibello-Filho, "Voltammetric determination of N-acetylcysteine using a carbon paste electrode modified with copper(II) hexacyanoferrate(III)," *Microchem. J.*, vol. 82, no. 2, pp. 163–167, 2006.

[78] A. C. de Sá, L. L. Paim, U. de O. Bicalho, and D. R. do Carmo, "Determination of N-acetylcysteine by cyclic voltammetry using modified carbon paste electrode with copper nitroprusside adsorbed on the 3-aminopropylsilica," *Int. J. Electrochem. Sci.*, vol. 6, no. 9, pp. 3754–3767, 2011.

[79] V. Arabali, H. Karimi-Maleh, H. Beitollahi, R. Moradi, M. Ebrahimi, and H. Ahmar, "A nanostructure-based electrochemical sensor for square wave voltammetric determination of N-acetylcysteine in pharmaceutical and biological samples," *Ionics (Kiel).*, vol. 21, no. 4, pp. 1153–1161, 2015.

[80] L. Li, Y. Li, S. Gao, and N. Koshizaki, "Ordered Co3O4 hierarchical nanorod arrays: tunable superhydrophilicity without UV irradiation and transition to superhydrophobicity," *J. Mater. Chem.*, vol. 19, no. 44, p. 8366, 2009.

[81] X. Tang, J. Li, and J. Hao, "Synthesis and characterization of spinel Co3O4 octahedra enclosed by the {1 1 1} facets," *Mater. Res. Bull.*, vol. 43, no. 11, pp. 2912–2918, 2008.

[82] A. C. Ngandjong, C. Mottet, and J. Puibasset, "Influence of the Silica Support on the Structure and the Morphology of Silver Nanoparticles: A Molecular Simulation Study," *J. Phys. Chem. C*, vol. 120, no. 15, pp. 8323–8332, 2016.

[83] T. D. Nguyen, T. C. Dang, A. T. Ta, and K. A. Dao, "Direct growth of CuO/ITO nanowires by the vapor solid oxidation method," *J. Mater. Sci. Mater. Electron.*, vol. 27, no. 5, pp. 4410–4416, 2016.

[84] S. Çetinkaya, H. A. Çetinkara, F. Bayansal, and S. Kahraman, "Growth and characterization of CuO nanostructures on si for the fabrication of CuO/p-Si schottky diodes," *Sci. World J.*, vol. 2013, 2013.

[85] S. Krishnan, C. J. Raj, S. M. N. Priya, R. Robert, S. Dinakaran, and S. J. Das, "Optical

and dielectric studies on succinic acid single crystals," *Cryst. Res. Technol.*, vol. 43, no. 8, pp. 845–850, 2008.

[86] H. R. Zare, M. Haji-Dehabadi, and Z. Shekari, "Electrocatalytic oxidation of N-acetyl-L-cysteine at a quercetin multiwall carbon nanotube modified GCE: application for simultaneous determination of ascorbic acid, L-DOPA, N-acetyl-L-cysteine, acetaminophen and tryptophan," *Anal. Methods*, vol. 7, no. 13, pp. 5511–5520, 2015.

[87] S. Shahrokhian, Z. Kamalzadeh, A. Bezaatpour, and D. M. Boghaei, "Differential pulse voltammetric determination of N-acetylcysteine by the electrocatalytic oxidation at the surface of carbon nanotube-paste electrode modified with cobalt salophen complexes," *Sensors Actuators, B Chem.*, vol. 133, no. 2, pp. 599–606, 2008.

[88] J. B. Raoof, R. Ojani, M. Amiri-Aref, and F. Chekin, "Catechol as an electrochemical indicator for voltammetric determination of N-Acetyl-L-cysteine in aqueous media at the surface of carbon paste electrode," *J. Appl. Electrochem.*, vol. 40, no. 7, pp. 1357–1363, 2010.

[89] M. H. Pournaghi-Azar and F. Ahour, "Palladized aluminum electrode covered by Prussian blue film as an effective transducer for electrocatalytic oxidation and hydrodynamic amperometry of N-acetyl-cysteine and glutathione," *J. Electroanal. Chem.*, vol. 622, no. 1, pp. 22–28, 2008.

[90] X. L. and M. W. Zafar Hussain Ibupoto, Kimleang Khun , Valerio Beni, "Synthesis of Novel CuO Nanosheets and Their Non-Enzymatic Glucose Sensing Applications," *Electroanalysis*, pp. 7926–7938, 2013.

[91] H. Karimi-Maleh, M. Moazampour, V. K. Gupta, and A. L. Sanati, "Electrocatalytic determination of captopril in real samples using NiO nanoparticle modified (9,10-dihydro-9,10-ethanoanthracene-11,12-dicarboximido)- 4-ethylbenzene-1,2-diol carbon paste electrode," *Sensors Actuators, B Chem.*, vol. 199, pp. 47–53, 2014.

[92] D. Habibi, A. R. Faraji, and A. Gil, "A highly sensitive supported manganese-based voltammetric sensor for the electrocatalytic determination of captopril," *Sensors Actuators, B Chem.*, vol. 182, pp. 80–86, 2013.

[93] H. Beitollahi, S. Ghofrani Ivari, R. Alizadeh, and R. Hosseinzadeh, "Preparation, Characterization and Electrochemical Application of ZnO-CuO Nanoplates for Voltammetric Determination of Captopril and Tryptophan Using Modified Carbon Paste Electrode," *Electroanalysis*, vol. 27, no. 7, pp. 1742–1749, 2015.

CURRICULUM VITAE

Personal Information	
Name Surname	MAWADA MOHAMED .E TUNESI
Place of Birth	Tripoli , Libya
Date of Birth	01.12 1988
Nationality	❐ T.C. ☑ Other:
Phone Number	05379693025
Email	mawadatunsi@gmail.com
Web Page	

Educational Information	
B. Sc.	
University	Tripoli University
Faculty	Science
Department	Chemistry
Graduation Year	2009-2010

M. Sc.	
University	Istanbul University
Institute	Institute of graduate studies in science and engineering
Department	Department of Chemistry
Programme	Chemistry
Graduation Year	22.12.2017

Publications

[1] M. M. Tunesi, R. A. Soomro, and R. Ozturk, "CuO nanostructures for highly sensitive shape dependent electrocatalytic oxidation of N-acetyl-L-cysteine," *J. Electroanal. Chem.*, vol. 777, pp. 40–47, 2016.

[2] M. Mohamed Tunesi, R. A. Soomro, and R. Ozturk, "The in situ growth of CuO nanostructures on an ITO substrate and its application as a highly sensitive electrode for the electrochemical determination of N-acetyl-l-cysteine," *J. Mater. Chem. C*, vol. 5, no. 10, 2017.

[3] R. A. Soomro, M. M. Tunesi, S. Karakus, and N. Kalwar, "Highly sensitive electrochemical determination of captopril using CuO modified ITO electrode: the effect of in situ grown nanostructures over signal sensitivity," *RSC Adv.*, vol. 7, no. 31, pp. 19353–19362, 2017.

[4]   N. H. Kalwar *et al.*, "Acetylsalicylic acid assisted hydrothermal growth of NiO, CuO and Co3O4nanostructures and their application in the electro-catalytic determination of nalbuphine hydrochloride," *J. Electroanal. Chem.*, vol. 807, pp. 137–144, 2017.

[5]   M. M. Tunesi, N. H. Kalwar, R. A. Soomro, S. Karakus, S. Jawaid, and M. I. Abro, "Tartaric acid assisted in-situ growth of CuO nanostructures over ITO substrate for the electrocatalytic detection of Sudan I," *Mater. Sci. Semicond. Process.*, vol. 75, no. August 2017, pp. 296–300, 2018.

[6]   M. M. Tunesi *et al.*, "Functionalised CuO nanostructures for the detection of organophosphorus pesticides: A non-enzymatic inhibition approach coupled with nano-scale electrode engineering to improve electrode sensitivity," *Sensors Actuators B Chem.*, 2018.